

Not in

Report No. 31



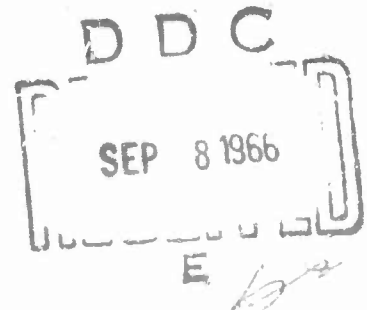
488251

Columbia University
in the City of New York

THERMONUCLEAR SHOCK WAVE STRUCTURE

by

Ann L. Fuller



PLASMA LABORATORY
SCHOOL OF ENGINEERING AND APPLIED SCIENCE
NEW YORK 27, N.Y.

⑥ THERMONUCLEAR SHOCK WAVE STRUCTURE .

⑨ Thermal Dept.
by

⑩ Ann L. Fuller

⑪ Jul 1966

⑫ 156 p.

⑬ AF/49-1-1631

⑭ TS-31

Plasma Laboratory
Report No. 31
S. W. Mudd Building
Columbia University
New York, N. Y. 10027

ABSTRACT

The structure of a very strong shock wave propagating through a deuterium-tritium gas mixture and a pure tritium gas is studied. The temperature behind the shock wave is sufficiently high so that thermonuclear reaction probabilities are large. The wave structure is similar to that of detonations in chemically reacting gases. It is assumed that the characteristic times for collisions and reactions are such that the von Neumann-Zeldovich model of detonations is applicable; i.e., the shock can be treated as a viscous gas dynamic shock followed by a deflagration wave inside of which all the reactions occur. The physical and mathematical assumptions involved in the analysis of thermonuclear shock wave structure are examined. The reaction probabilities for deuterium and tritium fusion reactions are computed and the appropriate reaction kinetics equations are developed. The effect of energy losses due to bremsstrahlung on the wave structure is considered for a gas that is optically thin to radiation of all frequencies. The resulting set of structure equations are solved numerically for several physically interesting cases. The neutron flux and power output due to reactions is calculated for a shock wave propagating in a electromagnetically driven shock tube filled

with a mixture of deuterium and tritium. A power of
1 kw/cm³ is predicted under specified operating conditions.

LIST OF ILLUSTRATIONS

<u>Figure</u>	<u>Page</u>	
1	2	detonation wave in a non-radiating gas viewed in a reference frame travelling with the wave
2	9	detonation in a non-radiating gas according to the von Neumann model
3	11	post-shock temperature vs. wave speed
4	29	post-shock and post-detonation temperature vs. detonation speed for deuterium-tritium mixture (1:1)
5	29	post-shock and post-detonation temperature vs. detonation speed for tritium
6	40	cross sections for deuterium fusion reactions
7	42	reaction probabilities for deuterium fusion reactions based on Maxwellian distributions
8	45	cross section for $T(d,n)He^4$ reaction [LA-2014]
9	47	reaction probabilities for $T(d,n)He^4$ and $T(t,2n)He^4$ reactions based on Maxwellian distributions
10	58	cross section for $T(t,2n)He^4$ reaction for triton energies below 60 kev
11	58	cross section for $T(t,2n)He^4$ reaction for triton energies above 60 kev
12	76	dimensionless speed, ω , vs. degree of fusion, α
13	78	dimensionless temperature, τ , vs. degree of fusion, α , for a detonation in a deuterium-tritium mixture (1:1)
14	82	dimensionless temperature, τ , vs. degree of fusion, α , for a detonation in tritium

<u>Figure</u>	<u>Page</u>	
15	86	radiation loss term, Δ , vs. degree of fusion, α
16	100	temperature profile behind gas dynamic shock in deuterium-tritium mixture (1:1)
17	101	speed profile behind gas dynamic shock in deuterium-tritium mixture (1:1)
18	102	density profile behind gas dynamic shock in deuterium-tritium mixture (1:1)
19	103	pressure profile behind gas dynamic shock in deuterium-tritium mixture (1:1)
20	104	degree of fusion behind gas dynamic shock in deuterium-tritium mixture (1:1)
21	105	temperature profile behind gas dynamic shock in tritium
22	106	speed profile behind gas dynamic shock in tritium
23	107	density profile behind gas dynamic shock in tritium
24	108	pressure profile behind gas dynamic shock in tritium
25	109	degree of fusion behind gas dynamic shock in tritium
26	118	temperature behind gas dynamic shock in deuterium-tritium mixture (1:1)
27	119	relative degree of fusion $\frac{\alpha}{\alpha_m}$ behind gas dynamic shock in deuterium-tritium mixture (1:1) for different shock speeds
28	120	ratio of radiative power loss to thermo-nuclear power behind gas dynamic shock in deuterium-tritium mixture (1:1) for different shock speeds

<u>Figure</u>	<u>Page</u>	
29	121	ratio of radiative power loss to thermo-nuclear power behind gas dynamic shock

TABLE OF CONTENTS

	<u>Page</u>
Abstract	i
List of Illustrations	iii
I. Introduction and Historical Survey	1
II. Physical and Mathematical Formulation of the Problem	7
2.1 von Neumann Model of Detonation Structure	7
2.2 Physical and Mathematical Assumptions	13
2.3 Shock Structure Equations Without Radiation	24
2.4 Reaction Rates	30
2.5 Shock Structure Equations with Radiation	33
III. Thermonuclear Shock Structure Equations for Three Different Gases	38
3.1 Fusion Reactions in Deuterium-Tritium Mixtures	38
3.2 Reaction Probabilities for the $T(d,n)He^4$ Reaction	44
3.3 Kinetics Equations for Deuterium-Tritium Reactions	48
3.4 Dimensionless Form of Shock Structure Equations for Deuterium-Tritium Mixtures	53
3.5 Dimensionless Parameters in the Energy Equation	55
3.6 Fusion Reactions in Tritium	56
3.7 Reaction Probabilities for the $T(t,2n)He^4$ Reaction	59
3.8 Kinetics Equations for Tritium Reactions	64
3.9 Kinetics Equations for $T(t,2n)He^4$ Reactions in Hydrogen-Tritium Mixtures	68
IV. Shock Structure Curves in Phase Space	74
4.1 Non-Radiative Shock Structure Curves in Phase Space	74
4.2 Radiative Shock Structure Curves in Phase Space	83
V. Shock Profiles in Real Space	92
5.1 Solution of the Shock Structure Equation for a Reacting and Radiating Gas	92
5.2 Solution of the Shock Structure Equation for a Radiating Gas	95

5.3	Profiles of the Flow Variables for Shocks Propagating with the Chapman-Jouguet Speed in Deuterium-Tritium and Tritium Gases	97
5.4	Profiles of the Flow Variables for Shocks Propagating with the Chapman-Jouguet Speed in Hydrogen-Tritium Mixtures	112
5.5	Profiles of the Flow Variables for Shocks Propagating with Speeds Below the Chapman-Jouguet Speed	115
	Acknowledgements	129
	List of Symbols	130
	References	134

CHAPTER I

INTRODUCTION AND HISTORICAL SURVEY

A shock wave is a disturbance that propagates with supersonic speed with respect to the undisturbed gas ahead of it. It compresses and heats the gas through which it moves. If the gas is capable of undergoing molecular, atomic or nuclear reactions, the gas composition may change across the shock front.

A shock wave in which exothermic reactions take place is called a detonation (see figure 1). A thermonuclear shock is defined as a detonation in which thermonuclear reactions occur. If the high temperature created by the shock wave is maintained, the gas may continue to react until all the fuel is consumed. Radiation is an important energy transfer mechanism at temperatures for which thermonuclear reaction rates are appreciable. If the gas is opaque to radiation, a steady state may be established behind the wave. If the gas loses energy through radiation, however, no steady state is established behind the wave; the gas continues to radiate until its temperature is the same as that of its surroundings.

The variation of temperature, pressure, density, speed and species concentration with space inside the shock wave

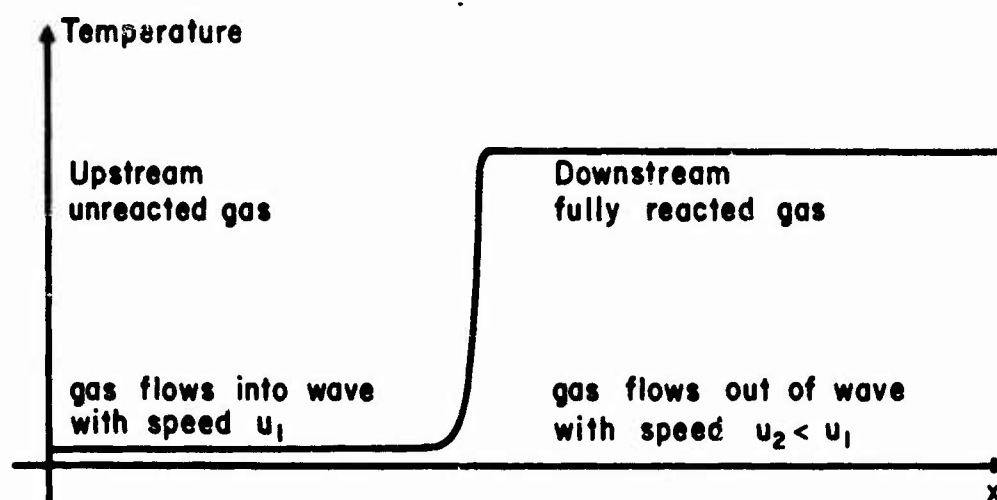


FIG. 1 DETONATION WAVE IN A NON-RADIATING GAS VIEWED IN REFERENCE FRAME TRAVELLING WITH THE WAVE

is called the shock structure. The flow variables change continuously from one side of the wave to the other. The interior of the wave is where viscous and thermal conducting processes are important and where all the reactions take place. However, for a gas in which radiation energy loss is negligible the conditions behind the wave are independent of the detailed transport and reaction processes occurring in the shock structure. If radiation energy loss cannot be neglected, the conditions behind the wave depend on the physical processes occurring in the structure.

In this paper the structure of detonations in gases capable of undergoing thermonuclear reactions is investigated. There is no known literature that deals directly with thermonuclear shock structure. However, studies of gas dynamic shocks, detonations in chemically reacting gases, and shocks in radiating gases are relevant.

The early theoretical work on gas dynamic shock waves was done by Rankine¹ and Hugoniot.² They derived the jump conditions across the wave and considered the gas dynamic shock structure equations in an inviscid gas with non-zero thermal conductivity. In general, the gas dynamic shock structure equations consist of two coupled non-linear first order differential equations. If either viscosity or thermal conductivity is neglected, one of the equations is algebraic.

Rayleigh³ studied shock structure in a viscid gas with zero thermal conductivity. The solution of the shock structure equations in a viscid-thermal conducting gas was obtained by Gilbarg and Paolucci⁴ using continuum theory and by Wang Chang⁵, Mott-Smith⁶, Zoller⁷ and Grad⁸ using the Boltzmann equation.

Detonations were first observed in 1881 by Berthelot.⁹ Chapman¹⁰ and Jouguet¹¹ studied detonations theoretically, postulating that the gas behind the detonation moved relative to the wave with the speed of sound. Von Neumann¹², Döring¹³, and Zeldovich¹⁴ analyzed the detonation structure problem in 1940 assuming that a detonation wave consists of a gas dynamic shock followed by a deflagration, a wave in which exothermic reactions take place that propagates with subsonic speed. Under this assumption, the shock structure equations include one algebraic equation and one first order non-linear differential equation. Hirschfelder and Curtiss¹⁵, assuming that the gas dynamic shock and deflagration are coupled, solved two simultaneous non-linear differential equations for the detonation structure. Detonations have been studied for many kinds of reacting gas mixtures. For example, Resler and Cary¹⁶ have studied detonations in dissociating air and Petchek and Byron¹⁷ have investigated ionizing shocks in argon.

Radiative shock wave structure has been studied extensively since 1952 when Prokof'ev¹⁸ investigated the case of steady flow with zero viscosity and thermal conductivity, i.e., the "radiation smoothed" case. Heaslet and Baldwin¹⁹ extended earlier work on the "radiation smoothed" shock by considering cases with discontinuous profiles. Marshak²⁰ and Traugott²¹ have included the effects of viscosity and thermal conductivity in their analyses of radiative shock structure. Shocks in optically thick atmospheres have been investigated by Koch²² for a plasma and Scala and Sampson²³ for a chemically reacting gas. Shocks in optically thin atmospheres have been studied by Gross²⁴ for an ordinary gas and by Scala and Sampson²³ for a gas undergoing chemical reactions.

In the present paper, the model of detonation structure that von Neumann used in his study of shocks in chemically reacting gases, is applied to an analysis of detonations in gases capable of undergoing thermonuclear reactions. First, a set of shock structure curves showing the effect of reactions is obtained for detonations in tritium and deuterium-tritium mixtures. We neglect the effects of viscosity and thermal conductivity of the gas and radiative energy loss in this initial treatment. Then, the more complicated problem of a coupled detonation and radiative shock wave

in tritium and deuterium-tritium mixtures is studied. As there are no applied magnetic fields in the problem, bremsstrahlung is the only type of radiation included in the analysis. The gas is assumed to be optically thin to radiation of all frequencies. A set of structure curves, showing the coupled effects of reactions and radiation on the shock structure, is obtained.

CHAPTER II

PHYSICAL AND MATHEMATICAL FORMULATION OF THE PROBLEM

In this chapter the problem of detonation wave structure in gases undergoing thermonuclear reactions will be formulated physically and mathematically. Before writing down the appropriate shock structure equations for thermonuclear shocks (first, assuming no radiation losses, and then including radiation losses), the von Neumann model of detonation structure will be described. A discussion of the physical and mathematical assumptions used to simplify the structure equations will follow.

2.1 Von Neumann Model of Detonation Structure

The model of detonation structure used by von Neumann in his study of shocks in chemically reacting gas mixtures, treats a detonation as a shock followed by a deflagration. The shock wave, which is thin compared to the deflagration that follows it, propagates supersonically into the undisturbed and unreacted gas; the deflagration, inside of which all the reactions occur, propagates subsonically into the gas through which the shock has already travelled.

The changes in pressure, density, speed, temperature and ratio of reaction product density to total density (λ) inside the detonation, viewed in a reference system moving

with the detonation, are depicted schematically in figure 2. Each variable asymptotically approaches its upstream value as x goes to $-\infty$ and its downstream value as x goes to $+\infty$. In the shock wave (points 1 to 2 in figure 2), the gas is compressed, decelerated and heated. In the deflagration (points 2 to 3 in figure 2), the gas, as the reactions proceed, is gradually expanded and accelerated. The temperature, which reaches almost its final value behind the shock, rises to a maximum inside the deflagration and then decreases slightly as the fuel gets used up and the random thermal energy is transferred into bulk kinetic energy of the gas.

The von Neumann model is a valid description of a detonation provided that the characteristic time for reactions to take place, τ_R , is long compared to the time involved in passage of the shock wave (Hirschfelder,²⁵ p. 801). The time for the shock wave to pass in a plasma depends on the ion-ion collision time, τ_c , behind the shock (Von Karman²⁶). Therefore the validity criterion for the von Neumann model is that $\tau_c/\tau_R \ll 1$ behind the gas dynamic shock.

In order to get some physical feeling for the conditions inside thermonuclear shocks, we shall note some typical values of parameters such as temperature, pressure and speed. The initial gas mixture (point 1 on figure 2) is assumed to be fully ionized to avoid the mathematical complications of

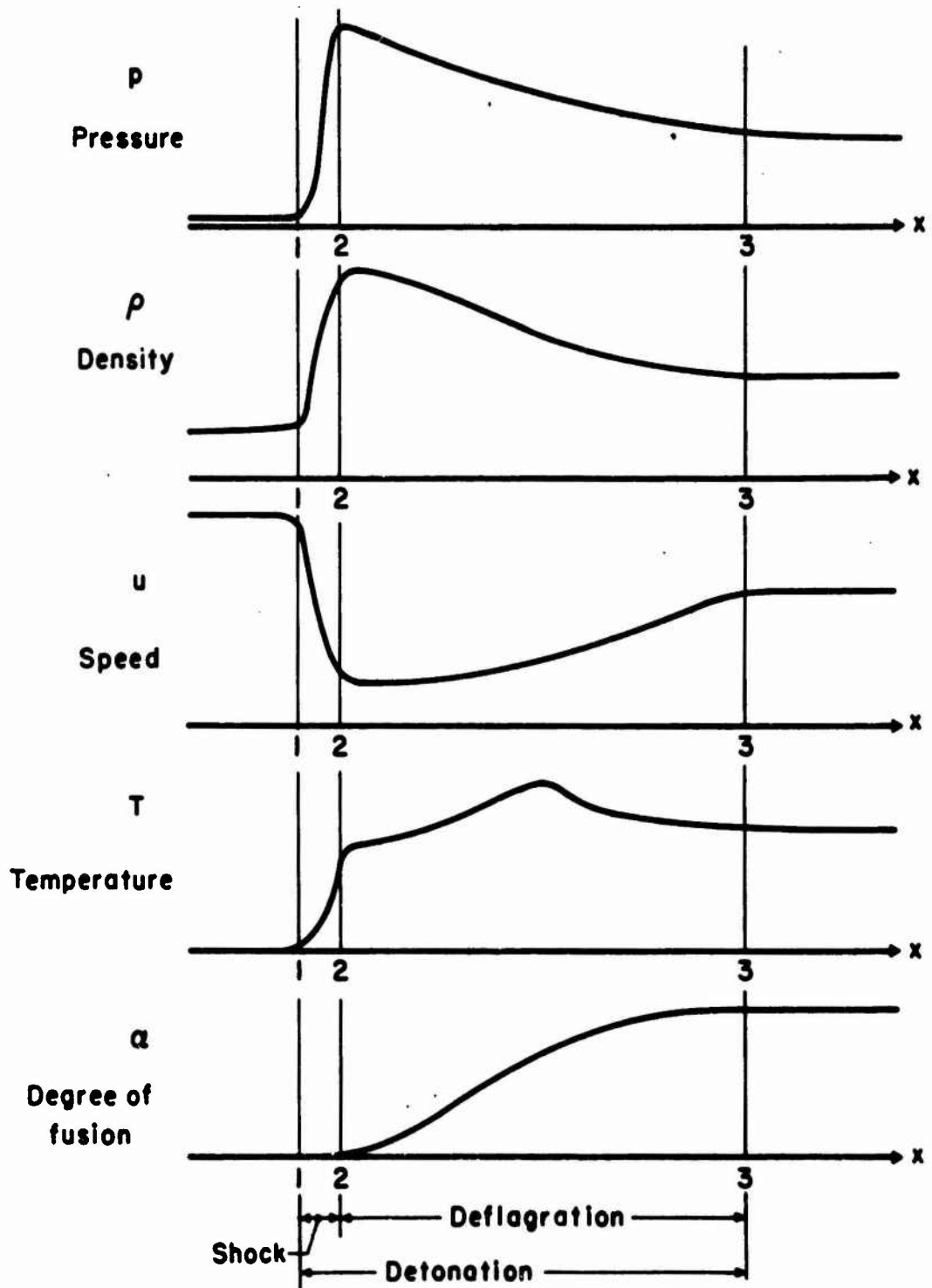


FIG. 2 DETONATION IN A NON-RADIATING GAS ACCORDING TO VON NEUMANN MODEL.

dissociation and ionization. Hydrogen is fully ionized at about 5×10^4 oK (Brezing²⁷). Initial number densities of interest for controlled thermonuclear fusion are $\approx 10^{15} - 10^{16} \text{ cm}^{-3}$ (Glasstone and Lovberg²⁸). The detonation speed, which is also the initial gas speed relative to a reference system moving with the detonation, is about 10^9 cm/sec .

The shock wave heats the gas to a temperature of about 10^{10} oK. Behind it (point 2 on figure 2), number densities have increased by a factor of four and gas speeds have decreased by the same factor (see section 2.3). As the reactions go to completion inside the deflagration wave, the density, speed, pressure and temperature change no more than a factor of two. The characteristic temperatures and number densities behind the deflagration (point 3 on figure 2) are about 10^{10} oK and 10^{15} cm^{-3} respectively.

The temperatures and speeds characteristic of thermonuclear shocks are much higher than those associated with other kinds of strong shock waves. A graph of post-shock temperature vs. wave speed for hydrogen is shown in figure 3. As the wave speed is increased, the gas first becomes dissociated and then ionized. As the wave speed is increased further, radiation processes in the gas become important. The post-shock temperature is given by the Rankine-Hugoniot

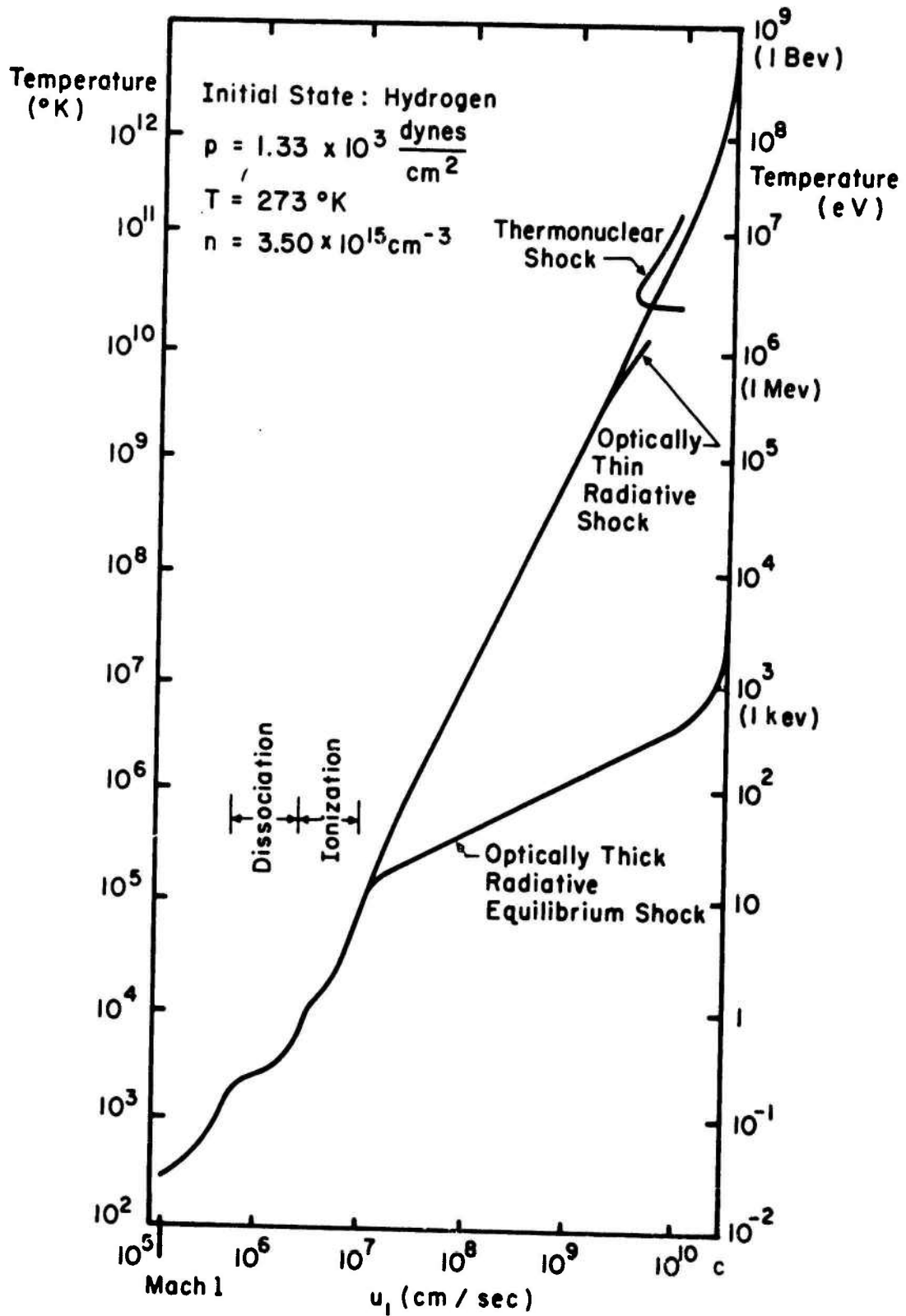


FIG. 3 POST-SHOCK TEMPERATURE vs. WAVE SPEED [GROSS 24]

conditions for a gas dynamic shock. In the dissociation and ionization speed-temperature regimes, the appropriate chemistry has been incorporated into the jump conditions (Taussig²⁹). In optically thick atmospheres, the radiation energy density becomes important compared to the internal energy of the gas for $u_1 > 10^7$ cm/sec (Koch²²). Radiation terms must be included in the jump conditions for such shock speeds. For an optically thin atmosphere, radiation energy losses become important only for shock speeds above 10^9 cm/sec. There are no Rankine-Hugoniot conditions for shocks in optically thin atmospheres because no steady state is established behind the shock. The post-shock temperature shown in figure 3 is the maximum temperature reached in the structure of the shock (Gross²⁴).

The post-shock temperature for thermonuclear shocks is the temperature behind the entire wave, gas dynamic shock plus deflagration. It is given by the set of Rankine-Hugoniot conditions that include the energy released and the change in gas composition due to reactions (see section 2.3). The lowest detonation speed which satisfies these Rankine-Hugoniot conditions is called the Chapman-Jouguet speed. If the detonation travels with the Chapman-Jouguet speed, the downstream flow is sonic. For speeds greater than the C-J speed, there are two solutions to the Rankine-

Hugoniot conditions. The upper branch, a strong detonation, has subsonic flow behind it; the lower branch, a weak detonation, has supersonic flow behind it (Hayes³⁰). A graph of post-shock temperature as a function of wave speed for deuterium is shown in the figure 3. Deuterium and tritium fusion reactions have much larger cross sections than hydrogen fusion reactions and are therefore of greater interest in problems of controlled thermonuclear fusion (Taylor and Tobolsky³¹).

2.2 Physical and Mathematical Assumptions

The physics to be described in a complete treatment of a thermonuclear shock structure problem includes (1) reactions, (2) radiation, (3) transport processes, (4) non-equilibrium effects due to the multi-component nature of gas, and (5) the effects of applied electromagnetic fields. Reactions occur in the gas which has been shock heated. Some of the energy added to the gas by reactions is lost through radiation. Transport processes due to the viscosity and thermal conductivity of the gas account for the bulk flow of momentum and energy. Since the gas is a mixture of several kinds of ions and electrons, non-equilibrium processes (e.g., diffusion, charge separation, and energy and momentum transfer between species) occur. External magnetic

fields, necessary to contain a thermonuclear plasma in order to tap its energy, further complicate the physics by adding cyclotron radiation and hydromagnetic effects.

A mathematical treatment of thermonuclear shock structure including all the relevant physics would require the solution of the set of non-linear differential equations that result from a coupling of the many species Boltzmann or continuum equations with the radiative transfer equation and Maxwell's equations. To reduce the number of differential equations in the problem to a manageable set, some of the physical effects must be ignored. The present treatment will include reactions and radiation while neglecting transport phenomena, non-equilibrium effects due to the presence of more than one species, and the containment problem. The many species nature of the gas is incorporated in the state and continuity equations only.

A list of assumptions used in the treatment of thermonuclear shock structure without radiation in tritium and deuterium-tritium mixtures is given below. It is followed by a discussion of their physical validity. The further assumptions that must be made when radiation is included in the problem are then listed and discussed.

PHYSICAL ASSUMPTIONS FOR THERMONUCLEAR SHOCK STRUCTURE

1. The von Neumann model of detonations is valid:

the shock wave is thin compared to the deflagration wave; all reactions take place in the deflagration region. Since the influence of reactions on the detonation structure is of primary interest, the shock is treated as a discontinuity and only the deflagration structure is studied.

2. Transport phenomena due to viscosity and thermal conductivity are negligible in the deflagration.
3. Non-equilibrium effects due to the presence of more than one species are negligible: All species travel with the local gas speed; the particles of each species have a Maxwellian distribution of energies at the local gas temperature; charge separation is negligible.
4. One-dimensional, single fluid, continuum equations provide an adequate description of the phenomena.
5. All macroscopic velocities and temperatures are low enough so that relativistic effects can be neglected.
6. There are no applied electromagnetic fields.

Assumptions 1, 2 and 3 were made in order to simplify both the mathematics and the physics of the thermonuclear shock structure problem. Their physical validity depends on the ratios of characteristic collision and reaction times

for typical temperatures and number densities inside thermonuclear shocks.

Spitzer³² defines the following characteristic times for a plasma: The time required for a single species, non-Maxwellian distribution to approach the Maxwellian distribution is

$$\tau_c = \frac{11.4 A^{\frac{1}{2}} T^{\frac{3}{2}} (\text{OK})}{n(\text{cm}^{-3}) Z^4 \ln \Delta} \text{ sec}, \quad (2.1)$$

where Z is the atomic number of the ion, A is its atomic weight, and

$$\Delta = \frac{3}{2 Z^2 e^3} \left(\frac{k^3 T^3}{\pi n_e} \right)^{\frac{1}{2}}. \quad (2.2)$$

The self collision time for electrons, τ_{ce} , is just τ_c with $A_e = 1/1836$, the atomic weight of electrons. The rate at which equipartition of energy between two groups of particles is established is

$$\tau_{eq} = 5.87 \frac{A_1 A_2}{n_2 Z_1^2 Z_2^2 \ln \Delta} \left(\frac{T_1}{A_1} + \frac{T_2}{A_2} \right)^{\frac{3}{2}} \text{ sec}. \quad (2.3)$$

If the two groups are ions and electrons, and if $T_1 \approx T_2$, then

$$\tau_{eq} = 5.87 \frac{A}{A_e^{\frac{1}{2}}} \frac{T^{\frac{3}{2}} (\text{OK})}{n Z^2 \ln \Delta} \text{ sec}. \quad (2.4)$$

The time associated with viscous processes, which is what von Karman²⁶ calls the characteristic time associated with thermodynamic transformations, is the ion-ion collision time. The time associated with thermal conduction processes is the ion-electron collision time. Another relevant characteristic time is the mean time between reactions

$$\tau_R = \frac{1}{n \langle \sigma v \rangle}, \quad (2.5)$$

where $\langle \sigma v \rangle$ is the reaction cross section times the relative speed of the interacting particles averaged over the product of their distribution functions (Osborn³⁵).

The ratios of the collision times, τ_c , τ_{ce} , τ_{eq} are independent of temperature and number density. For a tritium plasma ($A = 3$),

$$\frac{\tau_c}{\tau_{ce}} = 74.3 \quad \text{and} \quad \frac{\tau_{eq}}{\tau_c} = 38.2.$$

Ratios of collision times to the reaction time must be evaluated separately for each temperature and number density of interest. For $n = 10^{15} \text{ cm}^{-3}$ and $10^9 \text{ }^\circ\text{K} < T < 10^{10} \text{ }^\circ\text{K}$, $\ln \Lambda$ (which is not a very sensitive function of temperature and number density) ≈ 21 . The values of τ_{eq}/τ_R and τ_c/τ_R (with $A = 3$) are given in Table 1 for several temperatures in this range.

T (°K)	$\langle TV \rangle \left(\frac{\text{cm}^3}{\text{sec}} \right)$	$\tau_{\text{eq}}/\tau_{\text{R}}$	$\tau_{\text{c}}/\tau_{\text{R}}$
1×10^9	2×10^{-17}	0.02	0.0006
5×10^9	8×10^{-17}	1.02	0.027
1×10^{10}	1×10^{-16}	3.8	0.11
2×10^{10}	3×10^{-16}	30.5	0.79

TABLE 1. Ratios of Characteristic Times

The shock region is thin compared to the deflagration region (assumption 1) if $\tau_{\text{c}}/\tau_{\text{R}} \ll 1$ behind the shock. For a tritium plasma the temperature inside the shock rises from its downstream value, 5×10^4 °K, to 10^{10} °K before any reactions take place. However, as the temperature approaches its post-shock value, ion-ion collision times and reaction times become comparable. Therefore the reactions may not be completely confined to the deflagration wave; some may take place in the tail of the shock.

Viscosity is negligible inside the deflagration (assumption 2) if $\tau_{\text{c}}/\tau_{\text{R}} \ll 1$ for typical temperatures and number densities. The requirement for neglecting thermal conduction and diffusion is that $(\tau_{\text{c}}/\tau_{\text{R}}) \left(1/M^2 \right) \ll 1$ (von Karman²⁶).

M is the Mach number, the ratio of the local gas speed to the local sound speed:

$$M = \left(\frac{u^2}{\gamma \frac{R}{W} T} \right)^{\frac{1}{2}}. \quad (2.6)$$

γ , the ratio of specific heats at constant pressure to that at constant volume, has the value 5/3 for a plasma, a mixture of monatomic gases. It can be shown (see section 2.3) that inside the deflagration,

$$\frac{1}{5} \leq M^2 \leq 1.$$

Since $(\tau_c / \tau_R) (1/M^2) \geq 1$ inside the deflagration, the effects of viscosity, thermal conduction and diffusion would have to be included in a fuller treatment.

The requirement for the ions and electrons to be in thermal equilibrium (assumption 3) is that $\tau_{eq} / \tau_R \ll 1$ inside the deflagration. The reaction product ions are released with Mev energies. The electrons, since they are not involved in reactions, are cooler than the ions. Although reaction product ions transfer energy to fuel ions in a time comparable to the reaction time, energy transfer from the hot ions to the cooler electrons occurs much more slowly. (For $T = 2 \times 10^{10}$ oK, $\tau_c / \tau_R \approx 0.8$ while $\tau_{eq} / \tau_R \approx 30$).

The neutrons released in reactions, (which we assume are

kept in the gas), must be in equilibrium with the ions and electrons for the gas to be in thermal equilibrium. Cross sections for neutron-triton scattering, τ_N , are ≈ 1 barn for Mev neutron energies (Hughes and Schwartz³³). A 10 Mev neutron goes through 2-5 collisions before its energy reaches 2 Mev (Glasstone³⁴). The neutron collision time, $\tau_{cN} \approx (\text{number of collisions to thermalize}) \times 1/(n\tau_N\bar{v}_N)$. For $T=10^{10}$ oK, \bar{v}_N is 10^9 cm/sec. Therefore the ratio of the neutron-ion collision time to the ion-ion time, τ_{cN}/τ_c is ≈ 1 , and the neutrons thermalize with the ions in a time comparable to the ion-ion collision time. Equilibration times for neutrons and electrons, however, are much larger than those for neutrons and ions since neutron-electron collision cross sections are very small. The neutrons, like the ions, are therefore not in equilibrium with the electrons.

The gas has local charge neutrality if the electron Plasma frequency,

$$\omega_p = \left(\frac{4\pi n_e e^2}{m_e} \right)^{\frac{1}{2}} \quad (2.7)$$

(Spitzer³²) is much larger than the frequency associated with the shock wave, $\omega_R = 2\pi/\tau_R$. For the typical temperatures and number densities mentioned previously,

$$\frac{\omega_P}{\omega_R} \approx 10^{12} .$$

Therefore the assumption of charge neutrality is a good one.

One-dimensional, single fluid, continuum equations (assumption 4) have been used in many studies of shock structure (e.g. Gilbarg and Paolucci⁴ and Koch²²). A discussion of the use of continuum fluid equations rather than the Boltzmann equation is given by Gilbarg and Paolucci⁴ and by Gross.²⁴ Treatment of the ions, neutrons and electrons as a single fluid neglects the lack of thermal equilibrium between the electrons and the ions and neutrons. If the electrons are assumed to be as hot as the ions and neutrons, a significant fraction of them would have relativistic energies. The non-relativistic equations are valid (assumption 5) if $kT \ll mc^2$ for each species. (mc^2 for electrons is $\approx \frac{1}{2}$ Mev.) The use of non-relativistic equations is justified physically, however, since the electrons are actually cooler than the ions and neutrons.

The following physical assumptions are made in addition to those listed previously when radiation is included in the thermonuclear shock structure problem:

7. Radiation effects are significant in the deflagration region only.

8. The gas is optically thin to radiation of all frequencies.
9. The radiation comes from ion-electron bremsstrahlung only.

Since the von Neumann model of detonations is assumed, the effects of radiation are studied in the deflagration region only. In figure 3, it is seen that for thermonuclear shock speeds, the maximum temperature behind an optically thin shock is only slightly lower than the temperature behind a non-radiative gas dynamic shock. Therefore assumption 7 is valid.

A gas is optically thin to radiation if the photon absorption mean free path, λ_p^ν , for all frequencies, ν , is much larger than all the other characteristic lengths in the problem. The reaction mean free path is the largest characteristic length for non-radiative thermonuclear shocks. Therefore the gas is optically thin if $\lambda_p^\nu \gg \lambda_R$ for all frequencies. (For $T = 10^{10}$ OK and $n = 10^{15}$ cm⁻³, λ_R is $\approx 10^9$ cm). The only type of radiation occurring in a fully ionized plasma in the absence of magnetic fields is bremsstrahlung. Since non-relativistic equations are used, only ion-electron bremsstrahlung is considered; electron-electron bremsstrahlung is neglected. An approximate expression for the mean free path for absorption of a photon by a hydrogen

isotope plasma, as the result of a free-free transition, is (Glasstone and Lovberg²⁸),

$$\lambda_p^{\nu} \approx 7 \times 10^{-5} \frac{T^{\frac{1}{2}} \text{ (kev)}}{n^2} \nu^3 \text{ cm.} \quad (2.8)$$

The power emitted per unit wavelength per unit volume due to ion-electron bremsstrahlung (Glasstone and Lovberg²⁸) is

$$\frac{dP}{d\lambda} \approx 6.01 \times 10^{-23} n_e \sum_i (n_i Z^2) T^{-\frac{1}{2}} \lambda^{-2} \exp\left(-\frac{12.4}{\lambda T}\right) \frac{\text{ergs}}{\text{cm}^3 \text{ \AA-sec}}. \quad (2.9)$$

The maximum value of $\frac{dP}{d\lambda}$ occurs for

$$\lambda = \frac{6.2}{T \text{ (kev)}} \text{ \AA}. \quad (2.10)$$

For $T = 1 \text{ Mev}$, λ_{max} is $6.2 \times 10^{-3} \text{ \AA}$ ($\nu_{\text{max}} \approx 5 \times 10^{20} \text{ cps}$).

The photon absorption mean free path for this temperature and frequency is $\approx 10^{29} \text{ cm}$, which is much larger than the reaction mean free path. The smallest frequency for which λ_p^{ν} is $\gg \lambda_R$ is $\nu \approx 10^{15} \text{ cps}$ ($\lambda = 3 \times 10^3 \text{ \AA}$). The ratio of the power emitted at a frequency of 10^{15} cps to that emitted at a frequency of $5 \times 10^{20} \text{ cps}$ is $\approx 3 \times 10^{-11}$. Therefore the fraction of radiation energy emitted at frequencies for which the gas is not optically thin, is negligible. It is, therefore, a good assumption to treat

the gas as an optically thin atmosphere.

2.3 Shock Structure Equations Without Radiation

The following are the time-dependent continuum fluid conservation equations for the deflagration wave (von Karman²⁶):

The continuity equation for the i^{th} specie is

$$\frac{\partial n_i}{\partial t} + \frac{\partial}{\partial x} (n_i u) = W_i, \quad i = 1, 2, \dots, N, \quad (2.11)$$

where N is the number of species in the mixture, and W_i is the production rate of the i^{th} species (see section 2.4).

Multiplying each continuity equation by m_i and summing over all species, one obtains the mass flow equation,

$$\frac{\partial \rho}{\partial t} + \frac{\partial}{\partial x} (\rho u) = \sum_i m_i W_i, \quad (2.12)$$

where $\rho = \sum_i n_i m_i$. (2.13)

If no particles (e.g., neutrons) escape from the gas, and if negligible mass is lost or created in reactions, then

$$\sum_i m_i W_i = 0. \quad \text{The mass, } \Delta m, \text{ lost in a nuclear reaction is}$$

$$\Delta m = (m_1 + m_2) - (m_3 + m_4), \quad (2.14)$$

where m_1 and m_2 are the masses of the reacting nuclei and m_3 and m_4 the masses of the product nuclei (Evans³⁶). If $\Delta m / (m_1 + m_2)$ is $\ll 1$, the mass lost in reactions can be

neglected in the mass equation. For thermonuclear reactions, $\Delta m / (m_1 + m_2)$ is $\ll 0.01$, so mass is conserved to a high degree of accuracy.

A momentum flow equation for each species in the mixture, analogous to the species continuity equations for mass flow, can also be written down. The momentum flow equation for the mixture is obtained by summation of the species momentum equations. If the viscosity and thermal conductivity of the mixture and the diffusion of the species are neglected, the momentum flow equation for the mixture is,

$$\frac{\partial}{\partial t} (\rho u) + \frac{\partial}{\partial x} (\rho u^2) = - \frac{\partial p}{\partial x}, \quad (2.15)$$

$$\text{where } p = \sum_i n_i k T. \quad (2.16)$$

The energy flow equation for the mixture, which is derived by summing the energy equations for all the species, is

$$\frac{\partial}{\partial t} (\rho (e + \frac{u^2}{2}) - q_{TN}) + \frac{\partial}{\partial x} (\rho u (e + \frac{u^2}{2}) - q_{TN}) = - \frac{\partial}{\partial x} (\rho u), \quad (2.17)$$

where e is the internal energy of the mixture, and q_{TN} is a volume energy source due to thermonuclear reactions.

If the shock is viewed from a coordinate system moving with the shock speed, all time derivatives in the continuity, mass, momentum and energy equations vanish. If the resulting time-independent equations are integrated once with respect to the spatial variable, x , they become

$$\rho u = A, \quad (2.18)$$

$$p + \rho u^2 = B, \quad (2.19)$$

$$\text{and} \quad h + \frac{u^2}{2} - q_{\text{TN}} = C, \quad (2.20)$$

where $h = pu + e = \frac{\gamma}{\gamma-1} \frac{R}{W} T$ is the enthalpy of the gas (which is assumed to be ideal).

The constants of integration, A, B, and C, evaluated from the steady state conditions upstream and downstream from the shock (see figure 2), are

$$A = \rho_1 u_1 = \rho_3 u_3, \quad (2.21)$$

$$B = p_1 + \rho_1 u_1^2 = p_3 + \rho_3 u_3^2, \quad (2.22)$$

$$\text{and} \quad C = h_1 + \frac{u_1^2}{2} = h_3 + \frac{u_3^2}{2} - Q. \quad (2.23)$$

In state 1 the reactions have not begun so $q_{\text{TN}} = 0$. The reactions have gone to completion in state 3 so $q_{\text{TN}} = Q$, the energy released per unit mass of the initial mixture if it reacts completely.

Thermonuclear shocks are very strong shocks, i.e., $p_1 \ll \rho_1 u_1^2$. The Rankine-Hugoniot conditions for a thermonuclear shock follow from equations (2.21), (2.22), (2.23) and the assumption of a strong shock. The ratio of the gas speed behind the thermonuclear shock to the gas speed ahead of the thermonuclear shock, (the shock speed), is

$$\frac{u_3}{u_1} = \frac{f_1}{f_3} = \frac{\gamma}{\gamma+1} \pm \frac{(1 - 2(\gamma^2 - 1) Q/u_1^2)^{\frac{1}{2}}}{\gamma + 1}, \quad (2.24)$$

where $\gamma = \frac{5}{3}$.

The minimum shock speed that satisfies equation (2.24), the Chapman-Jouguet speed, is

$$u_1 = (2(\gamma^2 - 1) Q)^{\frac{1}{2}}. \quad (2.25)$$

For C-J flow conditions, equation (2.24) reduces to

$$\frac{u_3}{u_1} = \frac{\gamma}{\gamma+1} = \frac{5}{8}. \quad (2.26)$$

The ratio of the gas speeds behind the gas dynamic shock to that in front of it, $\frac{u_2}{u_1}$, is given by equation (2.24) with $Q = 0$.

The two values of $\frac{u_2}{u_1}$ that satisfy equation (2.24) with $Q = 0$ are

$$\frac{u_2}{u_1} = \frac{\gamma-1}{\gamma+1} = \frac{1}{4} \quad \text{and} \quad \frac{u_2}{u_1} = 1. \quad (2.27)$$

One feature of thermonuclear shocks is that the temperature of the gas behind the thermonuclear shock, T_3 , is independent of the initial temperature of the gas. T_3 is related to the energy released in reactions, Q , and the shock speed, u_1 , by

$$\frac{R}{W_3} T_3 = 2 \frac{\gamma-1}{\gamma+1} Q + \left(\frac{\gamma-1}{\gamma+1} \right)^2 u_1^2 \left[1 \pm \sqrt{1 - 2(\gamma^2 - 1) \frac{Q}{u_1^2}} \right]. \quad (2.28)$$

$$\text{For C-J flow, } \frac{R}{W_3} T_3 = 2 \left(\frac{\gamma-1}{\gamma+1} \right) \gamma Q = \frac{5}{6} Q. \quad (2.29)$$

The temperature of the gas behind the gas dynamic shock, T_2 , is given by equation (2.28) with $Q = 0$, i.e.,

$$\frac{R}{W_2} T_2 = \frac{2(\gamma-1)}{(\gamma+1)^2} u_1^2. \quad (2.30)$$

If the shock is propagating with the C-J speed,

$$\frac{R}{W_2} T_2 = 4 \frac{(\gamma-1)^2}{\gamma+1} Q = \frac{2}{3} Q. \quad (2.31)$$

The temperature behind the gas dynamic shock, T_2 , and that behind the thermonuclear shock, T_3 , are plotted as functions of the shock speed in figure 4. The gas is assumed to be a deuterium-tritium mixture containing equal numbers of tritium and deuterium ions. The C-J speed for the mixture is 3.48×10^9 cm/sec corresponding to a post-detonation temperature of 4.2×10^{10} °K. T_3 is higher than T_2 for all shock speeds. The increase in specific enthalpy across the deflagration is accompanied by an increase in temperature, since the mean molecular weight of the mixture remains constant as the reactions occur.

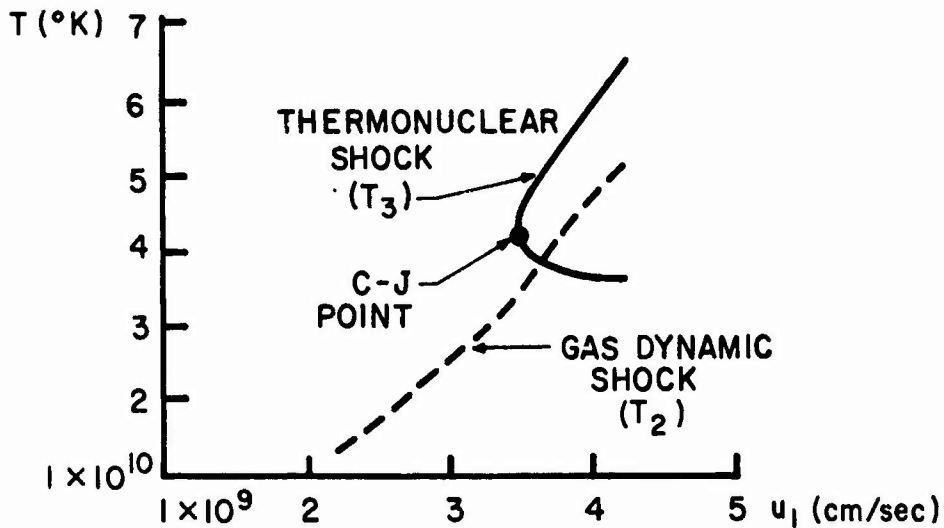


FIG. 4 POST-SHOCK AND POST DETONATION TEMPERATURE VS. DETONATION SPEED FOR DEUTERIUM-TRITIUM MIXTURE (1:1)

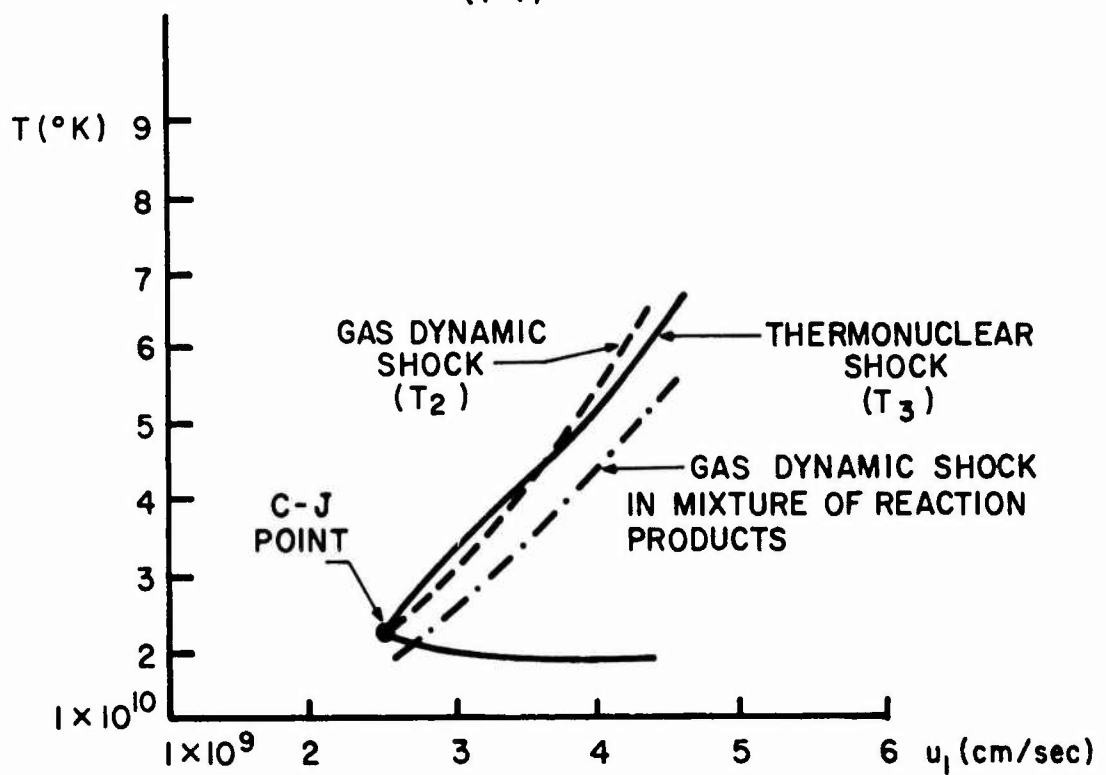


FIG. 5 POST-SHOCK AND POST-DETONATION TEMPERATURE VS. DETONATION SPEED FOR TRITIUM

The temperatures behind the gas dynamic and thermonuclear shocks as a function of shock speed for a tritium gas are shown in figure 5. The C-J speed is 2.55×10^9 cm/sec, creating a temperature of 2.2×10^{10} °K behind the thermonuclear shock. The temperature behind the deflagration (thermonuclear shock) is equal to the temperature behind the gas dynamic shock for shocks propagating with the C-J speed. T_3 is $\sim T_2$ for shocks propagating with speeds between the C-J speed and 3.4×10^9 cm/sec. If the shock speed is increased further, the temperature behind the deflagration will be lower than that behind the gas dynamic shock. An increase in the enthalpy of the gas as the reactions occur does not necessarily show up in increased temperatures, as the mean molecular weight of the mixture decreases with reactions. The temperature behind a gas dynamic shock propagating in a gas containing the reaction products of tritium fusion reactions, (alpha particles and neutrons in a 1:2 ratio by number), is also shown in figure 4 for comparison.

2.4 Reaction Rates

The source terms, W_i , in the species continuity equations, must be specified in order to solve the non-radiative shock structure equations across the deflagration. These functions

are related by the requirement for mass conservation,

$\sum_i m_i W_i = 0$. It can be shown that they all depend on the reaction rates for the fusion reactions taking place in the plasma.

The reaction rate for binary nuclear reactions is

$$W = \frac{n_1 n_2}{1 + \delta_{A_1 A_2}} \langle \tau v \rangle, \quad (2.32)$$

where n_1 and n_2 are the number densities of the interacting nuclei and where the Kronecker- δ takes into account the possibility that the reacting particles are of the same kind ($A_1 = A_2$). If each species has a Maxwellian distribution of velocities at the same temperature, the reaction probability $\langle \tau v \rangle$ is given by (Glasstone and Lovberg²⁸)

$$\langle \tau v \rangle = \frac{4}{\pi^{1/2}} \left(\frac{\mu}{2 kT} \right)^{3/2} \int_0^{\infty} \tau v \exp \left(- \frac{\mu v^2}{2 kT} \right) v^2 dv, \quad (2.33)$$

where $\mu = \frac{m_1 m_2}{m_1 + m_2}$ is the reduced mass of the system,

τ = cross section for binary nuclear reactions, and

v = relative speed of the interacting nuclei.

It is convenient to express $\langle \tau v \rangle$ as an integral over center-of-mass energy, E_{cm} . Since

$$E_{cm} = \frac{1}{2} \mu v^2, \quad (2.34)$$

the reaction probability can be written,

$$\langle \sigma v \rangle = \frac{8\pi}{\mu^{\frac{3}{2}}} \left(\frac{1}{2\pi kT} \right)^{\frac{3}{2}} \int_0^{\infty} \sigma(E_{cm}) \exp\left(-\frac{E_{cm}}{kT}\right) E_{cm} dE_{cm}. \quad (2.35)$$

Nuclear reactions are studied in the laboratory by sending beams of nuclear projectiles toward a target. Therefore nuclear reaction cross sections are usually given as a function of the laboratory energy of the incident particle E_L . If the target nuclei are in motion, as in a plasma, E_L is the relative energy of the interacting nuclei. With the relation between E_L and E_{cm} ,

$$E_L = \frac{m}{\mu} E_{cm}, \quad (2.36)$$

the reaction probability, written in terms of E_L , is

$$\langle \sigma v \rangle = \frac{8\pi}{m^2} \left(\frac{\mu}{2\pi kT} \right)^{\frac{3}{2}} \int_0^{\infty} \sigma(E_L) \exp\left(-\frac{\mu}{m} \frac{E_L}{kT}\right) E_L dE_L. \quad (2.37)$$

A reaction mean free path, λ_R , a mean reaction time, τ_R , and a reaction power density can be defined in terms of $\langle \sigma v \rangle$. If we let

$$\tau_R = \frac{1}{n \langle \sigma v \rangle}, \quad (2.38)$$

the reaction mean free path is defined as

$$\lambda_R = \langle v \rangle \tau_R, \quad (2.39)$$

where $\langle v \rangle = \left(\frac{8 kT}{\mu \pi} \right)^{\frac{1}{2}}$, for a Maxwellian velocity distribution. (2.40)

The power density is just the reaction rate multiplied by the energy released per reaction,

$$P_{TN} = \frac{n_1 n_2}{1 + \frac{c}{A_1 A_2}} \langle v \rangle Q_R, \quad (2.41)$$

where $Q_R = (\Delta m) c^2$.

2.5 Shock Structure Equations With Radiation

No steady state is established behind thermonuclear shocks propagating in a gas that is losing energy through radiation. Therefore, there are no Rankine-Hugoniot conditions which determine the post-shock state of the gas given its initial state. Since no steady state is established behind the shock, it is not obvious for the radiative case that a reference frame travelling with the shock speed is one in which all time derivatives in the structure equations vanish.

A physical argument can be used to show that the shock frame is a steady reference frame for shocks in optically thin atmospheres. It is apparent that successive particles of gas, passing through the shock, go through the same history in any region containing the shock that is much thinner than a photon absorption mean free path. The profiles of the

flow variables, viewed in the shock frame, are therefore steady throughout such a region. Thus, we can validly set time derivatives equal to zero in the structure equations if we limit the integration of these equations to a region containing the shock that is much thinner than a photon absorption mean free path. (The structure equations may be integrated over all space for thermonuclear shocks in a non-radiating gas.)

All of the non-radiative thermonuclear shock structure equations are valid for thermonuclear shocks in optically thin atmospheres except the energy equation. The radiation pressure in the radiative momentum equation and the energy density term in the energy equation are negligible because all of the radiation is assumed to escape from the gas. The only radiative term in the energy equation is $\frac{dq}{dx}$, the divergence of the radiative flux, (Vincenti and Kruger³⁷). The energy flow equation with radiation for thermonuclear shocks in an optically thin atmosphere is

$$\frac{d}{dx} \left(\rho u \left(h + \frac{u^2}{2} - q_{TN} \right) \right) + \frac{dq}{dx} = 0. \quad (2.42)$$

If equation (2.42) is integrated over all space and then divided by the mass flow constant, $\rho u = A$, then

$$h + \frac{u^2}{2} - q_{\text{TN}} + \frac{1}{A} \int_0^x \frac{dq}{dx'} dx' = c. \quad (2.43)$$

An expression for $\frac{dq}{dx}$ can be obtained from the radiative transfer equation,

$$\mu \frac{dI_v}{dx} = \rho (j_v - K_v I_v), \quad (2.44)$$

where I_v is the radiative intensity, μ is the cosine of the angle between the x-axis and the direction of observation of I_v , ρj_v is the volumetric emission coefficient, and ρK_v is the volumetric absorption coefficient (Goulard³⁸). For an optically thin gas, emission processes are more important than absorption processes so $\rho j_v \gg \rho K_v I_v$ (Vincenti and Kruger³⁷). The radiative transfer equation thus becomes,

$$\mu \frac{dI_v}{dx} = \rho j_v. \quad (2.45)$$

If it is integrated over all frequency and solid angle, assuming that the emission is isotropic, we get an expression for $\frac{dq}{dx}$,

$$\frac{dq}{dx} = 4\pi \int_0^\infty \rho j_v dv, \quad (2.46)$$

where $q = 2\pi \int_{-1}^1 \int_0^\infty \mu I_v d\mu dv. \quad (2.47)$

An expression for the volumetric emission coefficient, ρj_ν , must be obtained in order to evaluate the integral in equation (2.46). Since there are no magnetic fields and hence no cyclotron radiation, and since recombination of atoms is negligible at thermonuclear temperatures, the only non-negligible radiative process is ion-electron bremsstrahlung. Therefore the volumetric emission coefficient is just the power due to bremsstrahlung per unit volume per unit solid angle per unit frequency, which can be obtained from equation (2.9) by changing variables from wavelength to frequency. If the resulting volumetric emission coefficient is integrated over all frequency and solid angle, (assuming isotropic emission), one obtains an expression for the power per unit volume due to bremsstrahlung of all frequencies, P_{BR} (Glasstone and Lovberg²⁸):

$$P_{BR} = 1.57 \times 10^{-27} n_e \sum_i (n_i Z^2) T_i^{3/2} \text{ (OK) } \frac{\text{erg}}{\text{cm}^3 \text{ sec}} . \quad (2.48)$$

The radiation term in equation (2.43) is just $\frac{1}{A} \int_0^x P_{BR} dx'$.

In summary, the shock structure equations for a radiative thermonuclear shock in an optically thin atmosphere are

$$\rho u = A , \quad (2.18)$$

$$p + \rho u^2 = B, \quad (2.19)$$

$$h + \frac{u^2}{2} - q_{\text{TN}} + \frac{1}{A} \int_c^x P_{\text{BR}} dx' = C, \quad (2.49)$$

$$p = \rho \frac{R}{W} T, \quad (2.50)$$

$$\text{and } \frac{d}{dx} (n_i u) = W_i, \quad i = 1, 2, \dots, N, \quad (2.51)$$

where A, B, and C are defined by equations (2.21), (2.22), and (2.23) and where the expression for P_{BR} is given by equation (2.48). The remaining undefined quantities, the thermonuclear energy release term, q_{TN} , and the rate functions, W_i , depend on the specific nuclear chemistry and will be discussed in the next chapter.

The shock structure equations have now been developed as far as possible without reference to a particular reacting gas mixture. In the next chapter, the nuclear chemistry appropriate to three different reacting gas mixtures, will be discussed and incorporated into the equations.

CHAPTER III

THERMONUCLEAR SHOCK STRUCTURE EQUATIONS FOR THREE DIFFERENT
CASES

The general set of radiative thermonuclear shock structure equations derived in Chapter II will now be developed to apply to thermonuclear shocks in (1) deuterium-tritium gas mixtures with equal numbers of deuterium and tritium ions, (2) a pure tritium gas, and (3) hydrogen-tritium gas mixtures. The three cases will be discussed in succession. After an examination of the properties and cross sections of the nuclear reactions occurring in the gas mixture, the equations that govern reaction kinetics will be derived. The particular set of shock structure equations for the gas mixture will then be put into a convenient dimensionless form.

3.1 Fusion Reactions in Deuterium-Tritium Mixtures

The following reactions occur in deuterium-tritium gas mixtures (Wandel, Hesselberg Jensen and Kofoed-Hansen³⁹)

1. $D + D \rightarrow T + p,$
2. $D + D \rightarrow He^3 + n,$
3. $T + D \rightarrow He^4 + n,$
4. $He^3 + D \rightarrow He^4 + p,$

5. $T + T \rightarrow He^4 + 2n,$
6. $He^3 + He^3 \rightarrow He^4 + 2p,$
7. $T + He^3 \rightarrow He^4 + p + n.$

Reactions 5 through 7 have smaller cross sections at most energies than reactions 1 through 4 and are usually neglected in the treatment of thermonuclear problems. A graph of the cross sections for reactions 1 through 4 for deuteron energies up to 1 Mev is shown in figure 6.

The kinetics of deuterium reactions (reactions 1 through 4) are complicated because deuterium reacts with its reaction products, tritium and helium-3. Furthermore neutrons and protons are both intermediate and end products. Although problems involving the full set of deuterium reaction kinetics equations have been solved, it is considerably more difficult to deal with a coupled set of fluid and kinetics equations for deuterium.

It has been assumed, in the treatment of the thermonuclear shock structure in a deuterium-tritium mixture with equal numbers of deuterium and tritium ions, that only the $T(d,n) He^4$, (T-D), reaction occurs. This assumption is well justified for temperatures below 100 kev as reaction probabilities for T-D reactions are 100 times greater than those for the D-D reactions and 10 times greater than that

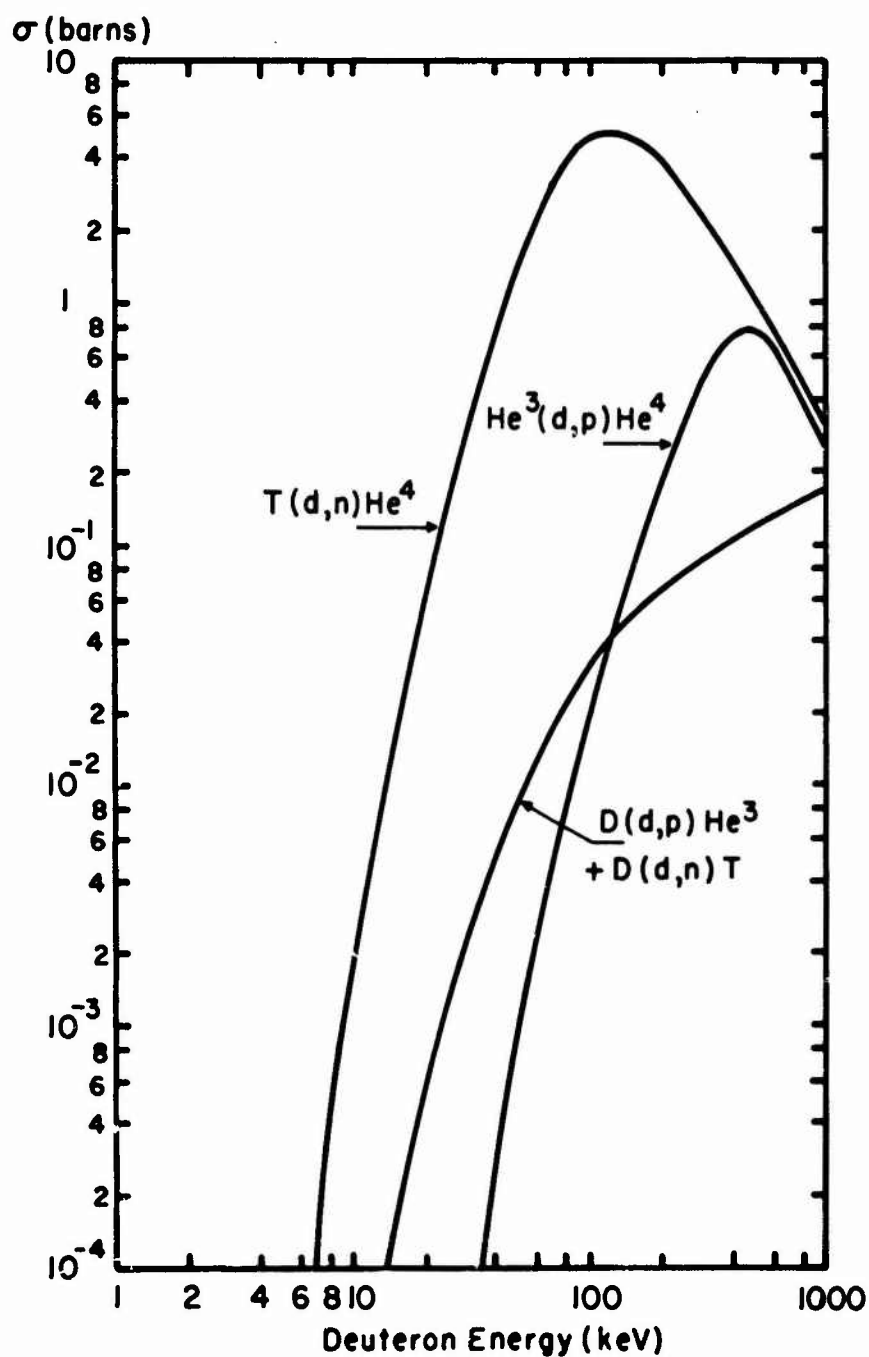


FIG. 6 CROSS SECTION FOR DEUTERIUM FUSION REACTIONS
[GLASSTONE AND LOVBERG²⁸]

for the reaction $\text{He}^3 (d,p) \text{He}^4$, $(\text{He}^3 - D)$, (see figure 7).

For Mev temperatures, the reaction probabilities for the three reactions are comparable. However, since reaction rates depend both on reaction probabilities and the products of number densities of the reacting nuclei,

$(W \equiv n_1 n_2 \langle \sigma v \rangle)$, $\text{He}^3 - D$ reactions can be neglected because of the small He^3 number densities. The ratio of the reaction rates for T-D and D-D reactions, assuming they have the same probability is

$$\frac{W_{TD}}{W_{DD}} \approx \frac{2n_T}{n_D} .$$

The triton population is enriched at the expense of the deuteron population as tritons are born in D-D reactions, so as the reactions proceed, the T-D reaction becomes more important than the D-D reaction.

The T-D reaction cross section has a wide resonance whose peak is at 0.107 Mev laboratory energy (see figure 8). The lifetime of the associated state is 2-3 times the natural nuclear lifetime, the time for a deuteron to traverse a tritium nucleus (Kaplan⁴⁰). The main reaction mechanism at these energies is formation of a He^5 compound nucleus which decays into a neutron and alpha particle. At higher energies, stripping reactions dominate; an alpha particle and neutron are formed directly when the deuteron strips

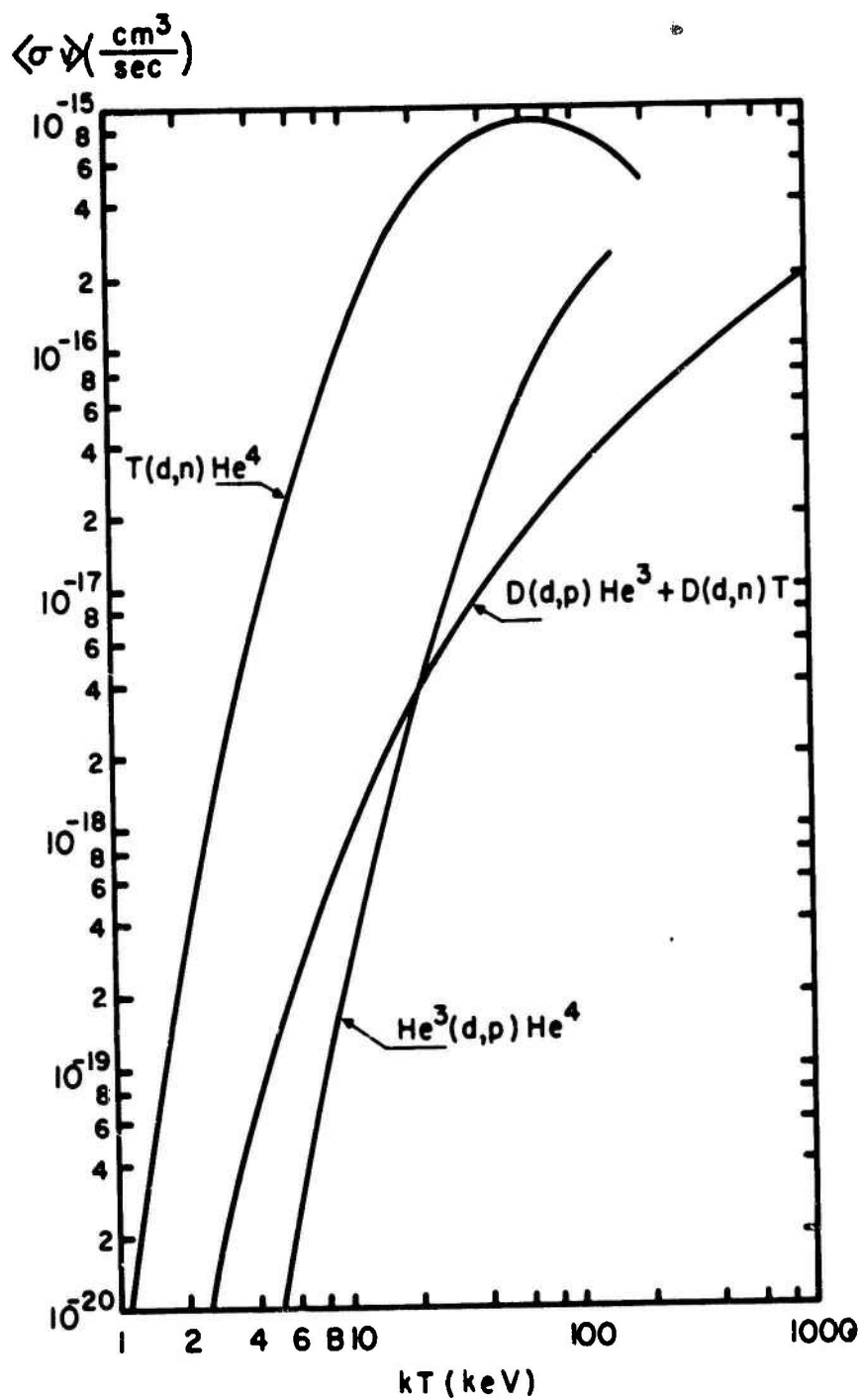


FIG. 7 REACTION PROBABILITIES FOR DEUTERIUM FUSION REACTIONS BASED ON MAXWELLIAN DISTRIBUTIONS.

[GLASSTONE AND LOVBERG²⁸]

a deuteron from a triton (or a triton strips a proton from a deuteron).

The only reaction between a deuteron and a triton that is observed at Mev temperatures is $T(d,n) He^4$. 17.6 Mev is released in this reaction. The threshold energies for two other reactions, $T(d,2n) He^3$ and $T(d,pn) T$, are 2.226 and 2.991 Mev (center of mass) respectively. These reactions are not observed for deuteron laboratory energies below about 12-14 Mev (Ajzenberg-Selove and Lauritsen⁴¹).

According to classical mechanics, no reactions should occur for deuteron energies less than the Coulomb barrier energy which is ≈ 660 kev for a tritium nucleus. Quantum mechanically, deuterons with energies less than the barrier energy have finite probabilities of tunneling through the barrier. The probability of penetrating the barrier, the Gamov factor, is

$$P = \exp\left(-\frac{r(E)}{\lambda(E)}\right) = \exp\left(-\frac{z_1 z_2 e^2 (2\mu)^{\frac{1}{2}}}{\hbar (E)^{\frac{1}{2}}}\right), \quad (3.1)$$

where $r = \frac{z_1 z_2 e^2}{E}$ is the classical distance of closest approach in a collision and $\lambda = \frac{\hbar}{(2\mu E)^{\frac{1}{2}}}$ is the de Broglie wavelength. The maximum reaction cross section for an s-wave interaction (neglecting Coulomb repulsion) is $\pi \lambda^2$. A plausible formula for the reaction cross section for

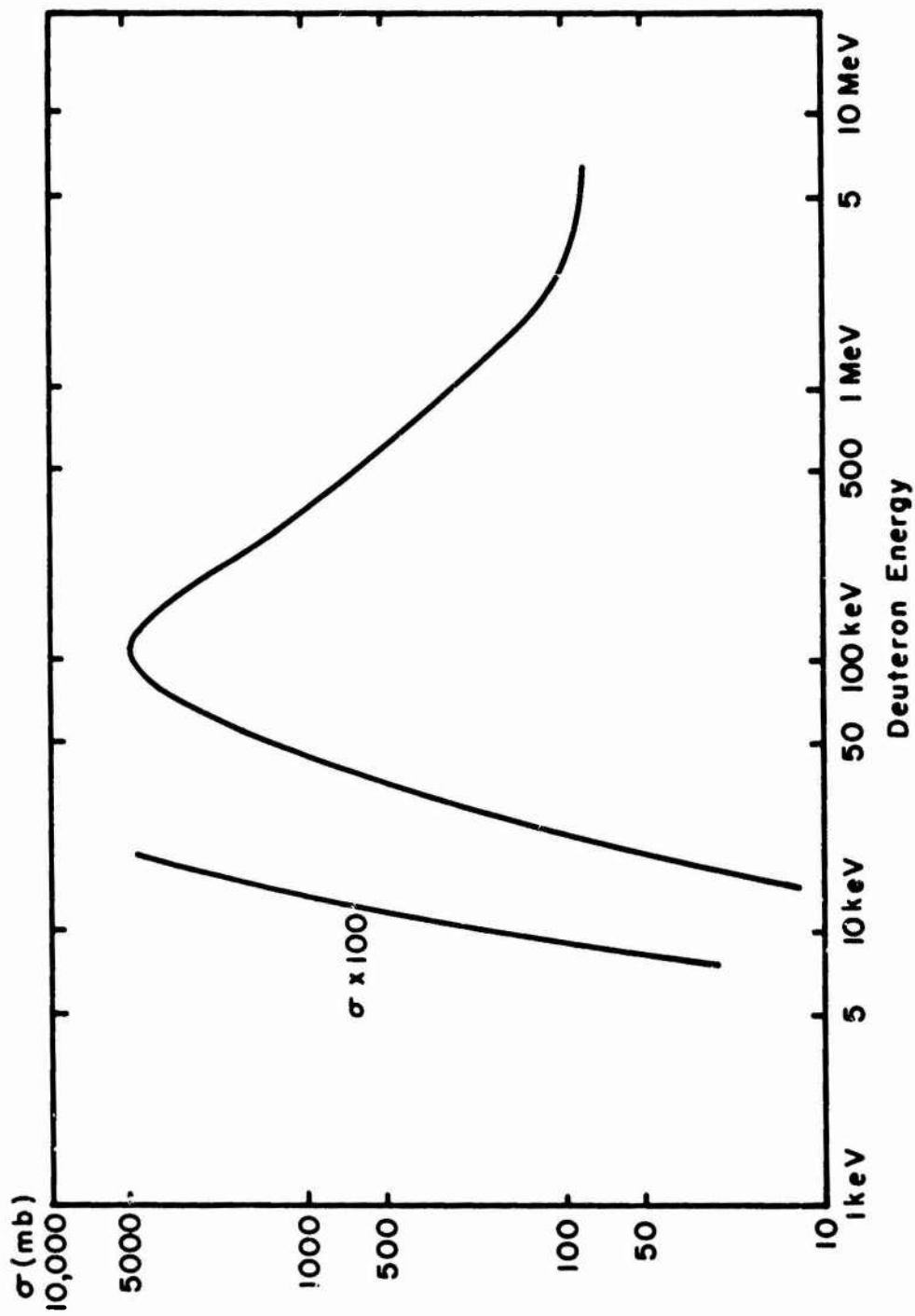
energies much less than the barrier height, is the product of the maximum collision cross section and the Gamov barrier penetration factor. The Gamov reaction cross section

$$\sigma = \frac{A'}{E} \exp\left(-\frac{B'}{(E)^{1/2}}\right), \quad (3.2)$$

has this energy dependence. Although the theoretical value of B' , given in equation (3.1) is sometimes used, the values of A' and B' are usually obtained from the best available low energy data. The Gamov cross section fits the experimental data well for deuteron energies less than 20 kev.

3.2 Reaction Probabilities for T(d,n)He⁴ Reactions

The reaction probability for T-D reaction must be computed numerically for the temperatures occurring in thermonuclear shocks. Cross sections for energies between 1 and 10 kev were computed from the Gamov formula with $A' = 2.19 \times 10^4$ barns kev and $B' = 44.24 (\text{kev})^{1/2}$. 106 other values of the cross section for energies between 10 kev and 10 Mev have been taken from the experimental data shown in figure 8 (LA-2014)⁴². $\langle\sigma v\rangle$ was evaluated with a Simpson's 1/3 rule adapted to unevenly spaced data points. (Uneven spacing of data points made it possible to determine the number of points according to how rapidly the cross section was changing with energy.) A graph of $\langle\sigma v\rangle$

FIG. 8 CROSS SECTION FOR $T(d,n)He^4$ REACTION [LA-2014]⁴²

for kT between 10 kev and 3 Mev is shown in figure 9.

Reaction probabilities, $\langle\sigma v\rangle$, for several values of kT between 1 kev and 150 kev were compared with the results of earlier calculations done by Wandel et al³⁹, Thompson⁴⁴, and those quoted by Glasstone and Lovberg³⁸ (p. 18, based on a combination of the work of Wandel, Thompson, and Tuck⁴⁵). These results are presented in Table 2.

The cross sections can be read accurately from the graph to two decimal places only. Therefore agreement to two decimal places between our results and those obtained by the others is all that is meaningful. The experimental data used by Thompson and Glasstone and Lovberg is not the data that was used in our calculation. Wandel et al, however, used the data presented in LA-2014 and their results agree with ours to two decimal places. Disagreement between our values of $\langle\sigma v\rangle$ and the values computed by Thompson and Glasstone and Lovberg for $kT= 2$ kev is explained, by the fact that the contribution of the cross section for lab energies below 1 kev was neglected in our calculation. However, for the purposes of this study, the value of $\langle\sigma v\rangle$ at $kT = 2$ kev is never used.

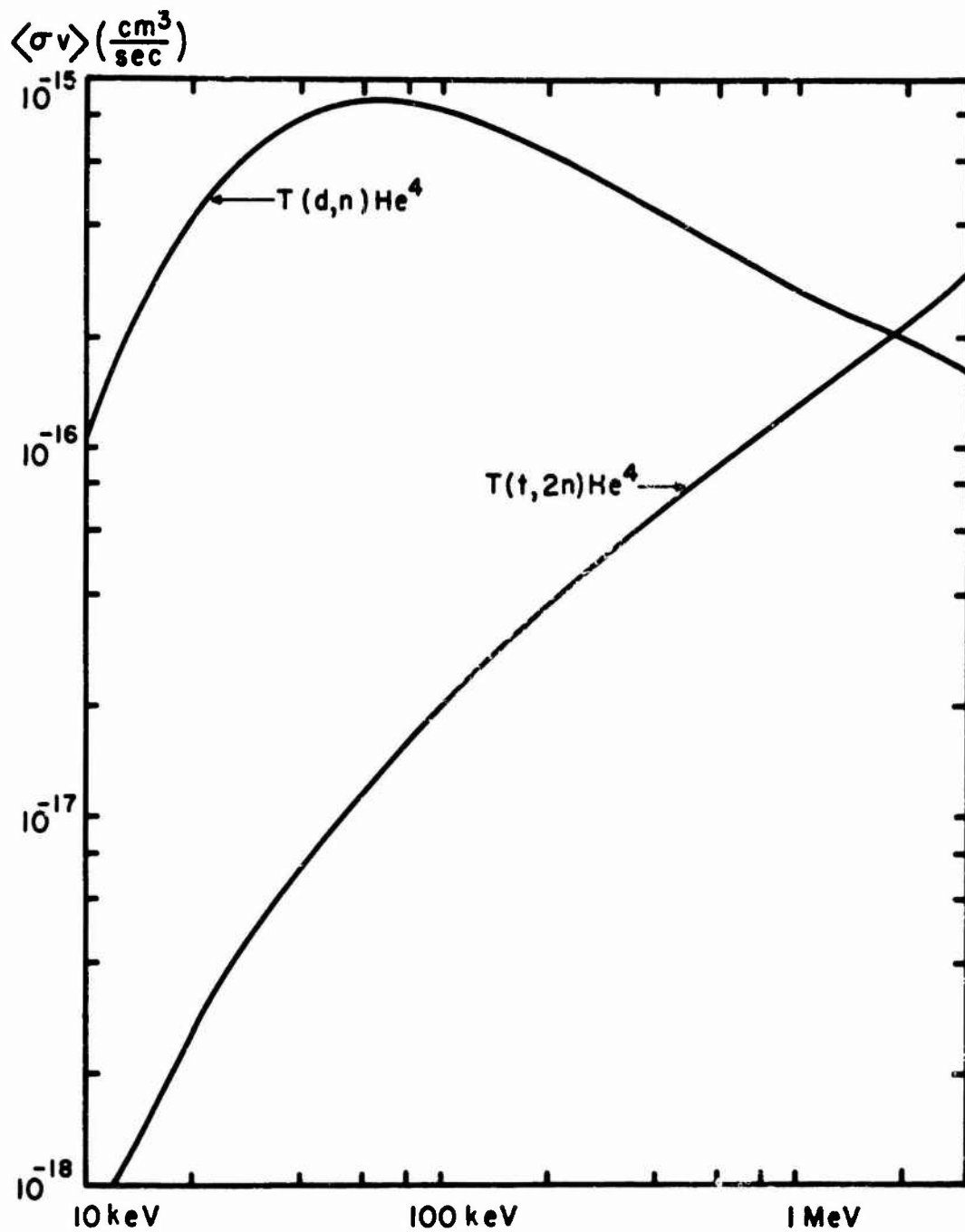


FIG. 9 REACTION PROBABILITIES FOR $T(d,n)He^4$ AND $T(t,2n)He^4$ REACTIONS BASED ON MAXWELLIAN DISTRIBUTIONS.

kT (kev)	Wandel et al	Glasstone and Lovberg	Thompson	$\langle \sigma v \rangle$ Fuller $\left(\frac{\text{cm}^3}{\text{sec}}\right)$
2		3×10^{-19}		2.76×10^{-19}
5	1.3×10^{-17}	1.4×10^{-17}		1.35×10^{-17}
10	1.11×10^{-17}	1.1×10^{-16}	1.05×10^{-16}	1.12×10^{-16}
20		4.3×10^{-16}		4.30×10^{-16}
25	5.58×10^{-16}			5.62×10^{-16}
50	8.54×10^{-16}			8.60×10^{-16}
60		8.7×10^{-16}		8.86×10^{-16}
100	8.45×10^{-16}	8.1×10^{-16}	8.0×10^{-16}	8.47×10^{-16}
150	7.04×10^{-16}			7.00×10^{-16}

TABLE 2. Reaction Probability for $T(d,n)He^4$ Reaction

3.3 Kinetics Equations for Deuterium-Tritium Reactions

If only the T-D reaction occurs, a reacting deuterium-tritium mixture is made up of tritons, deuterons, neutrons, alphas and electrons. The total pressure of the mixture is

$$p = (n_T + n_D + n_N + n_\alpha + n_e)kT. \quad (3.3)$$

The number densities of the different species can be related to each other by the equations of charge conservation,

$$n_e = n_T + n_D + 2n_\alpha, \quad (3.4)$$

electron number flux conservation (electrons do not participate in the reactions),

$$n_e u = F, \quad (3.5)$$

and mass conservation,

$$(n_T m_T + n_D m_D + n_N m_N + n_\alpha m_\alpha) u = A. \quad (3.6)$$

F , the electron flow constant and A , the mass flow constant can be evaluated from the initial conditions. Since the initial mixture contains deuterium and tritium ions in equal numbers,

$$n_{e_1} = 2n_{T_1}, \quad (3.7)$$

and therefore

$$F = 2n_{T_1} u_1, \quad (3.8)$$

and

$$A = \frac{5}{3} n_{T_1} m_T u_1. \quad (3.9)$$

A combination of equations (3.4) - (3.9) yields

$$(n_T - n_D) = 2(n_N - n_\alpha). \quad (3.10)$$

Since $n_{D_1} = n_{T_1}$, and since it is assumed that the species do not diffuse,

$$n_D = n_T, \quad (3.11)$$

for all x . Therefore, it follows from equation (3.10) that

$$n_N = n_\alpha, \quad (3.12)$$

for all x also.

The continuity equations for the species are not all independent. Tritons and deuterons are destroyed at the same rate, so $W_T = W_D$. Furthermore, neutrons and alpha particles are created at the same rate, so $W_N = W_\alpha$. Since mass is conserved in the reactions, $\sum_i m_i W_i = 0$, and therefore $W_N = -W_T$. As expected, the rate of triton and deuteron destruction is equal to the rate of neutron and alpha creation. There is only one independent continuity equation (which we choose to be the triton equation).

In order to eliminate number densities from the flow equations, we define a dimensionless variable α , the ratio of the density of the reaction products to the total density at the point x :

$$\alpha = \frac{n_N m_N + n_\alpha m_\alpha}{n_T m_T + n_D m_D + n_N m_N + n_\alpha m_\alpha}, \quad (3.13)$$

where

$$= n_T m_T + n_D m_D + n_N m_N + n_\alpha m_\alpha. \quad (3.14)$$

Before the gas begins to react, $n_N = n_D = 0$, so $\alpha = 0$.

After the gas has reacted completely, $n_D = n_T = 0$, so $\alpha = 1$.

A combination of equations (3.11) - (3.14) gives expressions for the neutron and triton number densities:

$$n_N = \frac{3}{5} \frac{\rho \alpha}{m_T}, \quad (3.15)$$

and
$$n_T = \frac{3}{5} \frac{\rho (1-\alpha)}{m_T}. \quad (3.16)$$

With these expressions for n_T and n_N , the state equation (3.3) becomes,

$$p = \frac{12}{5} \rho \frac{k}{m_T} T, \quad (3.17)$$

which is independent of α . Since $\frac{12k}{5m_T} = \frac{R}{5/4}$, the state equation can be written in its usual form for a mixture:

$$p = \rho \frac{R}{\bar{W}} T, \quad (3.18)$$

where $\bar{W} = \frac{5}{4}$.

In general, a state equation depends on the degree of reaction only if the number of particles before the reaction is not equal to the number of particles after the reaction. For the reaction, $T^3 + D^2 \rightarrow n^1 + He^4$, the number of particles before and after the reaction is the same; for the reaction, $T^3 + T^3 \rightarrow He^4 + 2n^1$, however, the particle number goes from

two to three. If the particle number does not change in the reaction, the mean molecular weight of the reacting mixture remains constant.

If we rewrite the continuity equation for tritons in terms of α , using equation (3.16), it becomes

$$\frac{3}{5} \frac{A}{m_T} \frac{d\alpha}{dx} = \left(\frac{3}{5}\right)^2 \frac{\rho^2}{m_T} (1-\alpha)^2 \langle \sigma v \rangle \quad (\text{cm}^{-3} \text{ sec}^{-1}). \quad (3.19)$$

The thermonuclear power per unit volume term, P_{TN} , in the differential form of the energy equation, (equation (2.17)), is $\frac{d}{dx} (\rho u q_{TN}) = A \frac{dq_{TN}}{dx}$. P_{TN} can also be written as the product of the reaction rate, W , and the energy released per reaction, Q_R . Equating these two expressions for P_{TN} we see that

$$A \frac{dq_{TN}}{dx} = \frac{3}{5} \frac{A}{m_T} Q_R \frac{d\alpha}{dx} \quad (3.20)$$

If both sides are integrated with respect to x , subject to the condition that $q_{TN} = 0$ for $\alpha = 0$, equation (3.20) becomes

$$q_{TN} = Q \alpha, \quad (3.21)$$

where $Q = \frac{3}{5} \frac{Q_R}{m_T}$.

It is easily verified that $Q = \frac{Q_R}{m_D + m_T}$, the maximum energy released per unit mass of initial mixture if it reacts completely.

3.4 Dimensionless Form of Shock Structure Equations for Deuterium-Tritium Mixtures

The shock structure equations can be put into dimensionless form, if they are multiplied by an appropriate combination of the mass, momentum, and energy flow constants, A, B and C. The dimensionless temperature is defined by

$$\tau \equiv \frac{k T H}{m_i}, \quad (3.22)$$

where $H \equiv \frac{A^2}{B^2}$, (3.23)

and m_i is the average ion mass for the initial mixture. For the deuterium-tritium mixture, with equal numbers of deuterium and tritium ions, $m_i = (m_D + m_T)/2$. Therefore,

$$\tau = \frac{k T H}{(m_D + m_T)/2} = \frac{R T H}{2.5}. \quad (3.24)$$

The dimensionless speed, density and pressure are defined in the following way:

$$u \equiv u (H)^{\frac{1}{2}}, \quad (3.25)$$

$$q \equiv \frac{B \rho}{A^2}, \quad (3.26)$$

$$\text{and } \pi = \frac{P}{B} . \quad (3.27)$$

In summary, the complete system of shock structure equations in dimensionless form is

$$\phi \omega = 1 , \quad (3.28)$$

$$\pi + \omega = 1, \quad (3.29)$$

$$\frac{5}{2} \frac{\pi}{\phi} + \frac{\omega^2}{2} - \alpha H Q + \Delta = C H, \quad (3.30)$$

$$\pi = 2 \phi \tau , \quad (3.31)$$

$$\frac{d\alpha}{dx} = \frac{3}{5} \frac{A H}{m_T} \frac{(1-\alpha)^2}{\omega^2} \langle \tau v \rangle = \frac{P_{TN}}{A Q} , \quad (3.32)$$

$$\text{where } \Delta = \frac{H}{A} \int_0^x P_{BR} dx' , \quad (3.33)$$

$$\text{and } P_{BR} = 2.261 \times 10^{-27} \frac{A B H}{m_T^2} \left(\frac{25}{R} \right)^{\frac{1}{2}} \frac{1+\alpha}{\omega^2} \tau^{\dagger} . \quad (3.34)$$

The function Δ , can be rewritten in a way that makes its physical significance apparent by changing variables of integration from x to α and by making use of equation (3.32).

It then becomes

$$\Delta = H Q \int_0^{\alpha} \frac{P_{BR}}{P_{TN}} d\alpha' . \quad (3.35)$$

There are two limiting cases of the shock structure equations, one including reactions and no radiation, the other including radiation but no reactions. The non-radiative limiting

case, ($\Delta = 0$ for all x), was discussed previously. The non-reactive limiting case is obtained if we set $\frac{d\alpha}{dx} = 0$ for all x and $\alpha(0) = 0$. The radiation is assumed to occur downstream from the gas dynamic shock, so the physical validity of this case is questionable. However the pure radiative solution of the equations is useful in providing a bounding curve for the solution of the physically more valid case that includes both reactions and radiation.

3.5 Dimensionless Parameters in the Energy Equation

There are three dimensionless parameters in the energy equation, CH, HQ, and Δ .

The parameter, CH, combines the constants of integration of the mass, momentum and energy equations. It depends only on the initial Mach number of the gas, M_1 , and not on the reaction chemistry, i.e.,

$$\begin{aligned} CH &= \left(\frac{5}{2} \frac{p_1}{\rho_1} + \frac{u_1^2}{2} \right) \left(\frac{\rho_1 u_1}{p_1 + \rho_1 u_1^2} \right)^2 \\ &= \frac{1}{2} \left(1 + \frac{5}{\gamma M_1^2} \right) \left(\frac{1}{1 + \frac{1}{\gamma M_1^2}} \right)^2 \end{aligned} \quad (3.36)$$

The initial Mach numbers, M_1 , for thermonuclear shocks are $\gg 1$, so $CH = 1/2$. The value of CH is therefore independent of the initial conditions.

The parameter, HQ, combines the mass and momentum flow constants with the energy per unit mass released in the reactions, i.e.,

$$HQ = \frac{Q}{u_1^2} \left(\frac{1}{1 + \frac{1}{\gamma M_1^2}} \right)^2 \quad (3.37)$$

For very large initial Mach numbers, HQ reduces to Q/u_1^2 ; since u_1 and Q are related by the Chapman-Jouguet condition, then

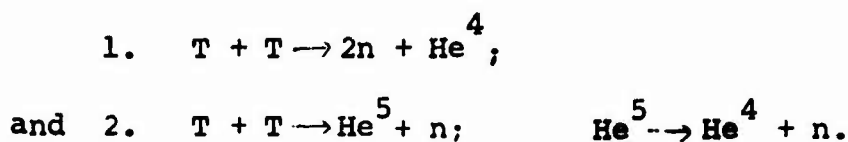
$$HQ = \frac{1}{2(\gamma^2 - 1)} = \frac{9}{32} \quad (3.38)$$

HQ is therefore independent of the reaction under consideration for shocks propagating with the C-J speed.

The third dimensionless parameter, Δ , is a measure of the relative importance of power lost in bremsstrahlung and power gained in thermonuclear reactions. When Δ is much smaller than other terms in the energy equation, ($\Delta \ll 1$), radiative losses are insignificant. When the value of Δ approaches 1, radiative power losses become comparable to the power gained in reactions. Unlike the parameters CH and HQ, Δ is neither constant nor independent of the reaction chemistry.

3.6 Fusion Reactions in Tritium

Two fusion reactions can occur in a pure tritium gas.



11.33 Mev is released in each reaction. If an incident triton strips a proton off a target triton, reaction 1 occurs, and He^4 and two neutrons are formed directly. The neutron energy spectrum is continuous since there are three bodies after the reaction. If an incident triton strips a deuteron off a target triton, the reaction occurs in two stages (reaction 2). The neutron energy spectrum is discrete because only two bodies come off in each stage of the reaction (Ajzenberg-Selove and Lauritsen³⁹).

T-T cross sections have been measured for incident lab energies between 60 kev and 1.14 Mev (Govorov et al⁴⁰). The cross section as a function of energy may be represented by the function

$$\sigma = (a + b \ln E \text{ (kev)}) \times 10^{-27} \text{ cm}^2 \quad (3.39)$$

where

$$a = -91.2 \pm 2.5,$$

$$b = (55.8 \pm 1) / \ln 10.$$

σ increases monotonically from 10 mb at 60 kev to 82 mb at 1.14 Mev (see figure 11).

Below these energies we can assume a cross section of the Gamov type. There is some question about the applicability of Gamov cross section to stripping reactions. However it is the only available cross sections for these energies

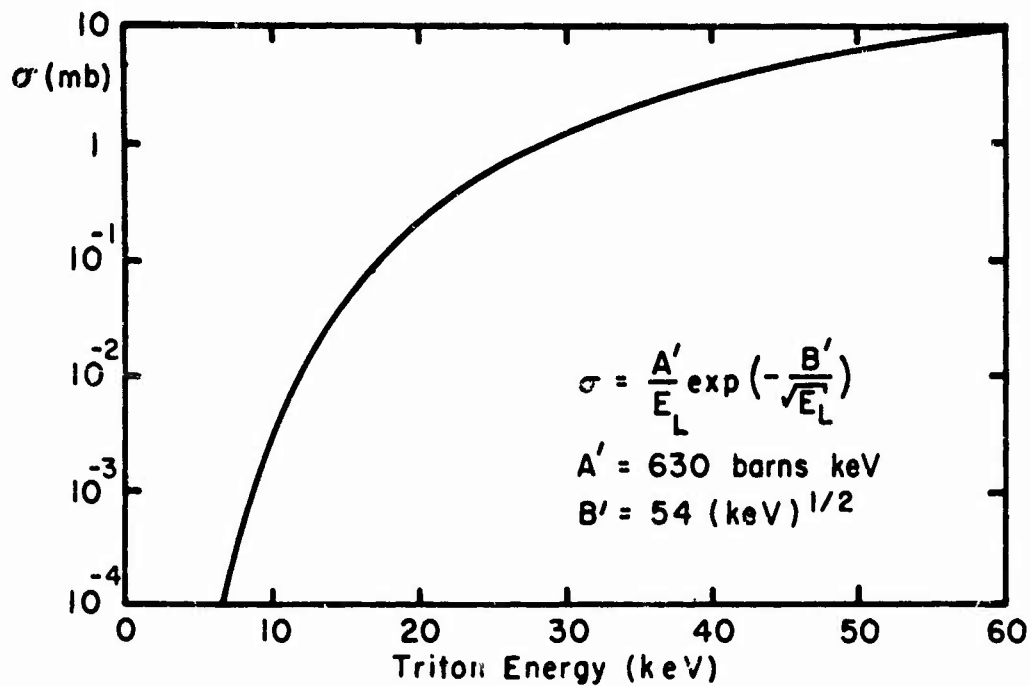


FIG. 10 CROSS SECTION FOR $T(t,2n)He^4$ REACTION FOR TRITON ENERGIES BELOW 60 keV

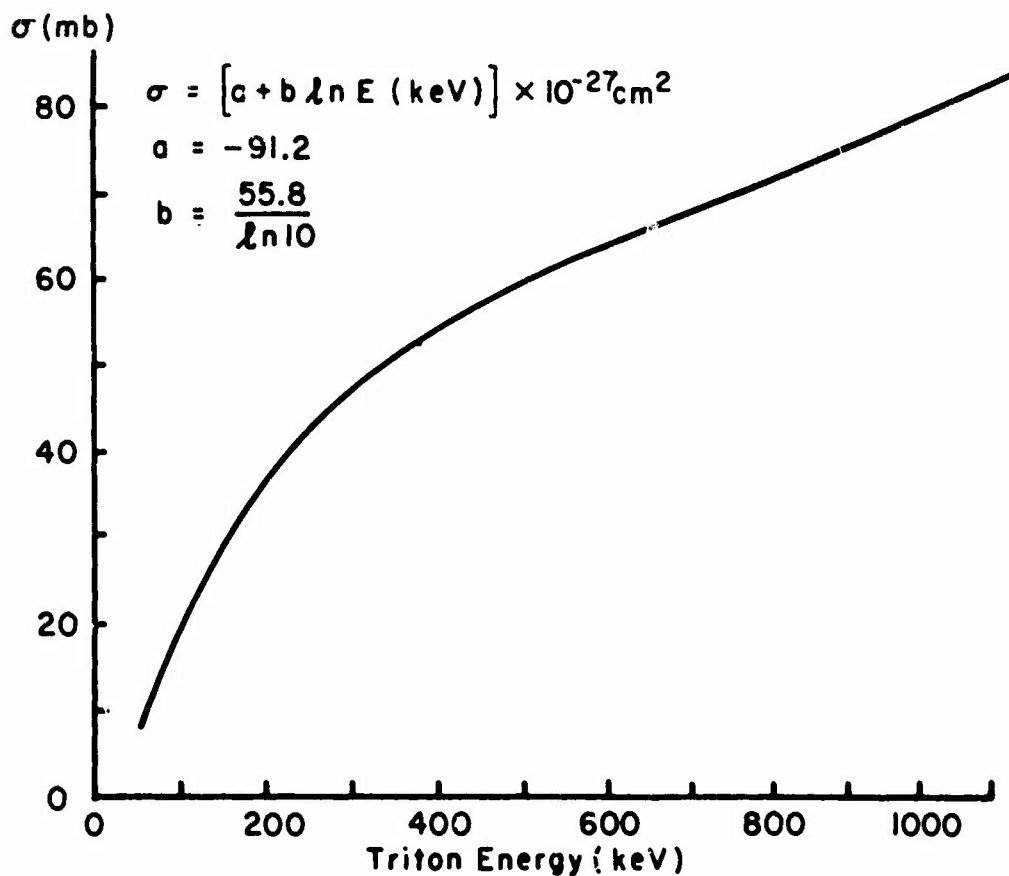


FIG. 11 CROSS SECTION FOR $T(t,2n)He^4$ REACTION FOR TRITON ENERGIES ABOVE 60 keV
 [GOVOROV ET AL ⁴³]

and has been used by Thompson⁴⁴. The theoretical value of the constant B' is $54 \text{ (kev)}^{1/2}$. The value of A' which gives Govorov's measured value of σ at 60 kev is *

$$A' = 0.6 \exp\left(\frac{54}{(60)^{1/2}}\right) \text{ barns kev.} \quad (3.40)$$

The T-T cross sections for $E_L < 60 \text{ kev}$ are shown in figure 10.

3.7 Reaction Probabilities for T(t,2n)He⁴ Reactions

kT \approx 1 Mev

An expression for the reaction probability for T-T reactions can be obtained analytically for the temperatures that occur in thermonuclear shocks ($kT \approx 1 \text{ Mev}$). In order to compute $\langle\sigma v\rangle$, an assumption must be made about the behavior of the cross section at energies for which no experimental values are available ($E_L < 60 \text{ kev}$ and $E_L > 1.14 \text{ Mev}$). For $kT \approx 1 \text{ Mev}$, collisions between particles with lab energies less than 60 kev do not contribute significantly to $\langle\sigma v\rangle$. Therefore, any convenient assumption about the behavior of the cross section at these energies, can be made. The Govorov cross section has been extrapolated to its crossing point on the energy axis, $E_0 = \exp(-\frac{a}{b})$. It is assumed to be zero for energies below E_0 . Collisions between particles with energies above 1.14 Mev make important contributions to $\langle\sigma v\rangle$. The Govorov cross section has been extrapolated

* An alternative way to match the Gamov and Govorov cross sections at 60 kev would be to choose values of A' and B' such that the cross section and its first derivative were continuous at 60 kev.

to all energies above 1.14 Mev for convenience in computing $\langle \sigma v \rangle$. The contribution of the cross sections for energies much higher than kT is damped out by the exponential in the integral.

$\langle \sigma v \rangle$ can be evaluated with the center of mass energy, E_{cm} , as the variable of integration. Since $\mu = \frac{m_T}{2}$ for pure tritium, the relation between lab and center of mass energy is just $E_{cm} = \frac{E_L}{2}$.

Therefore, it follows from equations (2.35) and (3.39), that

$$\langle \sigma v \rangle = \frac{8\pi \times 10^{-27}}{v^2} \frac{1}{(2\pi kT)^{3/2}} \times \int_{E_L}^{\infty} (a+b \ln(2E_{cm})) \exp\left(-\frac{E_{cm}}{kT}\right) E_{cm} dE_{cm} \quad (3.41)$$

The integral can be evaluated most simply by changing variables, from E_{cm} to the dimensionless variable, ϵ , where

$$\epsilon = \frac{E_{cm}}{kT} \quad (3.42)$$

Then

$$\langle \sigma v \rangle = \frac{4 \times 10^{-27}}{(\pi m_T)^{1/2}} (kT)^{1/2} \int_{\frac{E_L}{2kT}}^{\infty} (a' + b \ln \epsilon) e^{-\epsilon} \epsilon d\epsilon, \quad (3.43)$$

where $a' = a + b \ln(2kT)$

When the integral is performed, the resulting expression for $\langle \sigma v \rangle$ is

$$\langle \sigma v \rangle = \frac{4 \times 10^{-27}}{(\pi m_T)^{\frac{1}{2}}} (kT)^{\frac{1}{2}} b \left[E_1 \left(\frac{E_0}{2kT} \right) + \exp \left(-\frac{E_0}{2kT} \right) \right], \quad (3.44)$$

where $E_1(x) = \int_x^{\infty} \frac{\exp(-y)}{y} dy$.

Written in terms of our dimensionless variables, $\langle \sigma v \rangle$ becomes

$$\langle \sigma v \rangle = \left(\frac{16\tau}{\pi H} \right)^{\frac{1}{2}} b \left[E_1 \left(\frac{E_0 H/m_T}{2\tau} \right) + \exp \left(-\frac{E_0 H/m_T}{2\tau} \right) \right]. \quad (3.45)$$

Since $H \propto \frac{1}{u_1^2} = \frac{1}{2(\gamma^2 - 1)Q}$, $\frac{E_0 H}{m_T}$ is a dimensionless

parameter that depends on the Q of the reaction and the cut-off energy for the Govorov cross section, E_0 .

$kT \approx 100$ kev

If $kT \approx 100$ kev, the contribution of collisions of particles with lab energies below 60 kev becomes important. The Gamov cross section must be used for energies below 60 kev. There are now two contributions to $\langle \sigma v \rangle$. The Gamov cross section is integrated from some energy (which is much less than kT) to $E_L = 60$ kev. The Govorov cross section is integrated from $E_L = 60$ kev to $E_L = \infty$. The Gamov cross section was evaluated at 37 values of lab energy between 0.1 and 60 kev, and integrated over these energies with a Simpson's rule for unevenly spaced pivotal points. The

integral over the Govorov cross section was performed analytically with the result

$$\langle \sigma v \rangle_{\text{Gov}} = \frac{4 \times 10^{-27}}{(\pi m_p)^{\frac{1}{2}}} (kT)^{\frac{1}{2}} \left[\tau_0 \left(1 + \frac{E_{\infty}}{kT} \right) \exp \left(- \frac{E_{\infty}}{kT} \right) + \left(b \left(E_1 \left(\frac{E_{\infty}}{kT} \right) + \exp \left(- \frac{E_{\infty}}{kT} \right) \right) \right) \right] \quad (3.46)$$

where $\tau_0 = a + b \ln 50$ and $E_{\infty} = 30$ kev.

The results of the calculations for $\langle \sigma v \rangle_{\text{Gam}}$ and $\langle \sigma v \rangle_{\text{Gov}}$ are shown in Table 3. For $kT = 1$ kev, the Gamov contribution dominates; for $kT = 10$ kev, the Govorov contribution is roughly twice the Gamov contribution; for 100 kev, the Govorov contribution dominates.

kT (kev)	$\langle \sigma v \rangle_{\text{Gam}}$	$\langle \sigma v \rangle_{\text{Gov}}$	$\langle \sigma v \rangle \left(\frac{\text{cm}^3}{\text{sec}} \right)$
1	3.56×10^{-23}	1.04×10^{-30}	3.56×10^{-23}
5	6.64×10^{-20}	1.88×10^{-20}	8.52×10^{-20}
10	2.11×10^{-19}	3.99×10^{-19}	6.10×10^{-19}
20	2.44×10^{-19}	2.23×10^{-18}	2.47×10^{-18}
50	1.29×10^{-19}	8.97×10^{-18}	9.10×10^{-18}
100	5.84×10^{-20}	1.93×10^{-17}	1.93×10^{-17}
200	2.34×10^{-20}	3.68×10^{-17}	3.68×10^{-17}
500	6.38×10^{-21}	7.83×10^{-17}	7.83×10^{-17}
900	2.70×10^{-21}	1.22×10^{-16}	1.22×10^{-16}

TABLE 3. Contributions of Gamov and Govorov Reaction Probabilities to $\langle \sigma v \rangle$

An approximate formula for $\langle v \rangle$ for $kT < 10$ kev, is
(Thompson⁴⁴)

$$\langle v \rangle_{\text{app}} = \frac{0.8 \times 10^{-16} AB^{1/3}}{\mu_A^{1/2}} W^{-2/3} \exp\left(-3\left(\frac{B^2}{4W}\right)^{1/3}\right) \text{cm}^3/\text{sec}, \quad (3.47)$$

where, for T-T reactions,

$$\mu_A = \text{the reduced mass in a.m.u.} = \frac{3}{2},$$

$$W = kT,$$

$$A = \frac{\mu}{m_T} \quad A' = \frac{A'}{2},$$

$$B = \left(\frac{\mu}{m_T}\right)^{1/2} B' = \frac{B'}{(2)^{1/2}}.$$

Thompson has used the Gamov constants, $A' = 59.9$ barns kev and $B' = 668$ (kev)^{1/2}. However, the values of $\langle v \rangle$ for $kT = 1$ kev and $kT = 10$ kev, given in his paper, are inconsistent with the values of $\langle v \rangle_{\text{app}}$ obtained with his values of the Gamov constants. The Gamov constants, $A' = 54$ barns kev and $B' = 630$ (kev)^{1/2}, have been used in this study. The values of $\langle v \rangle_{\text{app}}$ are compared with the results of the numerical integration of the Gamov cross section for $kT = 1$ kev and 10 kev in Table 4. The agreement between the numerical results and the analytical results is quite good since the analytical formula is only approximate. This constitutes a check on the numerical integration for small values of kT .

kT (keV)	$\langle \sigma v \rangle_{\text{Gam}}$ A' = 54 B' = 630	$\langle \sigma v \rangle_{\text{app}}$ A' = 54 B' = 630	$\langle \sigma v \rangle_{\text{app}}$ A' = 59.9 B' = 668
1	3.56×10^{-23}	3.32×10^{-23}	0.795×10^{-23}
10	6.10×10^{-19}	7.00×10^{-19}	3.69×10^{-19}

TABLE 4. Reaction Probabilities for Low Temperatures

The T-T reaction probability for kT between 12 keV and 2 MeV, is shown in figure 9, along with the T-D reaction probability. The T-D reaction probability rises to a maximum value at ≈ 70 keV and then decreases with increasing temperature. This shape shows the influence of the resonance in the T-D reaction cross section. The T-T reaction probability, however, rises monotonically with increasing temperature. Although T-D reaction probabilities are about 100 times larger than T-T reaction probabilities for kT ≈ 10 keV, the two become comparable at ≈ 2 MeV.

3.8 Kinetics Equations for Tritium Reactions

A reacting tritium gas mixture consists of electrons, tritons, alphas and neutrons. He^5 has a lifetime of the order of 10^{-21} sec so it need not be included as one of the species of the mixture. The total gas pressure is

$$p = (n_T + n_N + n_\alpha + n_e)kT. \quad (3.49)$$

The number densities of the species are not independent.

Since the gas has local neutrality,

$$n_e = n_T + 2n_\alpha . \quad (3.50)$$

No electrons are created or lost in the reactions so the electron number flux is conserved:

$$n_e u = F, \\ \text{where } F = n_{T1} u_1 . \quad (3.51)$$

The total mass flux is also a constant,

$$(n_T m_T + n_N m_N + n_\alpha m_\alpha) u = A, \quad (3.52)$$

$$\text{where } A = n_{T1} m_T u_1 .$$

Since $A = m_T F$, it follows that

$$\rho = m_T n_e . \quad (3.53)$$

The electron number density profile has the same shape as the total density profile (which is reasonable since the electrons are inert). The relationship between the alpha and neutron number densities,

$$n_\alpha = \frac{n_N}{2} , \quad (3.54)$$

follows when the equations of electron flux conservation and mass flux conservation are combined with the condition for local charge neutrality.

The continuity equation for tritons is

$$\frac{d}{dx} (n_T u) = W_T \equiv -n_T^2 \langle \sigma v \rangle . \quad (3.55)$$

$|W_T|$ is twice the reaction rate for tritons since two tritons are lost in each reaction. The continuity equation for alpha particles is

$$\frac{d}{dx} (n_\alpha u) = W_\alpha . \quad (3.56)$$

The rate of neutron creation is twice the rate of alpha particle creation so

$$W_N = 2W_\alpha . \quad (3.57)$$

Since the total mass flux is conserved, $\sum_i m_i W_i = 0$, and therefore

$$W_T = -W_N . \quad (3.58)$$

It is convenient to eliminate number densities from the continuity and state equations. α is defined in the usual way as the ratio of the density of the reactions products to the total density,

$$\alpha \equiv \frac{n_N m_N + n_\alpha m_\alpha}{\rho} , \quad (3.59)$$

where $\rho = n_T m_T + n_N m_N + n_\alpha m_\alpha$. (3.60)

If equation (3.59) is solved for n_N and n_T , the resulting expressions are,

$$n_N = \frac{\rho \alpha}{m_T} , \quad (3.61)$$

and
$$n_T = \frac{\rho(1-\alpha)}{m_T} . \quad (3.62)$$

The state equation can be rewritten in terms of α . With the relation $\frac{k}{m_T} = \frac{R}{3}$, it becomes,

$$p = \rho \frac{R}{3} T (2 + \frac{\alpha}{2}). \quad (3.63)$$

This equation is recognized as the familiar equation for a mixture of gases, $p = \rho \frac{R}{\bar{W}} T$, if it is noted that the mean molecular weight per particle of the mixture, \bar{W} , instead of being constant, varies with α , i.e.,

$$\bar{W} = 3 / (2 + \alpha/2). \quad (3.64)$$

The set of dimensionless variables that were used to make the deuterium-tritium structure equations dimensionless, are now used to make the tritium structure equations dimensionless. The appropriate dimensionless temperature is,

$$\tau = \frac{k T H}{m_T} = \frac{R T H}{3} . \quad (3.65)$$

The mass and momentum equations are the same for the deuterium-tritium and pure tritium gases. The specific reaction chemistry is contained in the state equation,

$$\pi = (2 + \frac{\alpha}{2}) \phi \tau , \quad (3.66)$$

the continuity equation,

$$\frac{d\alpha}{dx} = \frac{AH}{m_T} \frac{(1-\alpha)^2}{\omega^2} \langle \tau v \rangle , \quad (3.67)$$

and the radiation term in the energy equation,

$$\Delta = HQ \int_0^{\alpha} \frac{P_{BR}}{P_{TN}} d\alpha', \quad (3.68)$$

where

$$P_{BR} = 1.57 \times 10^{-27} \frac{A B H}{m_T^2} \left(\frac{3}{R}\right)^{\frac{1}{2}} \frac{1+\alpha}{\omega^2} r^{\frac{1}{2}}, \quad (3.69)$$

and
$$P_{TN} = AQ \frac{d\alpha}{dx}. \quad (3.70)$$

3.9 Kinetics Equations for $T(t,2n)He^4$ Reactions in Hydrogen-Tritium Mixtures

If hydrogen is added to a tritium gas, the Chapman-Jouguet speed is reduced. An examination of the shock structure equations for a mixture of hydrogen and tritium is of interest in connection with shock tube experiments. The C-J speed for such mixtures can be reduced to a value which may be obtainable in an electromagnetically driven shock tube.

Let ϵ be a parameter that measures the initial density ratio of protons to tritons:

$$\epsilon \equiv \frac{n_H}{n_T} \frac{m_T}{m_H}. \quad (3.71)$$

Since reaction probabilities for proton fusion reactions are small, the only energy release comes from the tritium reactions.

Q_R is the energy released per reaction, the energy released per gram of gas of the initial mixture is

$$Q = \frac{Q_R}{2m_T} \frac{1}{1+\epsilon} . \quad (3.72)$$

The gas consists of five species: electrons, protons, tritons, alphas, and neutrons. The species number densities can be related by charge conservation,

$$n_e = n_H + n_T + 2n_\alpha , \quad (3.73)$$

conservation of electron flux,

$$n_e u = F, \quad (3.74)$$

conservation of proton flux,

$$n_H m_H u = G , \quad (3.75)$$

and conservation of mass,

$$u = (n_H m_H + n_T m_T + n_N m_N + n m) u = A$$

where F, A, and G are constants of integration which can be evaluated from the initial conditions. The initial electron density is

$$n_{e1} = n_{H1} + n_{T1} = n_{T1} (1+3\epsilon) . \quad (3.76)$$

Therefore,

$$F = n_{T1} (1+3\epsilon) u_1 , \quad (3.77)$$

$$G = m_H n_{H1} u_1 = \epsilon m_T n_{T1} u_1 , \quad (3.78)$$

and
$$A = (n_{H1} m_H + n_{T1} m_T) u_1 = n_{T1} m_T (1+\epsilon) u_1 . \quad (3.79)$$

Only one of the three constants of integration is independent, i.e.,

$$G = \frac{\epsilon}{1+\epsilon} A, \quad (3.80)$$

$$\text{and } F = \frac{1+3\epsilon}{(1+\epsilon)} \frac{1}{m_T} A. \quad (3.81)$$

If we solve for $1/u$ in the above equations, we obtain

$$\frac{1}{u} = \frac{\rho}{A} = \frac{n_e}{F} = \frac{n_H m_H}{G}. \quad (3.82)$$

This relationship can be used to get two different expressions for n_H :

$$n_H = \frac{n_N}{2} - n_\alpha + 3\epsilon \left(n_T + \frac{n_N}{2} + n_\alpha \right), \quad (3.83)$$

$$\text{and } n_H = \epsilon (3n_T + n_N + 4n_\alpha). \quad (3.84)$$

Setting the two expressions for n_H equal to each other, we see that

$$\frac{n_N}{2} - n_\alpha = \epsilon \left(n_\alpha - \frac{n_N}{2} \right). \quad (3.85)$$

Since ϵ is an arbitrary input parameter, equation (3.85) holds, (as in the pure tritium case, to which it reduces when $\epsilon = 0$), only if

$$\frac{n_N}{2} = n_\alpha, \quad (3.86)$$

for all x .

The total pressure of the gas mixture is

$$p = \left[2(1+3\epsilon) \left(n_T + n_N \right) + \frac{n_N}{2} \right] kT. \quad (3.87)$$

It is convenient to eliminate number densities from the state and continuity equations and express them in terms of

some appropriate reaction parameter α . One such choice of α puts the state equation into the same form as for the pure tritium case. Let

$$\alpha \equiv \left(\frac{n_N m_N + n_\alpha m_\alpha}{\rho} \right) \epsilon_R, \quad (3.88)$$

$$\text{where } \epsilon_R \equiv \frac{1+\epsilon}{1+3\epsilon}. \quad (3.89)$$

$$\text{Then } \left(\frac{1}{1+3\epsilon} - \alpha \right) = \frac{n_T m_T}{\rho} \epsilon_R. \quad (3.90)$$

An effective triton mass,

$$m_T^i = m_T \epsilon_R, \quad (3.91)$$

can be defined. Expressions for the neutron and triton number densities follow from equations (3.88) and (3.90):

$$n_N = \frac{\rho \alpha}{m_T^i}, \quad (3.92)$$

$$\text{and } n_T = \frac{\rho}{m_T^i} \left(\frac{1}{1+3\epsilon} - \alpha \right). \quad (3.93)$$

The sum of the neutron and triton number densities is independent of α . The number densities of the two inert components (protons and electrons) of the gas mixture are proportional to $(n_T + n_N)$, i.e.,

$$n_H = 3\epsilon(n_T + n_N),$$

$$\text{and } n_e = (1+3\epsilon)(n_T + n_N). \quad (3.95)$$

If equations (3.92) and (3.93) are substituted into the state equation, it becomes

$$p = \rho \frac{kT}{m'_T} \left(2 + \frac{\alpha}{2} \right) . \quad (3.96)$$

This is identical to the state equation for pure tritium if we replace the triton mass by its effective mass. It must be noted that when the reactions are complete, $n_T = 0$ and therefore from equation (3.90), $\alpha = \frac{1}{1+3\epsilon}$.

The energy equation for the hydrogen-tritium mixture is the same as equation (3.30). The expression for Δ must be modified to contain the appropriate reaction chemistry, and the constant Q in the thermonuclear energy release term must be redefined. The thermonuclear energy release term, αQ , has the value Q for a tritium gas when all the reactions are completed. The maximum value of α for the hydrogen-tritium mixture is $\frac{1}{1+3\epsilon}$. The maximum energy released per unit mass of the initial mixture, (given by equation (3.72)), is $Q = \frac{Q_R}{2m'_T} \frac{1}{1+\epsilon}$. We define a constant Q_{eff} such that αQ_{eff} approaches Q as α approaches $\frac{1}{1+3\epsilon}$.

It follows that

$$Q_{\text{eff}} = \frac{Q_R}{2m'_T} . \quad (3.97)$$

The flow variables are made dimensionless in the same

way as those for the pure tritium case. The dimensionless temperature becomes

$$\tau \equiv \frac{k T H}{m_T'} . \quad (3.98)$$

As in the state equation, the mass of the triton has been replaced by its effective mass.

The dimensionless mass, state and momentum equations for the hydrogen-tritium mixture are the same as those for pure tritium. The dimensionless energy equation is

$$\frac{5}{2} \frac{\pi}{\phi} + \frac{\omega^2}{2} - \alpha H Q_{\text{eff}} + \Delta = CH, \quad 0 \leq \alpha \leq \frac{1}{1+3\epsilon}, \quad (3.99)$$

where Δ is defined in the usual way and

$$P_{BR} = 1.57 \times 10^{-27} \frac{ABH}{m_T'^2} \left(\frac{3\epsilon}{R} \right)^{\frac{1}{2}} \frac{1+\alpha}{\omega^2} \tau^{\frac{1}{2}} . \quad (3.100)$$

The continuity equation is,

$$\frac{d\alpha}{dx} = \frac{AH}{m_T'} \left(\frac{1}{1+3\epsilon} - \alpha \right)^2 \frac{\langle \sigma v \rangle}{\omega^2} . \quad (3.101)$$

CHAPTER IV

SHOCK STRUCTURE CURVES IN PHASE SPACE4.1 Non-Radiative Shock Structure Curves in Phase Space

The system of non-radiative shock structure equations, developed in Chapter III for three different gas mixtures, includes four algebraic equations, (mass, momentum, energy and state equations) and one non-linear, first order, differential equation, (the continuity equation). In order to integrate the differential equation for the shock profiles in real space, all the flow variables except one must be eliminated. The algebraic equations are solved for relationships between the variables. These relationships are called the phase space shock curves.

A relationship between the dimensionless speed, ω , and the degree of fusion, α , can be obtained from the non-radiative mass, momentum, and energy equations. A combination of equations (3.28) and (3.29) gives an expression for $\frac{\pi}{\phi}$, which can be substituted into equation (3.30). The resulting equation is

$$\omega^2 - \frac{5}{4}\omega + \frac{1}{2}(\text{CH} + \text{HQ}\alpha) = 0, \quad (4.1)$$

or

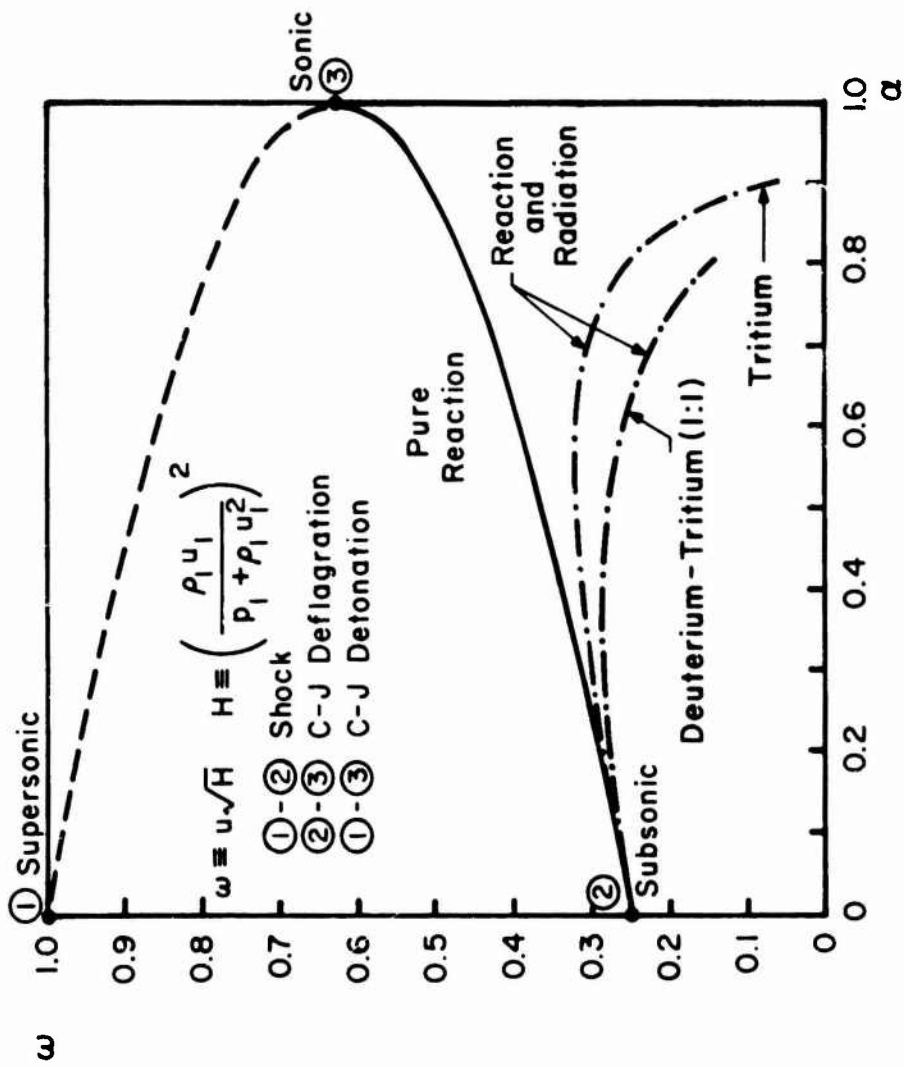
$$\alpha - \frac{1}{\text{HQ}} \left(\frac{25}{32} - \text{CH} \right) = - \frac{2}{\text{HQ}} \left(\omega - \frac{5}{8} \right)^2. \quad (4.2)$$

Since $CH = 1/2$ and $HQ = 9/32$, equation (4.2) becomes,

$$\alpha - 1 = -\frac{64}{9} \left(\omega - \frac{5}{8} \right)^2. \quad (4.3)$$

Equation (4.3) is independent of the specific reaction chemistry since the dimensionless mass, momentum and energy equations are identical for all three cases considered in Chapter III. The $\omega - \alpha$ curve is a parabola that opens to the left with an axis of symmetry parallel to the α -axis. The vertex of the parabola is located at $(\omega, \alpha) = (\frac{5}{8}, 1)$. The $\omega - \alpha$ relation is plotted in figure 12. (Points 1, 2 and 3 are the same as in figure 2.)

The two branches of the $\omega - \alpha$ curve join at the vertex of the parabola. The lower branch, (ω_-) , corresponds physically to a gas dynamic shock followed by a C-J deflagration. It is the familiar solution assumed by the von Neumann model. Ahead of the shock, ω is equal to 1. Behind the shock, ω is equal to 1/4, while behind the deflagration, ω has the value 5/8. The upper branch, (ω_+) , is also a solution of the non-viscous non-thermal conducting shock structure equations. It corresponds physically to a C-J detonation. ω is a continuous function of α , monotonically decreasing as α increases from 0 to 1. The C-J detonation has not been observed experimentally and is therefore not considered in most theoretical treatments,

FIG. 12 DIMENSIONLESS SPEED, ω , VS. DEGREE OF FUSION, α

(e.g., von Karman²⁶). It is presented in the phase plane diagrams for completeness sake; shock structure curves in real space have not been computed for this branch.

A relationship between the dimensionless temperature, τ , and the degree of fusion, α , is obtained by combining the mass, momentum, and energy equations with the state equation. The mass, momentum and energy equations are first combined to give a relation between ω and τ for the deuterium-tritium mixture:

$$\omega^2 - \omega + 2\tau = 0; \quad (4.4)$$

and a relationship between ω , τ and α for the pure tritium gas:

$$\omega^2 - \omega + \left(2 + \frac{\alpha}{2}\right)\tau = 0. \quad (4.5)$$

Combining these relations with the appropriate energy equation, we obtain a relationship between τ and α . The τ - α relation, unlike the ω - α relation, depends on the reaction chemistry because it contains the state equation.

The relationship between temperature and degree of fusion for the deuterium-tritium mixture is

$$16\tau^2 + \left(\frac{1}{2} + 2D' - 8HQ\alpha\right)\tau + \frac{D'^2 - 1}{16} + HQ\alpha(HQ\alpha - \frac{D'}{2}) = 0, \quad (4.6)$$

where $D' = 1 - 4CH = -1. \quad (4.7)$

τ as a function of α is plotted in figure 13. The jump conditions for temperature are obtained by setting

$$\tau \equiv \frac{kTH}{(m_D + m_T)/2} \quad H = \left(\frac{\rho_1 u_1}{\rho_1 + \rho_1 u_1^2} \right)^2$$

$$\alpha \equiv (n_N m_N + n_a m_a) / \rho$$

REACTION $T(d, n) He^4$

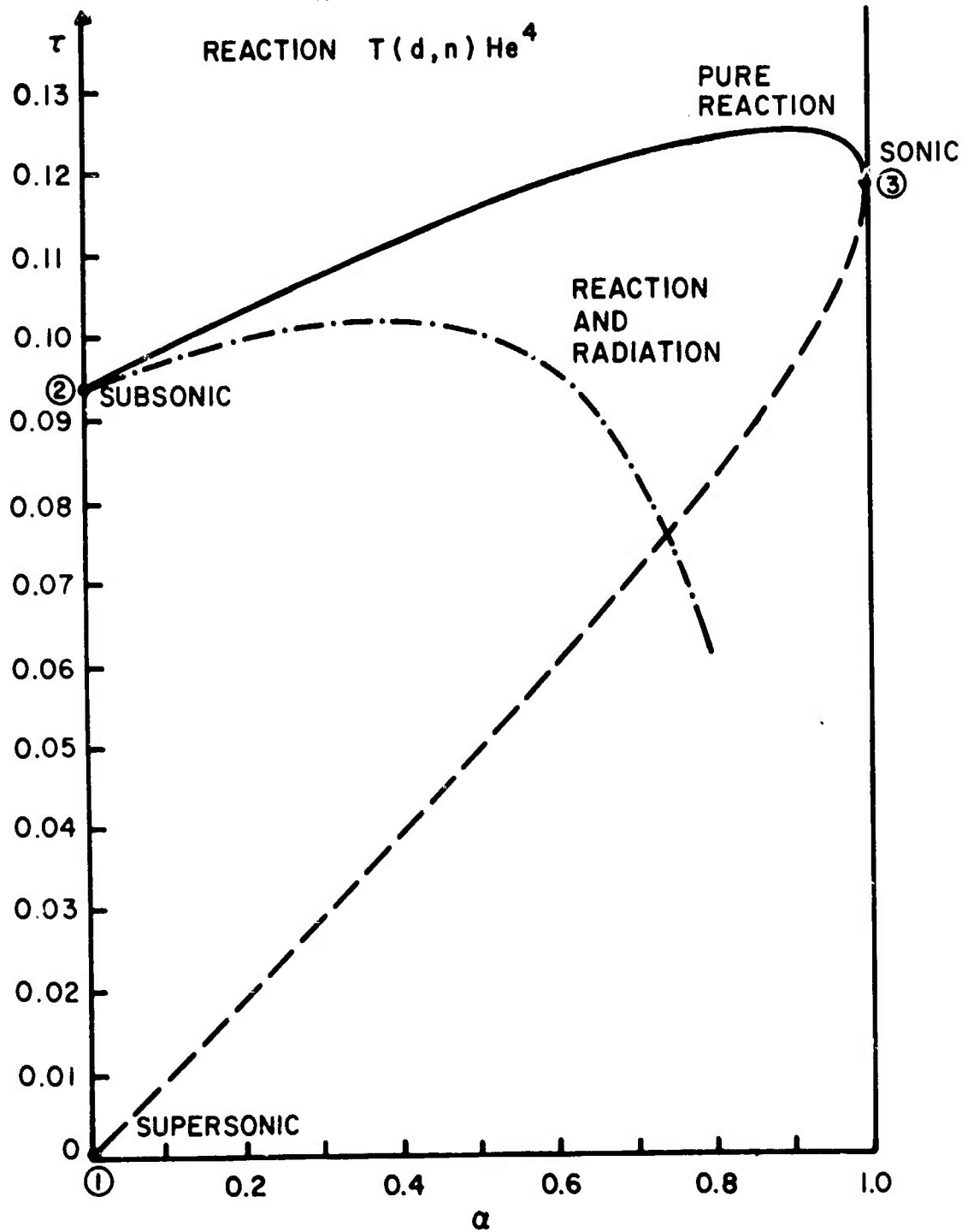


FIG. 13 DIMENSIONLESS TEMPERATURE, τ , vs. DEGREE OF FUSION, α , FOR A DETONATION IN A DEUTERIUM-TRITIUM MIXTURE (1:1)

$\alpha = 0$ and 1 in equation (4.6). When $\alpha = 0$,

$$16\tau^2 + \left(\frac{1}{2} + 2D'\right)\tau + \frac{D'^2 - 1}{16} = 0, \quad (4.8)$$

and $\tau_{\pm} = \frac{3}{32}, 0. \quad (4.9)$

The zero root comes from assuming that $D' = -1$. Actually D' is not exactly -1 and when its correct value is used, the zero root of equation (4.8) becomes $\approx 10^{-6}$. The other root is only different from $3/32$ in about the sixth decimal place. When $\alpha = 1$,

$$16\tau^2 + \left(2D' + \frac{1}{2} - 8HQ\right)\tau + \frac{D'^2 - 1}{16} + HQ\left(HQ - \frac{D'}{2}\right) = 0, \quad (4.10)$$

and $\tau_{\pm} = \frac{15}{128} \approx 0.117. \quad (4.11)$

The branch, τ_{-} , (like ω_{+}), corresponds to a C-J detonation. The other branch, τ_{+} , corresponds to a gas dynamic shock followed by a C-J deflagration. The two branches meet at the downstream point.

The $\tau - \alpha$ curve is not any simple shape like the $\omega - \alpha$ curve. However, the existence, location, and nature of extremal points on it can be determined analytically. If equation (4.4) is differentiated with respect to α , a relationship between $\frac{d\tau}{d\alpha}$ and $\frac{d\omega}{d\alpha}$ is obtained:

$$2 \frac{d\tau}{d\alpha} = (1 - 2\omega) \frac{d\omega}{d\alpha}. \quad (4.12)$$

If $\frac{d\tau}{d\alpha} = 0$, then either $\frac{d\omega}{d\alpha} = 0$ or $\omega = \frac{1}{2}$. There are no points on the $\omega - \alpha$ curve where $\frac{d\omega}{d\alpha} = 0$, but ω does go through

the value $1/2$ on the ω -curve. Therefore, there is some point on the τ -curve where $\frac{d\tau}{d\alpha} = 0$. If equation (4.4) is differentiated a second time, the extremum is found to be a maximum; (since $\frac{d\omega}{d\alpha} > 0$ for $\omega = \frac{1}{2}$ and therefore $\frac{d^2\tau}{d\alpha^2} < 0$). It can be shown from equations (4.3) and (4.4) that the coordinates of the maximum are $(\tau, \alpha) = (\frac{1}{8}, \frac{8}{9}) = (0.125, 0.889)$.

The value of the Mach number at any point on the $\tau - \alpha$ curve is given by the easily verifiable relation

$$\frac{\omega^2}{\tau} = 2 \gamma M^2. \quad (4.13)$$

The temperature maximum occurs when $M^2 = \frac{1}{\gamma} = \frac{3}{5}$. Therefore the temperature increases with increasing α for $\frac{1}{5} \leq M^2 < \frac{3}{5}$ and decreases with increasing α for $\frac{3}{5} < M^2 \leq 1$. When $M^2 = \frac{3}{5}$, the static pressure, p , is equal to the kinetic pressure, ρu^2 . The temperature therefore rises with decreasing pressure when $p > \rho u^2$, and falls with decreasing pressure when $p < \rho u^2$. The competing physical processes are the reactions, which add energy to the gas, thereby raising the temperature, and the transformation of random thermal energy into directed kinetic energy, which lowers the temperature. As the reactions go to completion, the reaction rates decrease and eventually the second effect dominates the first.

The relation between the dimensionless temperature, τ , and the degree of fusion, α , for pure tritium and hydrogen-tritium mixtures is

$$(4+\alpha)^2 \tau^2 + (4+\alpha) \tau \left(\frac{D'}{2} + \frac{1}{8} - 2HQ\alpha \right) + \frac{D'^2 - 1}{16} + HQ\alpha \left(HQ\alpha - \frac{D'}{2} \right) = 0. \quad (4.14)$$

τ as a function of α is depicted in figure 14. The $\tau\alpha$ cross terms in equation (4.14) are of higher degree than those for the deuterium-tritium case because the state equation depends on α . The upstream ($\alpha = 0$) roots of this equation, which are the pre-shock and post-shock dimensionless temperature, are identical to those for the deuterium-tritium relation between τ and α , (equation (4.6)). This is reasonable since the structure equations are made dimensionless in a way that eliminates their dependence on the mean molecular weight of the initial gas mixture, and since no reactions take place in the gas dynamic shock. The downstream ($\alpha = 1$) temperature satisfies the equation

$$25\tau^2 + 5 \left(\frac{D'}{2} + \frac{1}{8} - 2HQ \right) \tau + \frac{D'^2 - 1}{16} + HQ \left(HQ - \frac{D'}{2} \right) = 0, \quad (4.15)$$

which has the double root,

$$\tau_2 = \frac{3}{32}. \quad (4.16)$$

For the discontinuous solution, $\tau_2(\alpha = 0) = \tau_2(\alpha = 1)$. In other words, the decrease in mean molecular weight per

$$\tau \equiv \frac{kTH}{m_T} \quad H = \left(\frac{\rho_1 u_1}{\rho_1 + \rho_1 u_1^2} \right)^2$$

$$\alpha \equiv (\eta_N m_N + \eta_a m_a) / \rho$$

REACTION $T(t, 2n) He^4$

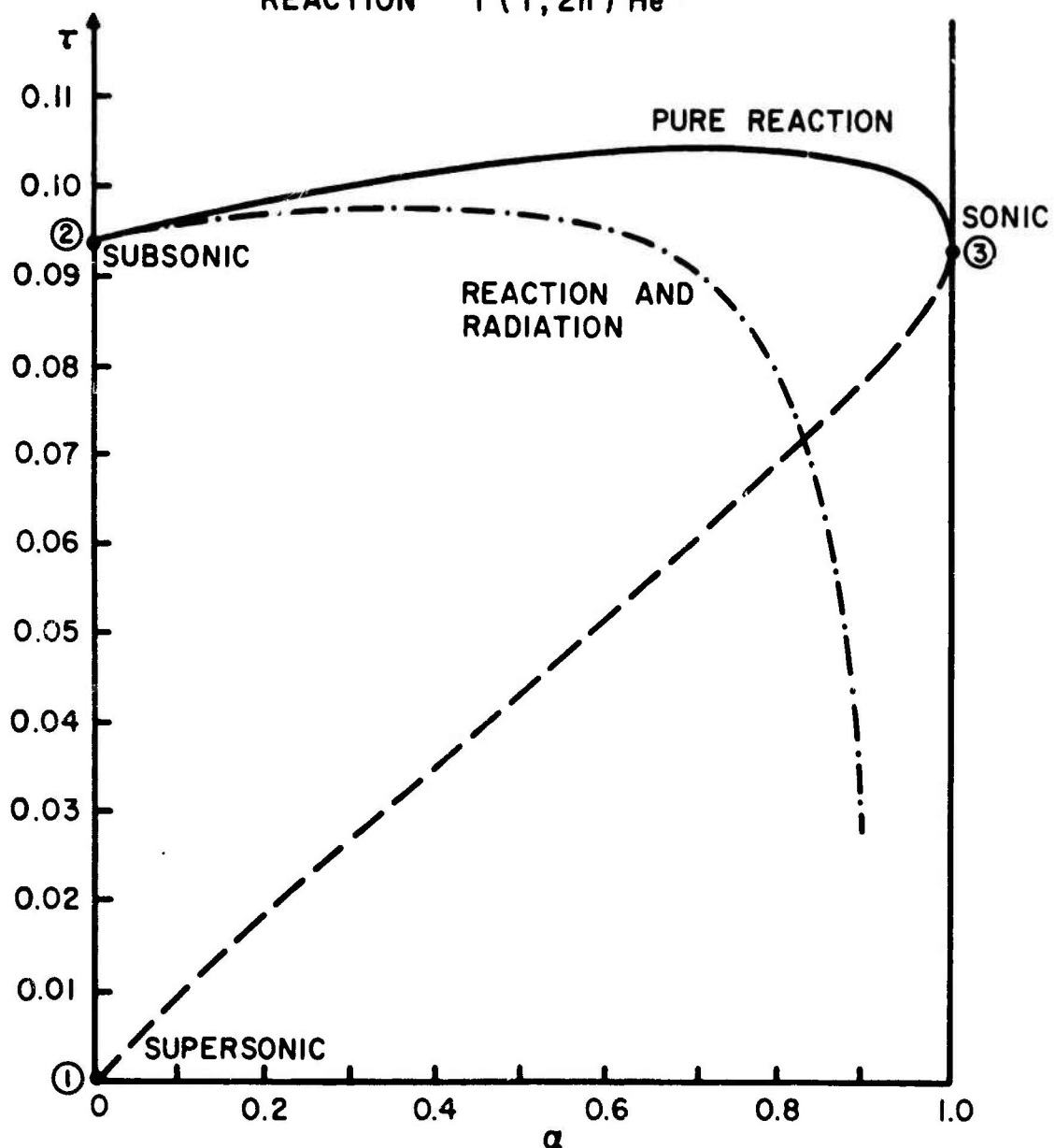


FIG. 14 DIMENSIONLESS TEMPERATURE, τ , vs. DEGREE OF FUSION, α , FOR A DETONATION IN TRITIUM

particle just cancels any net rise in temperature across the deflagration region.

The existence of extremal points on the τ - α curve can be shown also. If equation (4.5) is differentiated with respect to α , then,

$$(1-2\omega) \frac{d\omega}{d\alpha} = \left(2 + \frac{\alpha}{2}\right) \frac{d\tau}{d\alpha} + \frac{\tau}{2} . \quad (4.17)$$

This expression, unlike its counterpart for the deuterium-tritium mixture, does not give a simple condition for the existence of an extremum on the τ - α curve. However, if the τ - α curve is differentiated directly, and we set $\frac{d\tau}{d\alpha} = 0$ in the resulting equation, we find an expression which τ and α satisfy at the extremal point. If this expression is substituted into equation (4.14), the coordinates of the extremum are found to be $(\tau, \alpha) = (0.1036, 0.72)$, which corresponds to a dimensionless speed, $\omega = 0.427$. It can be shown, although the algebra is more complex than for the deuterium-tritium example, that this extremal point is a maximum. There is a second extremal point which has been discarded because it does not correspond to a physically allowed value of α .

4.2 Radiative Shock Structure Curves in Phase Space

When radiation energy loss is considered, the energy equation changes from an algebraic equation to an integral equation (see equations (3.30) and (3.33)). The radiative

energy loss term, Δ , can be written as a function of α (see equation 3.35). The mass, momentum, and state equations can be used to eliminate all variables except τ and α from the energy equation. The resulting equation, relating τ and α for the radiative case, is the same as that for the non-radiative case, (equation (4.6) for the deuterium-tritium mixture and equation (4.14) for the tritium gas), if D' is replaced by

$$D = D' + 4\Delta(\alpha), \quad (4.18)$$

where $\Delta = HQ \int_0^\alpha R_p d\alpha'$,

and $R_p \equiv \frac{P_{BR}}{P_{TN}}$. (4.19)

It follows from equation (3.32) and (3.34) that R_p can be written as the product of a function of α , and a function of τ , i.e.,

$$R_p = K A(\alpha) B(\tau), \quad K > 0, \quad (4.20)$$

where $A(\alpha) = \frac{1+\alpha}{(1-\alpha)^2}$,

and $B(\tau) = \frac{\tau^{\frac{1}{2}}}{\langle \tau v \rangle(\tau)}$.

An iterative method is used to solve the integral equation relating the dimensionless temperature to the degree of fusion. The non-radiative solution ($\Delta = 0$, for all α) is assumed for the first iteration. The first non-zero

approximation to the radiative loss term, $\Delta_1(\alpha)$, can be evaluated with the non-radiative τ - α relation (if $\langle v \rangle$ is a known function of τ). A first approximation to the radiative relation between τ and α is then obtained. It is used to evaluate $\Delta_2(\alpha)$. This iterative process is continued until $\tau(\alpha)$ does not change to some required degree of accuracy from one iteration to the next. The numerical procedure converges to three significant figures in about six iterations. The results of the integration for $\tau(\alpha)$ are shown in figure 13 for the deuterium-tritium case, and in figure 14 for the pure tritium case. $\Delta(\alpha)$ for both cases is plotted in figure 15.

The radiative relation between the dimensionless speed and the degree of fusion is

$$\alpha - 1 - \frac{\Delta}{H_0} = - \frac{64}{9} \left(\omega - \frac{5}{8} \right)^2. \quad (4.21)$$

It can be evaluated once $\Delta(\alpha)$ is known. The results for both the deuterium-tritium mixture and the tritium gas are shown in figure 12. For $\frac{\Delta}{H_0} \ll 1$, the radiative solution is asymptotic to the non-radiative solution. Away from the non-radiative asymptotic limit, equation (4.21) depends on the specific reaction chemistry through Δ which is a function of the reaction and bremsstrahlung rates.

Certain features of the radiative phase space solutions,

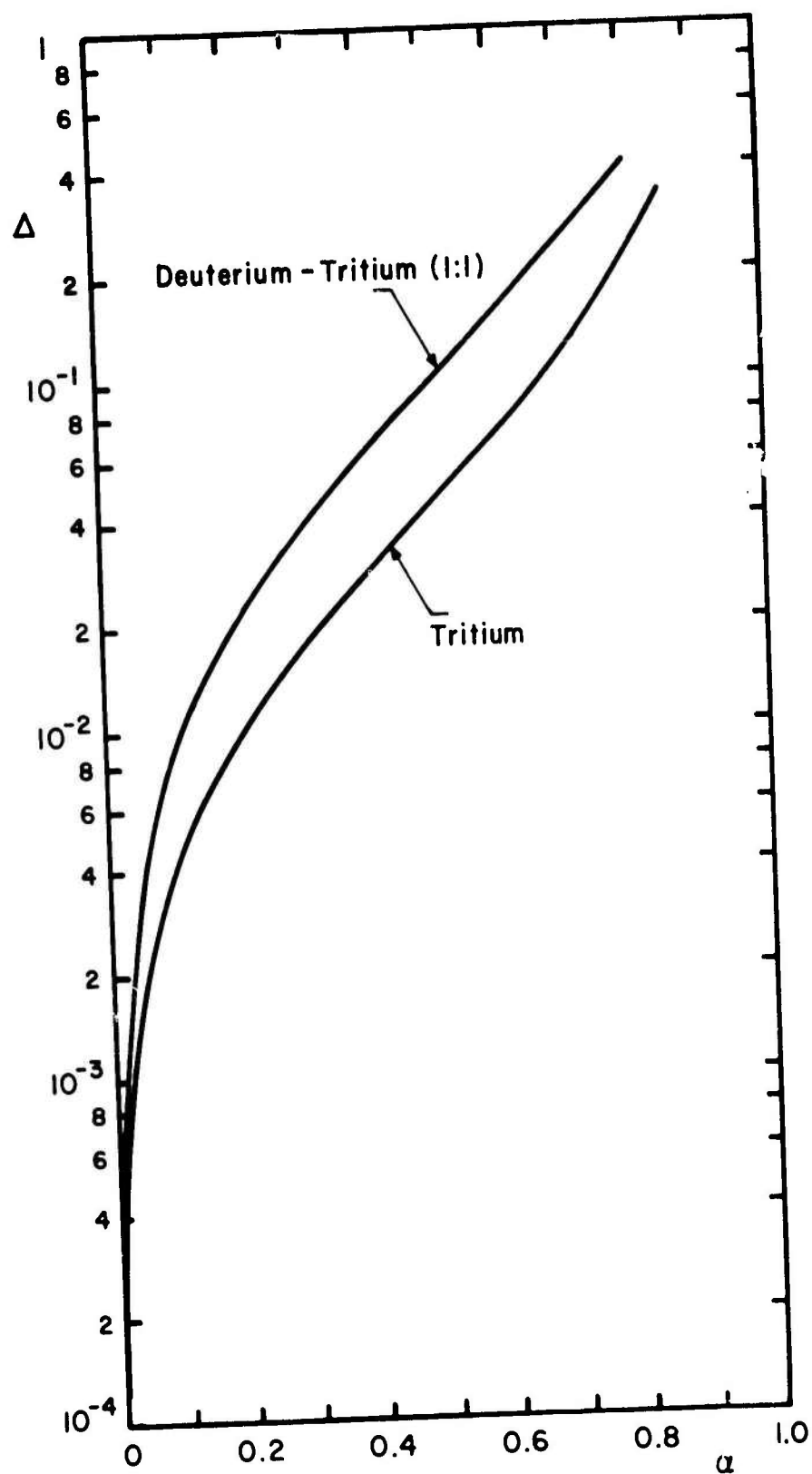


FIG. 15 RADIATION LOSS TERM, Δ , vs. DEGREE OF FUSION, α

e.g., the existence of extremal points, can be ascertained without solving the radiative phase space integral equation. The existence of extremal points on the $\omega - \alpha$ shock curve can be determined by differentiating equation (4.21) with respect to α . The resulting expression is

$$1 - \frac{1}{HQ} \frac{d\Delta}{d\alpha} = - \frac{128}{9} \left(\omega - \frac{5}{8} \right) \frac{d\omega}{d\alpha}. \quad (4.22)$$

Since

$$\frac{1}{HQ} \frac{d\Delta}{d\alpha} = R_p, \quad (4.23)$$

solving equation (4.22) for $\frac{d\omega}{d\alpha}$, we see that

$$\frac{d\omega}{d\alpha} = - \frac{9}{128} \frac{1 - R_p}{\omega - \frac{5}{8}}. \quad (4.24)$$

It follows that ω has an extremal value when the bremsstrahlung power loss just equals the thermonuclear power gain, ($R_p = 1$).

The nature of the extremal point of equation (4.21) depends on the sign of the second derivative evaluated at the extremum. An expression for $\frac{d^2\omega}{d\alpha^2}$ is obtained by differentiating equation (4.24) with respect to α . The resulting expression is

$$\frac{d^2\omega}{d\alpha^2} = \frac{9}{128} \left[\frac{(1 - R_p)}{\left(\omega - \frac{5}{8}\right)^2} \frac{d\omega}{d\alpha} + \frac{1}{\omega - \frac{5}{8}} \frac{dR_p}{d\alpha} \right]. \quad (4.25)$$

At the extremum, $\frac{d\omega}{d\alpha} = 0$, so

$$\frac{d^2\omega}{d\alpha^2} = \frac{9}{128} \frac{1}{\omega - \frac{5}{8}} \frac{dR_p}{d\alpha} \quad (4.26)$$

For the deflagration branch, ω is $< \frac{5}{8}$. Therefore, if $\frac{dR_p}{d\alpha}$ is positive, the extremum is a maximum. Differentiating equation (4.20) with respect to α , we see that

$$\frac{dR_p}{d\alpha} = K \left[\frac{1}{A(\alpha)} \frac{dA}{d\alpha} + A(\alpha) \frac{dB}{d\tau} \frac{d\tau}{d\alpha} \right] \quad (4.27)$$

$\frac{dR_p}{d\alpha}$ must be evaluated separately for the tritium-deuterium and pure tritium cases.

For the deuterium-tritium case, it follows from equation (4.12), (which is valid for the radiative case since it is derived from the mass, momentum and state equations which have no radiative terms in them), that if $\frac{d\omega}{d\alpha} = 0$, then $\frac{d\tau}{d\alpha} = 0$. This result holds for any gas whose equation of state is independent of α . Therefore, if we evaluate $\frac{dA}{d\alpha}$, we see that $\frac{dR_p}{d\alpha}$ is positive at the extremal point, i.e.,

$$\frac{dR_p}{d\alpha} = K \frac{3+\alpha}{1+\alpha} \frac{1}{1-\alpha} > 0 \quad (4.28)$$

Therefore, the extremum is a maximum. In other words, when radiation is taken into account in the structure equations,

the speed of the gas increases until the radiative losses just equal the gains due to reactions. The speed then begins to decrease as the temperature of the gas falls and the density of the gas increases.

If the state equation depends on α , as it does for the pure tritium case, then $\frac{d\omega}{d\alpha} = 0$ does not imply that $\frac{d\tau}{d\alpha} = 0$. In fact, it follows from equation (4.17) that when $\frac{d\omega}{d\alpha} = 0$, then $\frac{d\tau}{d\alpha} = \frac{-\tau}{2(2+\frac{\alpha}{2})}$, which is negative. The first term in equation (4.27) is $K \frac{3+\alpha}{1+\alpha} \frac{1}{1-\alpha}$. Therefore, if $\frac{dB}{d\tau}$ is negative, then $\frac{dR}{d\alpha}$ is positive and the extremum is a maximum. It can be shown from equation (4.20) that $\frac{dB}{d\tau}$ is negative if

$$\frac{2\tau}{\langle v \rangle} \frac{d\langle v \rangle}{d\tau} > 1. \quad (4.29)$$

The reaction probability for T-T reactions has the form,

$$\langle v \rangle = \text{const} \times \tau^{\frac{1}{2}} \left(\exp\left(-\frac{\text{const}}{\tau}\right) + E_1\left(\frac{\text{const}}{\tau}\right) \right),$$

(see section 3.7). Therefore the requirement on $\frac{dB}{d\tau}$, given in equation (4.29), is satisfied and the extremal point on the tritium $\omega - \alpha$ curve is a maximum.

The existence of extrema on the radiative $\tau - \alpha$ curves can also be determined analytically. For the deuterium-tritium case, $\frac{d\tau}{d\alpha} = 0$ implies either $\omega = \frac{1}{2}$ or $\frac{d\omega}{d\alpha} = 0$. When the entire system of equations is integrated, we see that the dimensionless speed never reaches the value 1/2. Therefore if $\frac{d\tau}{d\alpha} = 0$,

then $\frac{d\omega}{d\alpha} = 0$ and the extremal values of temperature and speed occur for the same value of α . Since $1-2\omega$ is positive, a speed maximum corresponds to a temperature maximum.

The temperature and speed extremal values do not occur at the same value of α for the tritium gas. It follows from equation (4.17) that when $\frac{d\tau}{d\alpha} = 0$, then $\frac{d\omega}{d\alpha} = \frac{\tau}{2(1-2\omega)} > 0$. Since the slope of the $\omega-\alpha$ curve is positive when $\frac{d\tau}{d\alpha} = 0$, and since ω goes through only one maximum value, the temperature maximum occurs for a smaller value of α than the speed maximum. In fact, the physical condition for the existence of a temperature maximum is not that the bremsstrahlung power equal the thermonuclear power as it is for the deuterium-tritium case. There is no such simple criterion for a gas whose equation of state depends on α .

The coordinates of the maximum points on the radiative $\tau-\alpha$ and $\omega-\alpha$ phase space curves can be found only if the phase space integral equation is solved. The maximum on the deuterium-tritium $\tau-\alpha$ curve occurs at the point $(\tau, \alpha) = (0.1019, 0.38)$. The maximum on the $\omega-\alpha$ curve occurs for $(\omega, \alpha) = (0.285, 0.38)$. A comparison between the non-radiative and radiative phase space solutions shows that the effect of the radiative energy loss is to lower the maximum temperature inside the wave and to shift its occurrence from $\alpha = 0.89$ to $\alpha = 0.38$. The speed, which

monotonically increases with increasing α when radiation losses are neglected, rises to a maximum value and then falls when radiation losses are included in the analysis.

The coordinates of the maximum point on the $\tau - \alpha$ curve for tritium are $(\tau, \alpha) = (0.0974, 0.37)$, corresponding to a dimensionless speed of $\omega = 0.308$. Those of the maximum point on the $\omega - \alpha$ are $(\omega, \alpha) = (0.322, 0.56)$. When radiation is included in the equations, the temperature maximum occurs when 37% of the material has fused compared to the non-radiative value of 72%.

CHAPTER V

SHOCK PROFILES IN REAL SPACE5.1 Solution of the Shock Structure Equation for a Reacting and Radiating Gas

The profiles of the temperature, speed, density, pressure and degree of fusion in the reaction zone can be found by solving the full system of shock structure equations. The phase space solutions are used to eliminate all of the flow variables except α from the continuity equation. The resulting non-linear differential equation is

$$\frac{d\alpha}{dx} = g(\alpha), \quad (5.1)$$

where
$$g(\alpha) = \frac{\delta A H}{m_T} \frac{(H - \alpha)^2}{\omega^2} \langle \tau v \rangle,$$

and $\delta = 0.6$, $H = 1$, for the deuterium-tritium mixture,

$\delta = 1$, $H = 1$, for pure tritium, and

$\delta = \frac{1}{\epsilon_R}$, $H = \frac{1}{1+3\epsilon}$ for the hydrogen-tritium mixture.

No reactions occur in front of the wave. This physical fact is incorporated into the differential equation by assuming that the reaction probability cuts off at the initial temperature of the gas, i.e., $\langle \tau v \rangle(T_1) = 0$. No reactions occur behind the wave because the fuel has been consumed, i.e., $\alpha = H$. Therefore $g(\alpha)$ approaches 0 as x approaches $+\infty$ and $-\infty$.

$\alpha(x)$ varies directly with the initial number density and inversely with the shock speed since $AH \approx \frac{A}{u_1}$. This dependence may be eliminated if the continuity equation is made dimensionless. An appropriate scale length with which to make the continuity equation dimensionless is the reaction mean free path at the beginning of the reaction zone, λ_2 . The dimensionless spatial variable becomes

$$\xi = \frac{x}{\lambda_2}, \quad (5.2)$$

where $\lambda_2 = \langle v \rangle_2 \frac{1}{n_2 \langle \tau v \rangle_2}$.

The dimensionless continuity equation is

$$\frac{d\alpha}{d\xi} = \frac{\delta A H \lambda_2}{m_T} \frac{(H - \alpha)^2}{\omega^2} \langle \tau v \rangle. \quad (5.3)$$

The constant $AH \lambda_2 / m_T$ is proportional to $(n_1/n_2)(\langle v \rangle_2 / u_1)$. Since n_1 and n_2 are linearly related by the jump conditions across the gas dynamic shock, equation (5.3) is independent of the initial number density of the gas. It follows from equations (2.30) and (2.40) that $\langle v \rangle_2$ is proportional to $T_2^{1/2}$ which is proportional to the shock speed. The differential equation thereby becomes independent of u_1 also.

In most shock structure problems, one must integrate the differential equation from $\xi = -\infty$ to $\xi = +\infty$ because the boundary condition is known only at $\xi = -\infty$.

In this problem, the boundary condition is known for a finite value of ξ which for convenience we assume to $\xi = 0$. The assumption of the von Neumann model of thermonuclear shocks requires that $\alpha = 0$ throughout the gas dynamic shock. Although $\frac{d\alpha}{d\xi} = 0$ ahead of the gas dynamic shock, $\frac{d\alpha}{d\xi} \neq 0$ behind it since $\langle \tau v \rangle (T_2)$ is non-zero. The differential equation for $\xi(\alpha)$ in the reaction zone can thus be reduced to the quadrature,

$$\xi(\alpha) = \frac{1}{\lambda_2} \int_0^\alpha \frac{d\alpha'}{g(\alpha')} \quad (5.4)$$

Equation (5.4) can be integrated analytically for $\frac{\alpha}{H} \ll 1$. ω^2 and $\langle \tau v \rangle$ are constant over the range of integration and can be taken outside the integral. Therefore,

$$\xi(\alpha) = \frac{m_T \omega_2^2}{\delta A H \lambda_2 \langle \tau v \rangle_2} \int_0^\alpha \frac{d\alpha'}{(\kappa - \alpha')^2} \quad (5.5)$$

Performing the integration, we see that

$$\xi(\alpha) = \frac{m_T \omega_2^2}{\delta A H \lambda_2 \langle \tau v \rangle_2} \left[\frac{1}{1 - \frac{\alpha}{H}} - 1 \right] \quad (5.6)$$

This expression can be simplified if $1/(1 - \frac{\alpha}{H})$ is expanded to first order in $\frac{\alpha}{H}$. The resulting linear relation between ξ and α is

$$\xi(\alpha) = \left[\frac{m_T \omega_2^2}{\delta A H \lambda_2 \langle \tau v \rangle_2} \cdot \frac{1}{H^2} \right] \alpha \quad (5.7)$$

The relation between ξ and α , obtained by numerically integrating equation (5.4), establishes that the linear relation between ξ and α is valid for $\frac{\alpha}{\mu} < 0.001$.

Equation (5.4) cannot be integrated analytically when $\frac{\alpha}{\mu} > 0.001$. ω^2 and $\langle \tau v \rangle$ remain inside the integral. Their functional dependence on α is complicated. A closed form expression for $\langle \tau v \rangle(\tau)$ exists only for T-T reactions at Mev temperatures. In all other cases $\langle \tau v \rangle$ must be evaluated numerically (see sections 3.2 and 3.7). A change of variables in $\langle \tau v \rangle$ from τ to α results in an integral that cannot be evaluated analytically. Therefore the integration has been performed numerically with an Euler forward integration scheme.

5.2 Solution of the Shock Structure Equations for a Radiating Gas

The shock structure equations for a reacting gas, and for a reacting and radiating gas, were presented in Chapter IV. If the gas radiates but does not react, equations (4.6) and (4.14) reduce to

$$16 \tau^2 + \left(\frac{1}{2} + 2D \right) \tau + \frac{D^2 - 1}{16} = 0, \quad (5.8)$$

where $D = D' + 4\Delta$,

and
$$\Delta = \frac{H}{A} \int_c^x P_{BR}(\tau', \omega') dx'.$$

The relation between the dimensionless speed, τ , and Δ , obtained from the energy equation, is

$$\omega = (2CH - 2\Delta - 10\tau)^{\frac{1}{2}} \quad (5.9)$$

An iterative method, (similar to that used to solve the phase space equations for a reacting and radiating gas), can be used to solve the structure equations for a radiating gas. The values of τ and ω behind the gas dynamic shock (given by the jump conditions) are used for the first iteration. Since these values of τ and ω are constant for all x , $\Delta_1(x)$ (which can be evaluated analytically), varies linearly with x . $\Delta_1(x)$ is substituted into equation (5.8) to obtain $\tau_1(x)$. Once $\Delta_1(x)$ and $\tau_1(x)$ are known, $\omega_1(x)$ can be evaluated with equation (5.9). Given $\tau_1(x)$ and $\omega_1(x)$, $\Delta_2(x)$ can be computed numerically. The process is repeated until $\tau(x)$, $\omega(x)$ and $\Delta(x)$ remain the same to some required accuracy from one iteration to the next. The scheme converges to three decimal places in a few iterations for the cases we have considered.

One feature of the no reaction limiting case of the structure equations is that the time-independent flow equations are not satisfied for all values of x . As the gas radiates, its temperature and speed decrease. It follows from equation (5.9), that for values of τ which are $\ll 0.1$,

the maximum value that Δ can have is $CH = 0.5$. Therefore the solution of these equations is meaningful only for those values of x for which $\Delta < CH$. The cut off distance occurs about one reaction mean free path behind the gas dynamic discontinuity.

5.3 Profiles of the Flow Variables for Shocks Propagating with the Chapman-Jouquet Speed in Deuterium-Tritium and Tritium Gases

The profiles of the flow variables behind the gas dynamic shock have been computed for thermonuclear shocks propagating with the Chapman-Jouquet speed. The profiles of dimensionless temperature, speed, density, and pressure are shown in figures 16 to 19 for the deuterium-tritium mixture and figures 21 to 24 for the tritium gas. Three cases are displayed in each figure: (1) pure reaction, (2) reaction and radiation, (3) pure radiation. The pure reaction curves are computed for values of α up to $\alpha = 0.99$. The Euler forward integration procedure is inadequate for values of the spatial variable corresponding to α greater than 0.99. However, the behavior of the curves as they approach the values given by the jump conditions across a thermonuclear shock is not of much interest. The reaction and radiation curves are computed for values of α up to $\alpha = 0.80$ for the deuterium-tritium mixture, and

$\alpha = 0.91$ for the tritium gas. The flow variables are changing very rapidly with space for larger values of α , so a higher order integration scheme is needed. However, the behavior of the variable for $\alpha > 0.80$ is of no physical interest. The pure radiative curves are computed for values of x such that the radiation energy loss parameter, Δ , is $\leq CH$.

The reaction and radiation shock profiles combine the features of the pure reaction and pure radiation solutions. As $\xi \rightarrow 0$, all three curves approach the values given by the jump conditions behind the gas dynamic shock. For $\xi \ll 1$, the reaction and radiation solution coincides with the pure reaction curve. For $\xi \gg 1$, it follows the general shape of the pure radiation curve. However, the two do not coincide because the composition of the gas changes as the reactions occur, and the pure radiative case is valid only for a gas consisting of reactants.

The pure reaction and pure radiation shock profiles put upper and lower bounds on the values of the flow variables at each point ξ . For the pure reaction case, the dimensionless speed, w , rises monotonically from $\xi = 0$ to $\xi = \infty$. The dimensionless density, $\phi = \frac{1}{w}$, and pressure, $\pi = 1 - w$, decrease monotonically over the same range. The temperature

rises to a peak and then decreases gradually to its post-detonation steady state value. The temperature peak occurs at $\xi = 13.9$ for the deuterium-tritium mixture and at $\xi = 2.6$ for the tritium gas. For the pure radiation case, all of the variables are monotonic functions of ξ . The temperature and speed of the gas decrease from $\xi = 0$ to $\xi = \infty$; there is no energy source (e.g., reactions) to accelerate and heat the gas. The gas density and pressure increase monotonically with increasing ξ .

When the coupled effects of reactions and radiation are included in the equations, ω , ϕ , and π are no longer monotonic functions of ξ . At first the speed of the gas increases, as in the pure reaction case. It continues to increase until the power input due to reactions is equal to the power loss due to bremsstrahlung, ($R_p = 1$). Then the speed begins to decrease, as in the limiting pure radiative case. The curves of dimensionless density and pressure also undergo a shift in slope for $R_p = 1$; the pressure and density decrease with increasing ξ for $R_p < 1$ and increase with increasing ξ for $R_p > 1$. The turning point of the ω , ϕ , and π curves occurs at $\xi = 0.356$ for the deuterium-tritium case and at $\xi = 0.947$ for the tritium case. The temperature increases with increasing ξ until $R_p = 1$ for the deuterium-tritium mixture and $R_p = 0.425$ ($\xi = 0.386$)

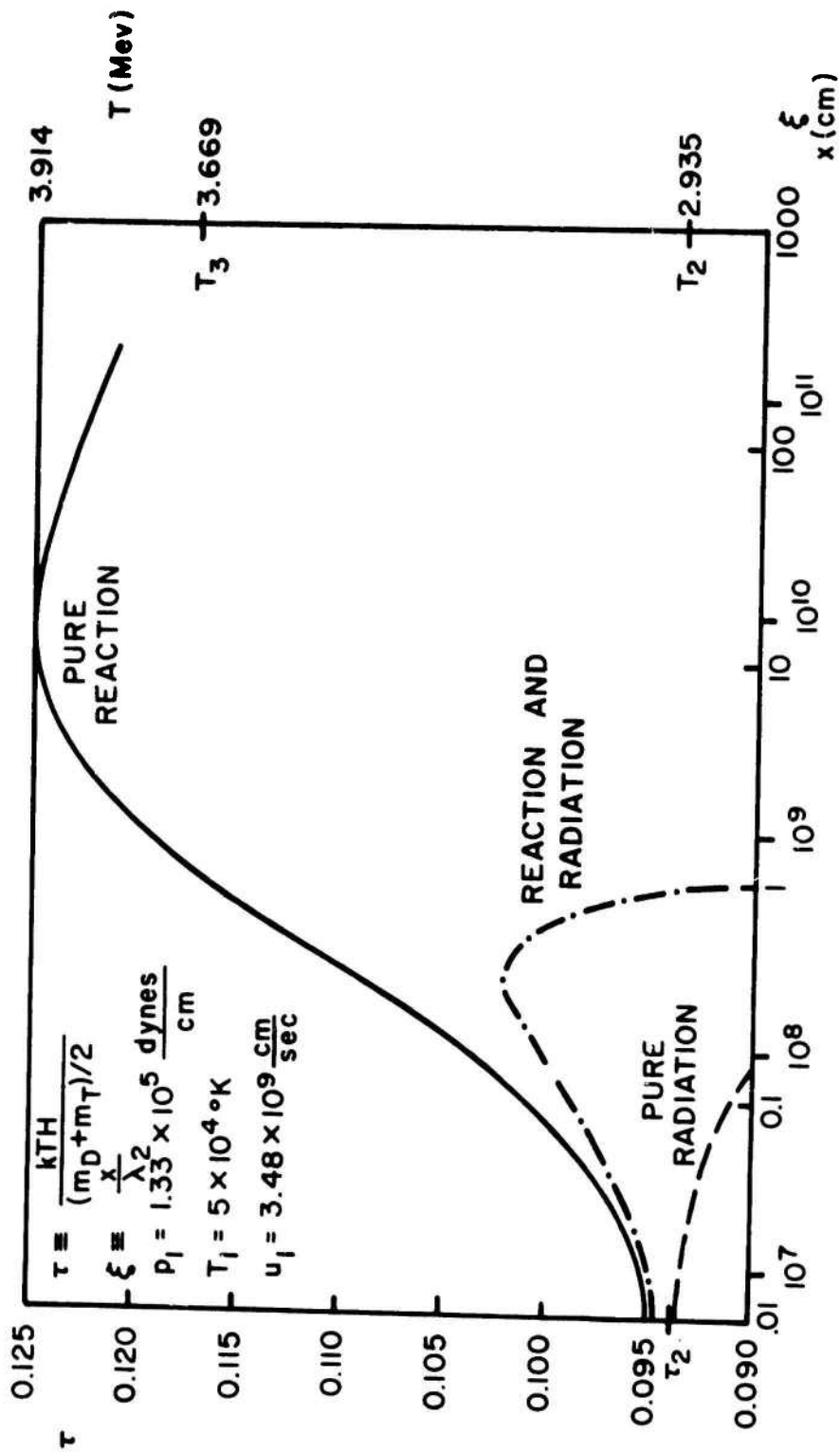


FIG. 16 TEMPERATURE PROFILE BEHIND GAS DYNAMIC SHOCK IN DEUTERIUM - TRITIUM MIXTURE (1:1)

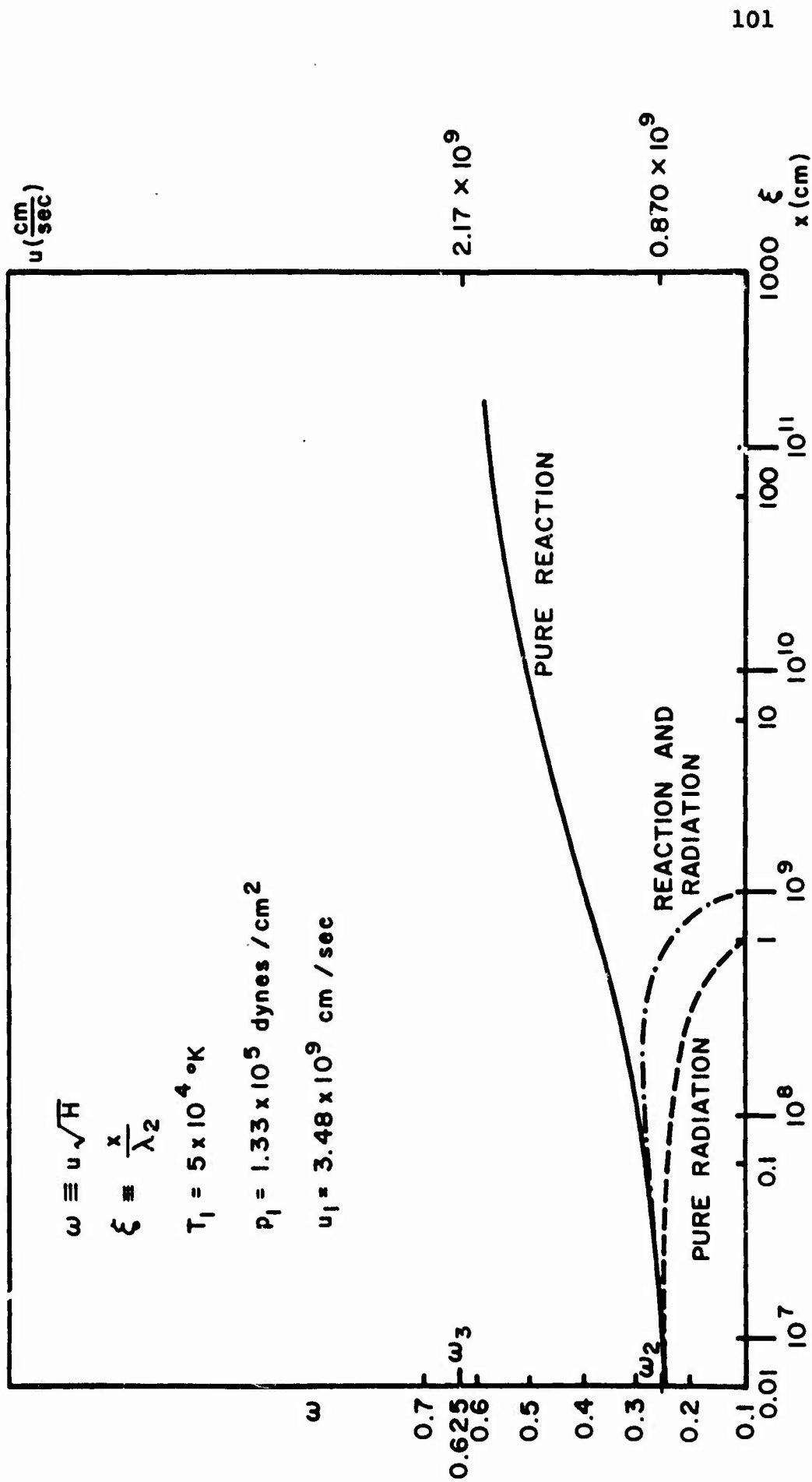
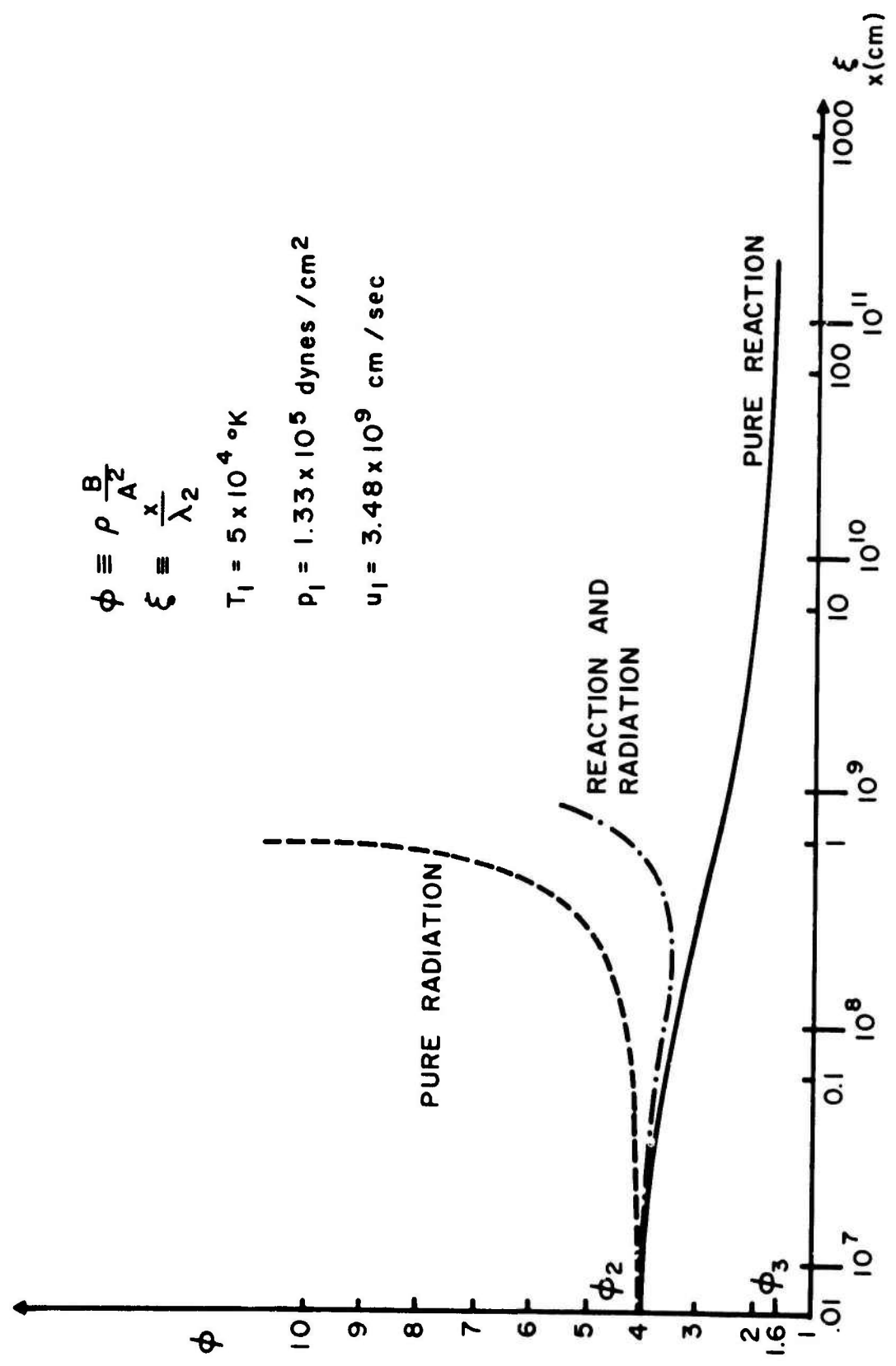


FIG. 17 SPEED PROFILE BEHIND GAS DYNAMIC SHOCK IN DEUTERIUM-TRITIUM MIXTURE



$$\phi \equiv \rho \frac{B}{A^2}$$

$$\xi \equiv \frac{x}{\lambda_2}$$

$$T_1 = 5 \times 10^4 \text{ } ^\circ\text{K}$$

$$\rho_1 = 1.33 \times 10^5 \text{ dynes / cm}^2$$

$$u_1 = 3.48 \times 10^9 \text{ cm / sec}$$

FIG. 18 DENSITY PROFILE BEHIND GAS DYNAMIC SHOCK IN DEUTERIUM-TRITIUM MIXTURE

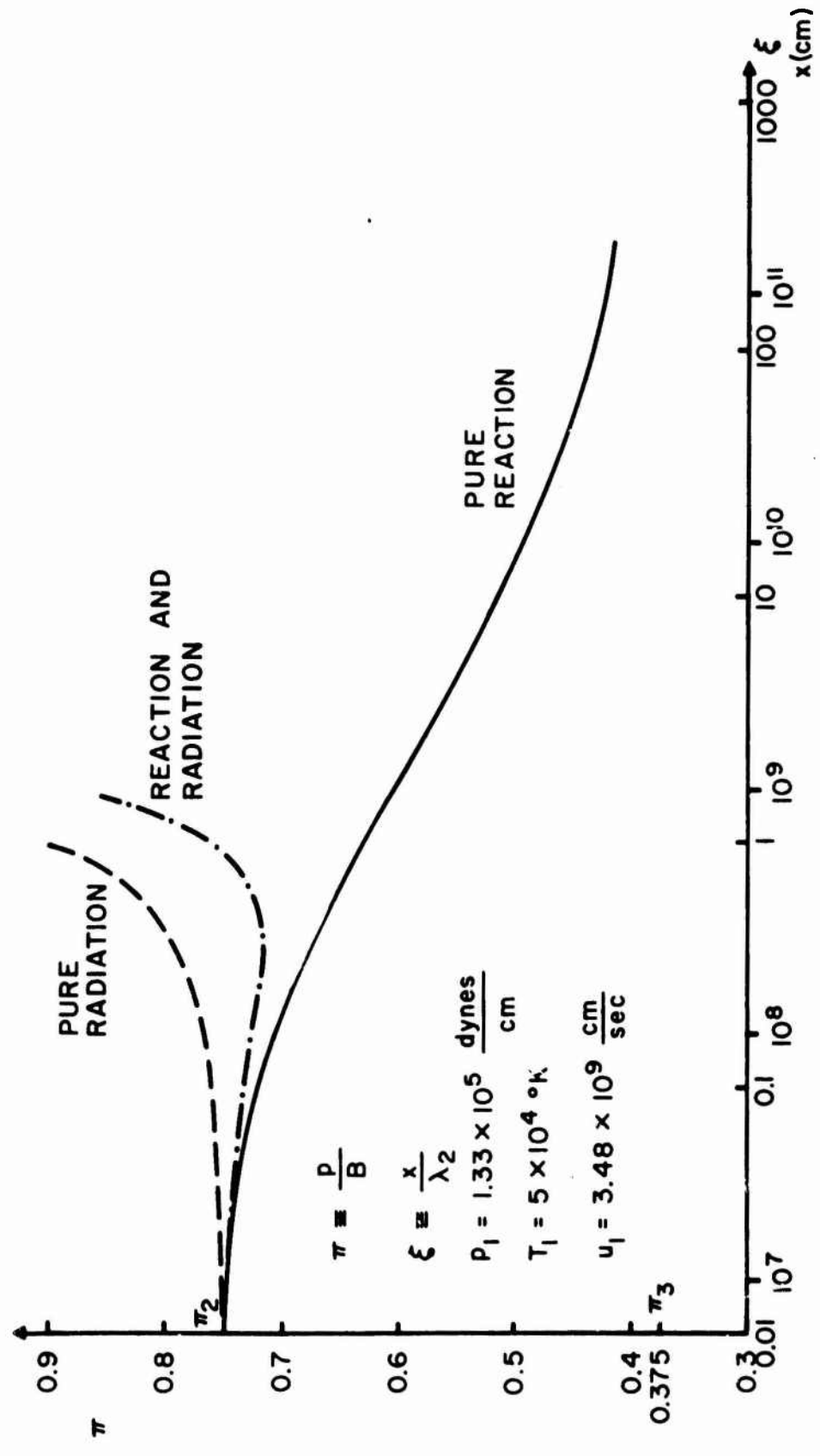


FIG. 19 PRESSURE PROFILE BEHIND GAS DYNAMIC SHOCK IN DEUTERIUM-TRITIUM MIXTURE (1:1)

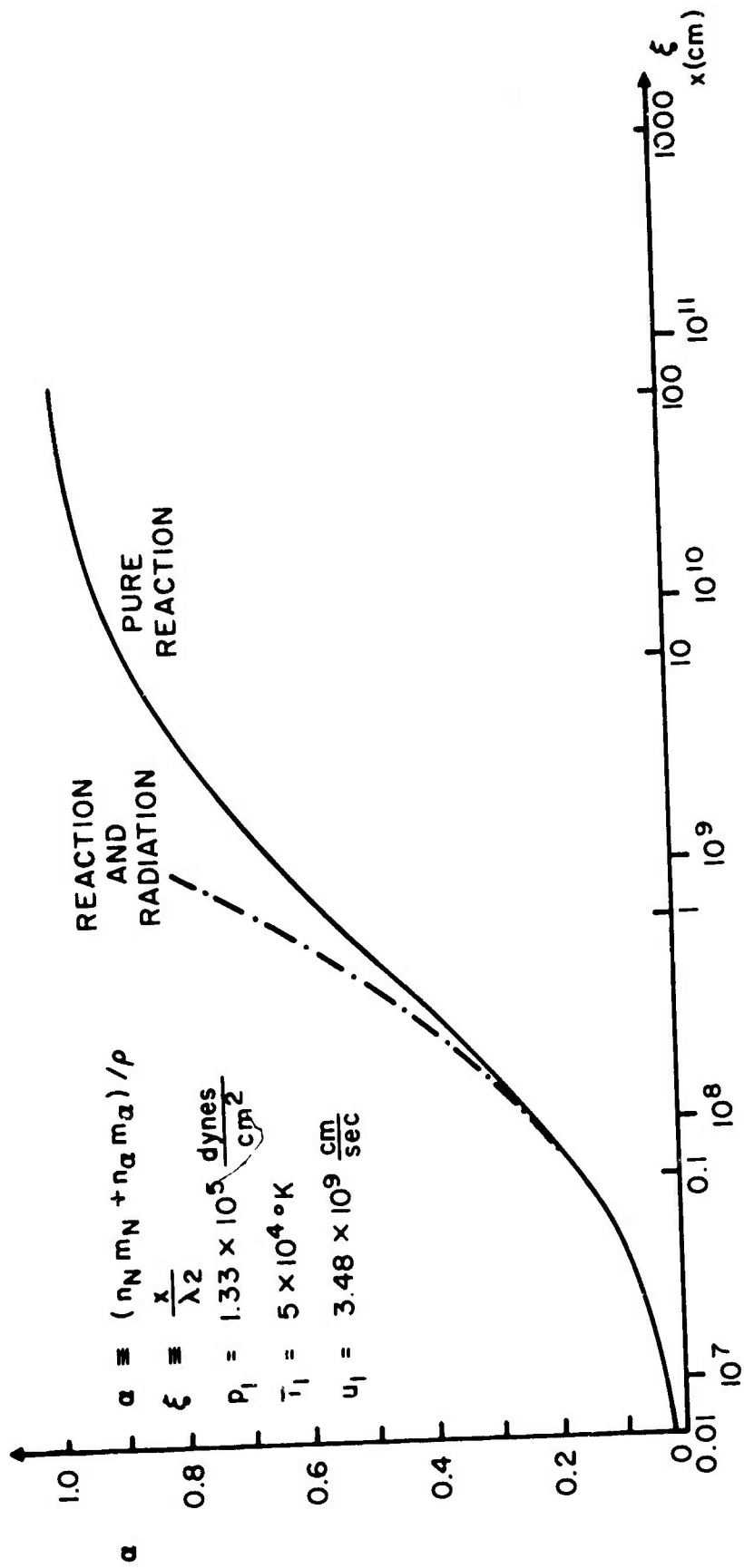


FIG. 20 DEGREE OF FUSION BEHIND GAS DYNAMIC SHOCK IN DEUTERIUM-TRITIUM MIXTURE (1:1)

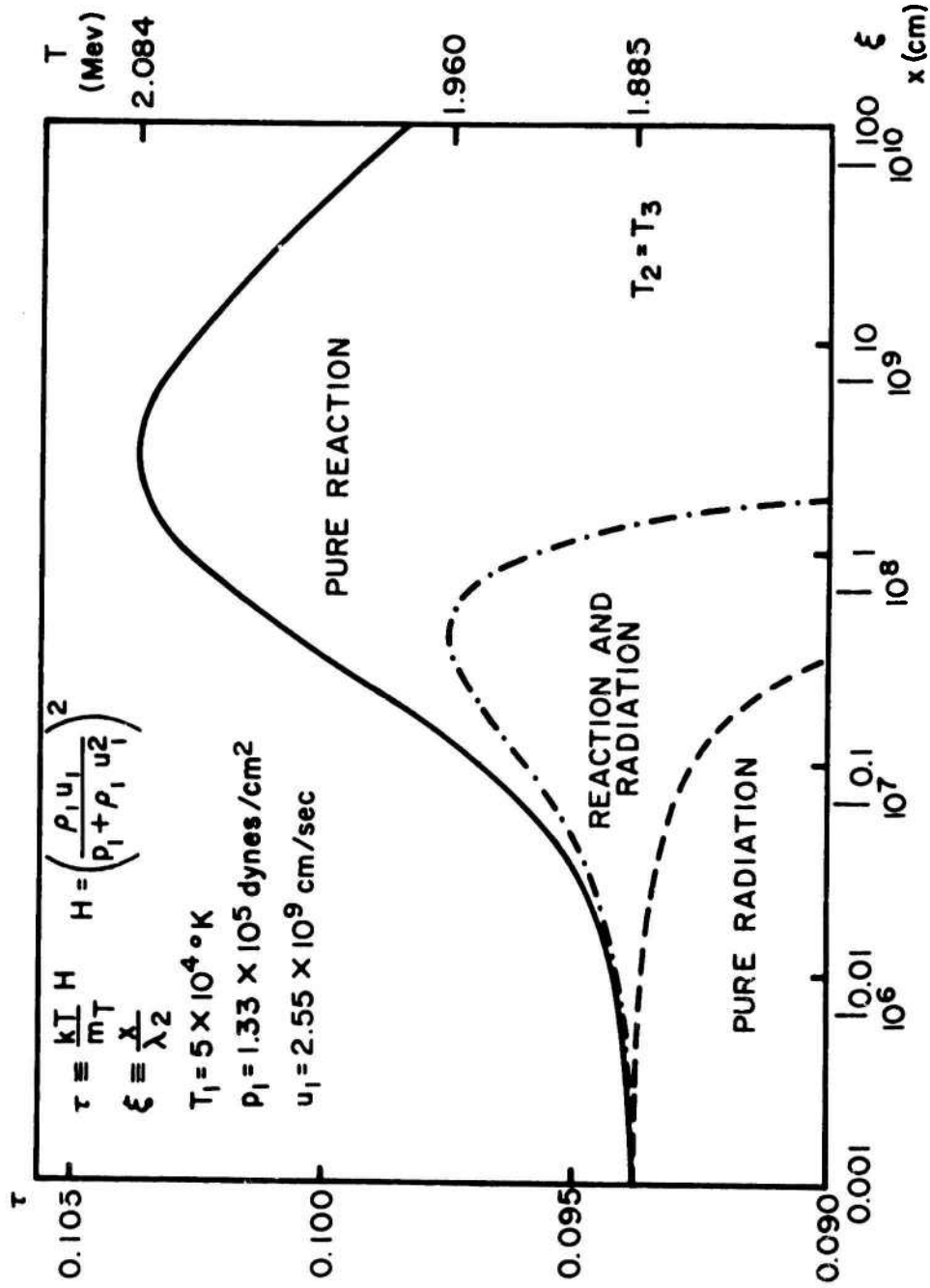


FIG. 21 TEMPERATURE PROFILE BEHIND GAS DYNAMIC SHOCK IN TRITIUM

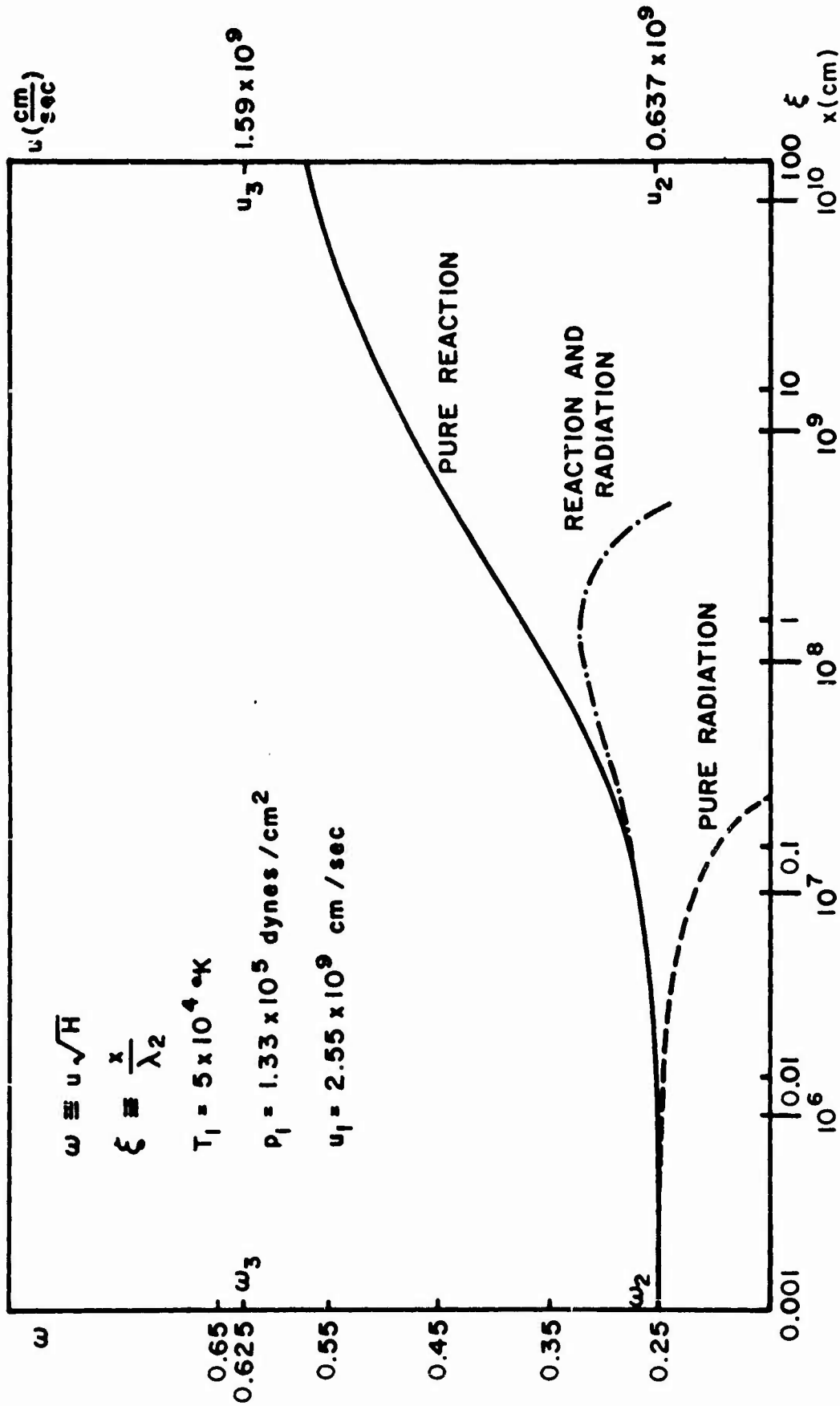


FIG. 22 SPEED PROFILE BEHIND GAS DYNAMIC SHOCK IN TRITIUM

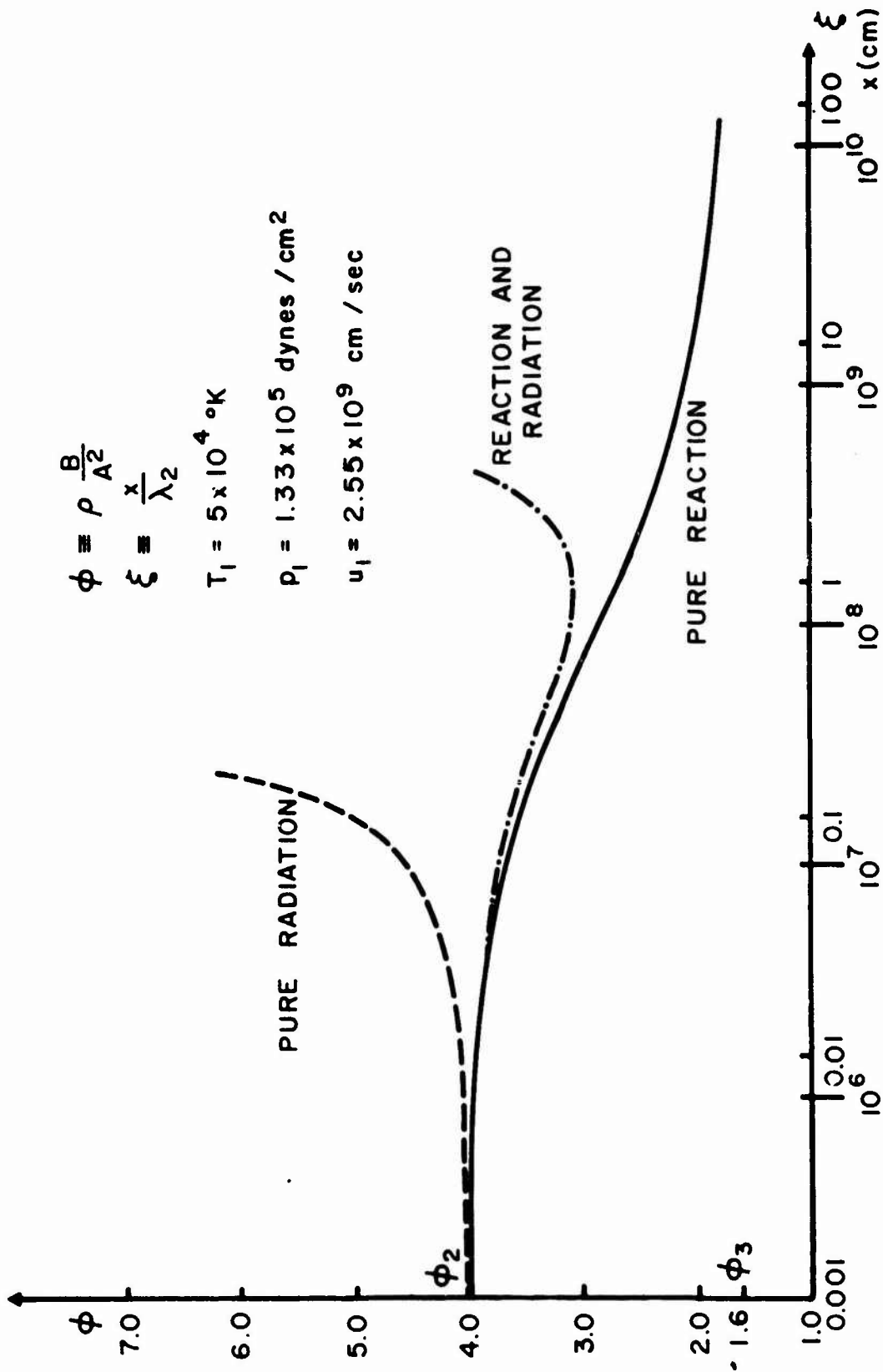


FIG. 23 DENSITY PROFILE BEHIND GAS DYNAMIC SHOCK IN TRITIUM

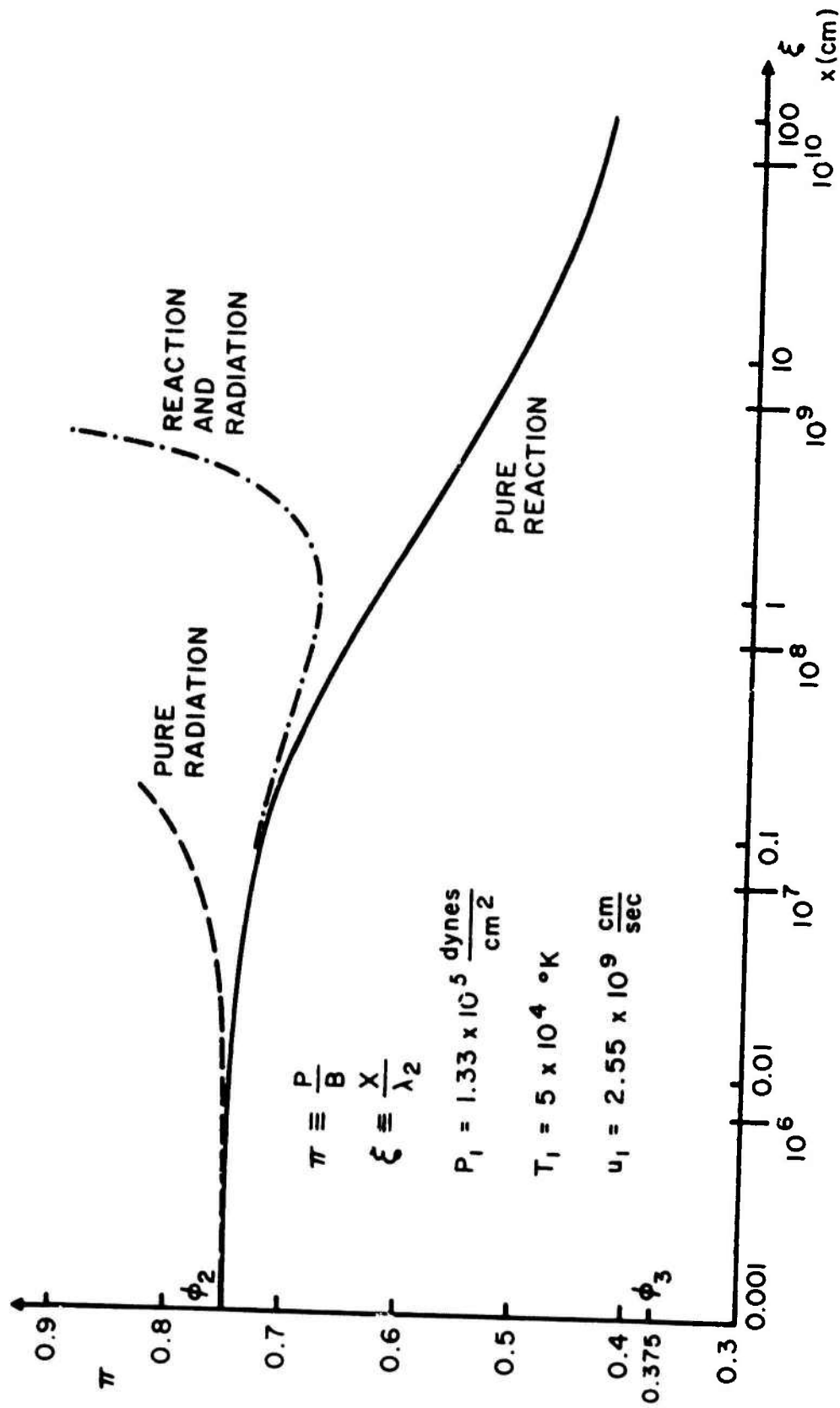


FIG. 24 PRESSURE PROFILE BEHIND GAS DYNAMIC SHOCK IN TRITIUM

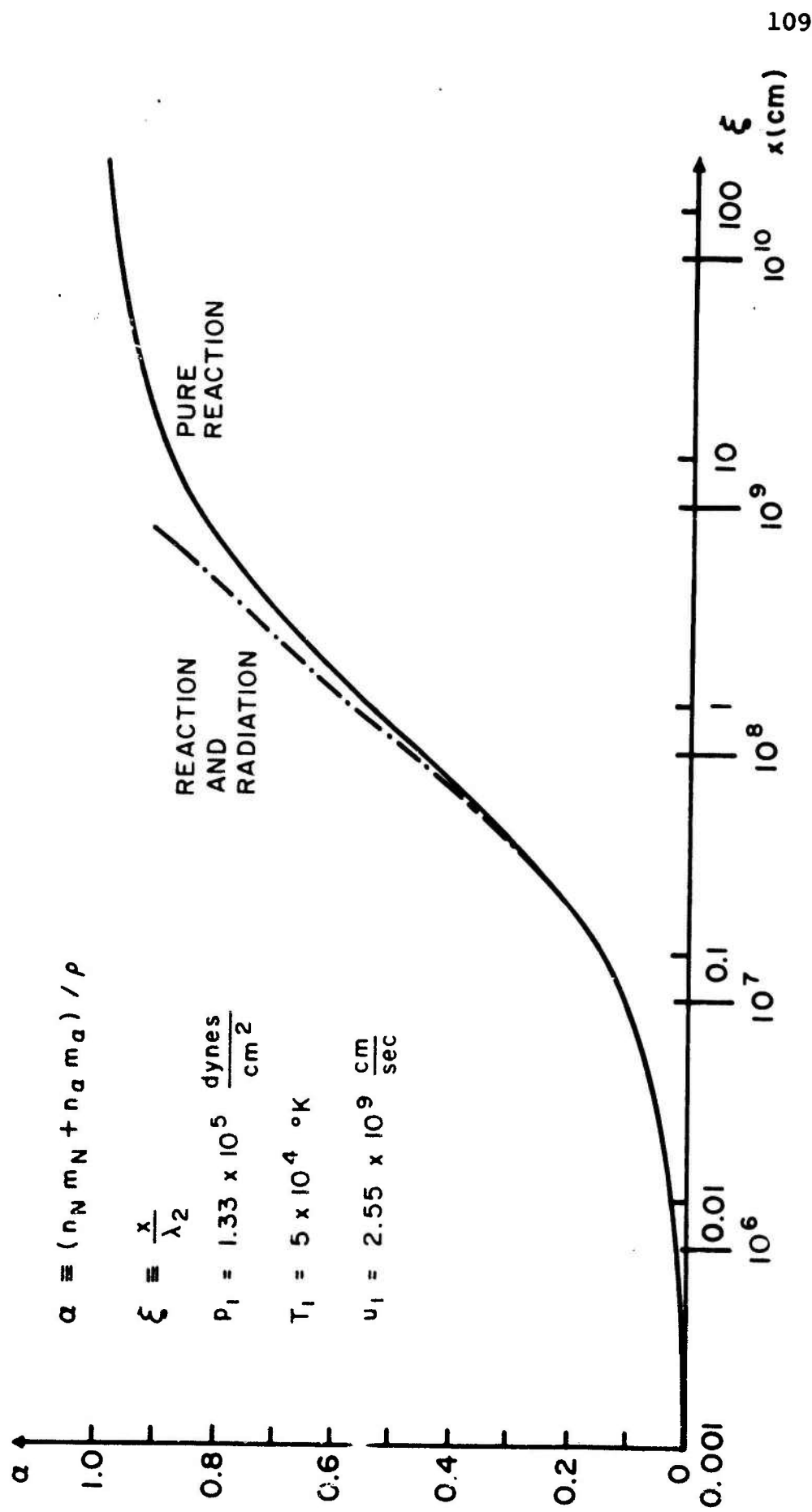


FIG. 25 DEGREE OF FUSION BEHIND GAS DYNAMIC SHOCK IN TRITIUM

for the tritium gas. It then falls as radiative effects become dominant.

The variation of α , the degree of fusion, with space behind the wave front is shown in figures 20 and 25 for the two gas mixtures. α increases monotonically with increasing ξ since thermonuclear reactions are irreversible. The reaction and radiation curve coincides with the pure reaction curve for small values of α . As ξ increases, $\alpha(\xi)$ increases faster for the reaction and radiation case than for the pure reaction case. The following argument can be used to explain this result.

The ratio of the reaction rate for the radiating gas (R) and the non-radiating gas (NR) is

$$\frac{\frac{d\alpha}{d\xi}_R}{\frac{d\alpha}{d\xi}_{NR}} = \frac{\rho_R^2 \langle \sigma v \rangle (T_R)}{\rho_{NR}^2 \langle \sigma v \rangle (T_{NR})}$$

The density for a given ξ for a radiating gas is greater than (or equal to) that for a non-radiating gas (see figures 18 and 23). The temperature for a given ξ for a radiating gas is less than (or equal to) that for a non-radiating gas (see figures 16 and 21). The reaction probability for T-T reactions decreases with decreasing temperature. The reaction rate is proportional to the reaction probability and

to the density squared. Since

$$\frac{\rho_R^2}{\rho_{NR}^2} \geq \frac{\langle \sigma v \rangle (T_{NR})}{\langle \sigma v \rangle (T_R)}$$

for each value of ξ , the reaction rate is larger (or the same) when radiation losses are included in the equations than when they are neglected for the tritium gas. The reaction probability for T-D reactions, (unlike that for T-T reactions), increases with decreasing temperature for $kT > 70$ kev, i.e.,

$$\frac{\langle \sigma v \rangle (T_R)}{\langle \sigma v \rangle (T_{NR})} \geq 1.$$

Therefore, even if $\rho_R^2 = \rho_{NR}^2$,

the reaction rate is greater for the radiating gas than it is for the non-radiating gas for the deuterium-tritium mixture.

The general properties of the shock profiles can be discussed with the variables in dimensionless form, but in order to compute the thickness of the reaction zone, the actual values of the physical variables must be known. For an initial temperature of 5×10^4 °K, and an initial pressure of 1.33×10^5 dynes/cm², ($n_1 \approx 10^{16}$ (cm⁻³)), the reaction mean free path behind the gas dynamic shock is $\approx 10^8$ cm. One

possible definition of the width of the reaction zone is the distance over which 80% of the material fuses, $\Delta_{.80}$. It is expressed in the units of λ_2 , in Table 5.

Gas	$(kT)_2$ (Mev)	λ_2 (cm)	$\Delta_{.80}$	
			pure reaction	reaction & radiation
deuterium-tritium	2.93	6.01×10^8	5.43	1.54
tritium	1.88	1.59×10^8	4.83	2.96

TABLE 5. Reaction Zone Thickness

The distance behind the gas dynamic shock over which 80% of the reactions occur is the order of several earth radii. The thickness of the reaction zone varies inversely with the initial pressure of the gas. Therefore, it will be reduced if the pressure is increased. Reaction zone thicknesses for smaller degrees of fusion can be computed also. There is no need for such a high degree of fusion in order to obtain useful power from thermonuclear reactions.

5.4 Profiles of the Flow Variables for Shocks Propagating with Chapman-Jouquet Speeds in Hydrogen-Tritium Mixtures

It was shown in section 2.3 that the minimum shock speed satisfying the Rankine-Hugoniot conditions for a non-radiative

thermonuclear shock is the Chapman-Jouguet speed. For shocks travelling with the C-J speed, the fusion reactions go to completion inside the wave and a steady state is established behind it. Shock speeds of the order of 10^7 cm/sec are presently obtainable in electromagnetically driven shock tubes. Shock speeds of 10^8 cm/sec have been reported. Therefore, a study of thermonuclear shocks which travel with speeds lower than the C-J speed for tritium, or a deuterium-tritium mixture, is of interest for shock tube experiments.

The C-J speed for a hydrogen-tritium mixture is a function of the relative concentration of the two species. Since the C-J speed for the mixture is proportional to $\left(\frac{1}{1 + \epsilon}\right)^{\frac{1}{2}}$, (see equations (2.29) and (3.72)), the C-J speed decreases as more hydrogen is added to the mixture. The C-J speed is reduced to 10^8 cm/sec for $\epsilon = 643$. Although the power yield would be small for such mixtures, there would be a measurable neutron flux in the shock tube. Neutron fluxes can be measured with appropriate counters. Such measurements could be used to determine whether the plasma temperature had its predicted value behind the gas dynamic shock.

The flux of neutrons per unit area per unit time is defined as

$$\phi_N = n_N u \quad . \quad (5.10)$$

The neutrons are assumed to be in equilibrium with the other species and to travel with the local fluid speed. If

$\alpha \ll \frac{1}{1+3\epsilon}$, it follows from equations (3.92) and (5.7)

that

$$\phi_N = \left[\frac{A^2 H \langle \sigma v \rangle_2}{m_T^2 \omega^2} \frac{1}{(1+3\epsilon)^2} \right] x . \quad (5.11)$$

The distance, x , behind the wave in the shock reference frame is related to the time, t , elapsing after the wave has passed a given point by

$$x = u_1 t . \quad (5.12)$$

Therefore the neutron flux also increases linearly with time behind the wave for $\alpha \ll \frac{1}{1+3\epsilon}$. The values of the neutron flux at 2, 4, 6, 8 and 10 meters behind the gas dynamic shock have been computed for hydrogen-tritium mixtures with $\epsilon = 33.3$ and $\epsilon = 643$. The C-J shock speed is 4.34×10^8 cm/sec for mixtures with $\epsilon = 33.3$. A 10 meter gas sample behind the gas dynamic shock has a temperature of 18.67 kev. The shock speed for mixtures with $\epsilon = 643$ is 1×10^8 cm/sec. The temperature behind the gas dynamic shock is 0.981 kev. The neutron flux as a function of space and time is given in Table 6. The degree of fusion corresponding to each value of the flux is also included.

ϵ	$\phi_N \left(\frac{1}{\text{cm}^2\text{-sec}} \right)$	$x(\text{m})$	t (μ sec)	α
33.3	6.34×10^{13}	2	0.46	1.53×10^{-11}
	1.27×10^{14}	4	0.92	3.06×10^{-11}
	1.90×10^{14}	6	1.38	4.59×10^{-11}
	2.54×10^{14}	8	1.84	6.12×10^{-11}
	3.17×10^{14}	10	2.30	7.15×10^{-11}
643	2.48×10^6	2	2	2.56×10^{-18}
	4.96×10^6	4	4	5.12×10^{-18}
	7.44×10^6	6	6	7.68×10^{-18}
	9.92×10^6	8	8	1.02×10^{-17}
	1.24×10^7	10	10	1.28×10^{-17}

TABLE 6. Neutron Flux Behind Gas Dynamic Shock in Hydrogen-Tritium Mixtures

5.5 Profiles of the Flow Variables for Shocks Propagating with Speeds Below the Chapman-Jouquet Speed

In the preceding sections, shocks travelling at the Chapman-Jouquet speed have been considered. One method of reducing shock speeds to experimentally obtainable values was proposed: the addition of inert material like ordinary hydrogen to a fusible gas like tritium. This method has the

disadvantage of increasing the bremsstrahlung rate without increasing the reaction rate. Another method of obtaining thermonuclear shocks might be to send shocks with speeds less than the Chapman-Jouguet speed into a deuterium-tritium mixture. The approximations that we make in order to solve for the structure of shocks travelling with the C-J speed become better for shocks travelling at lower speeds (see section 2.2).

The analysis of thermonuclear shocks propagating with speeds below the Chapman-Jouguet speed follows very simply from the analysis of the C-J case. In order to keep the jump conditions across the gas dynamic shock in the same form as those for the C-J case, we define a constant Q_m , such that the C-J relation between the shock speed and Q_m is preserved for any value of the shock speed, i.e.,

$$u_1^2 = 2(\gamma^2 - 1) Q_m . \quad (5.13)$$

$$\text{Then, } \frac{R}{W_2} T_2 = 4 \frac{(\gamma - 1)^2}{\gamma + 1} Q_m . \quad (5.14)$$

The shock structure equations for deuterium-tritium mixture, presented in section 3.4, are valid only for $\alpha < \alpha_m = \frac{Q_m}{Q}$, where Q is the value of Q_m when the shock speed is equal to the C-J speed. The time independent equations are not satisfied for larger values of α .

Temperature profiles in the reaction zone have been computed for shock speeds of 1.10×10^8 cm/sec, 3.48×10^8 cm/sec and 1.10×10^9 cm/sec (which correspond to $\alpha_m = 0.001$, 0.01, and 0.1, respectively). The results are displayed in figure 26. The profiles of the relative degree of fusion, $\frac{\alpha}{\alpha_m}$, in the reaction zone are shown in figure 27. A graph of the ratio of the bremsstrahlung power to the thermonuclear power, R_p , for the reaction zone is shown in figures 28 for the three cases and figure 29 for shocks travelling with the C-J speed in a deuterium-tritium mixture and a tritium gas.

Radiative effects are not important for shocks travelling with speeds between 3.48×10^8 and 1.10×10^9 cm/sec. R_p remains at the roughly constant value of 6×10^{-3} for shocks travelling with a speed of 3.48×10^8 cm/sec and 2.5×10^{-2} for shocks propagating at 1.10×10^9 cm/sec. The temperature profiles for the two cases look like the non-radiative temperature profile for shocks travelling with the C-J speed; the temperature rises to a peak value and then decreases as approaches α_m . The details of the shape of each curve depend on the temperatures occurring in the reaction zone (which depend on the shock speed). The reaction probability does not have the same functional dependence on temperature for all temperatures. The temperature and relative degree of fusion rise fastest for temperatures close to the

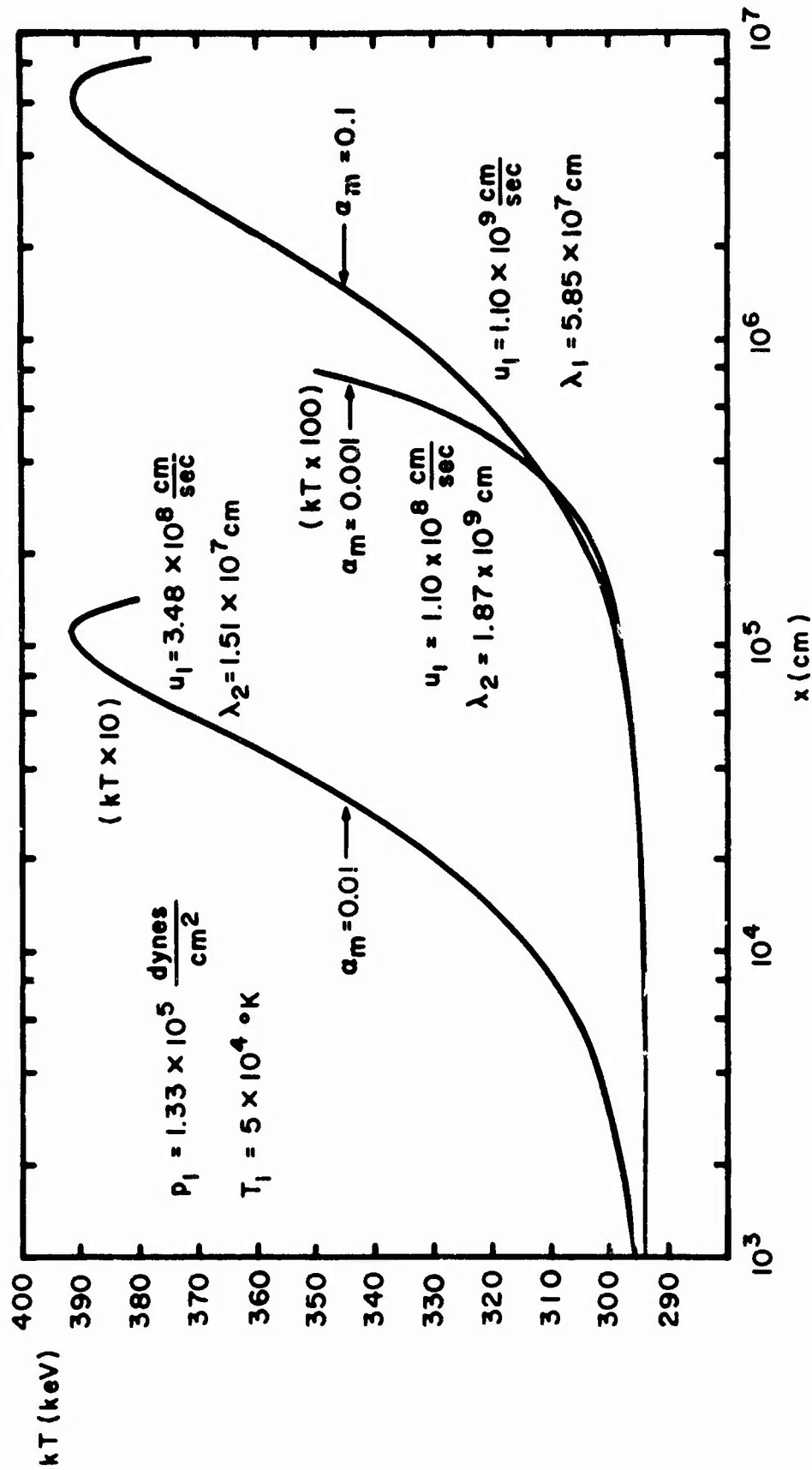


FIG. 26 TEMPERATURE BEHIND GAS DYNAMIC SHOCK IN DEUTERIUM - TRITIUM MIXTURE (1:1)

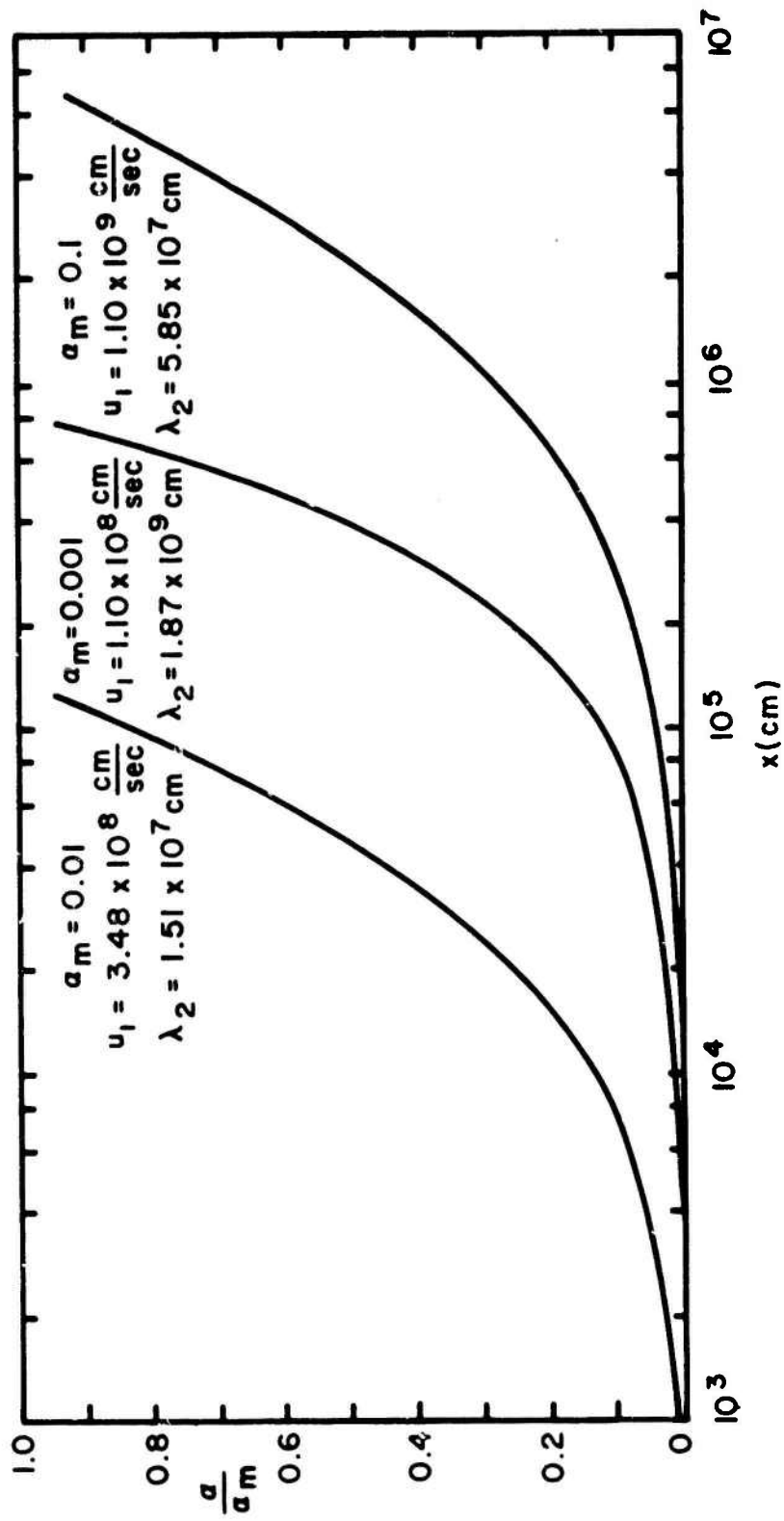


FIG. 27 RELATIVE DEGREE OF FUSION $\frac{\alpha}{\alpha_m}$ BEHIND GAS DYNAMIC SHOCK IN DEUTERIUM - TRITIUM MIXTURE (1:1) FOR DIFFERENT SHOCK SPEEDS

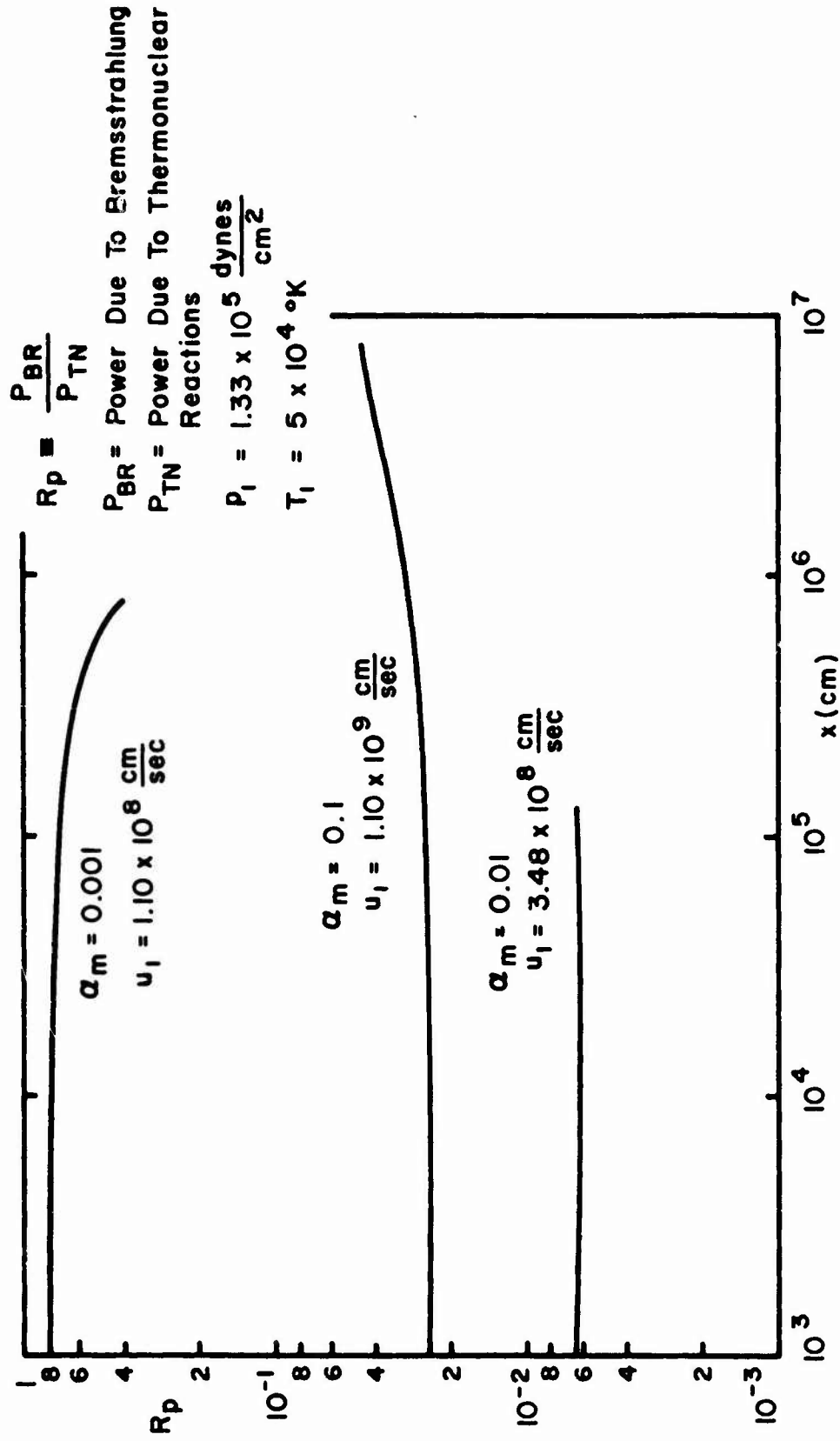


FIG. 28 RATIO OF RADIATIVE POWER LOSS TO THERMONUCLEAR POWER BEHIND GAS DYNAMIC SHOCK IN DEUTERIUM - TRITIUM MIXTURE (1:1) FOR DIFFERENT SHOCK SPEEDS

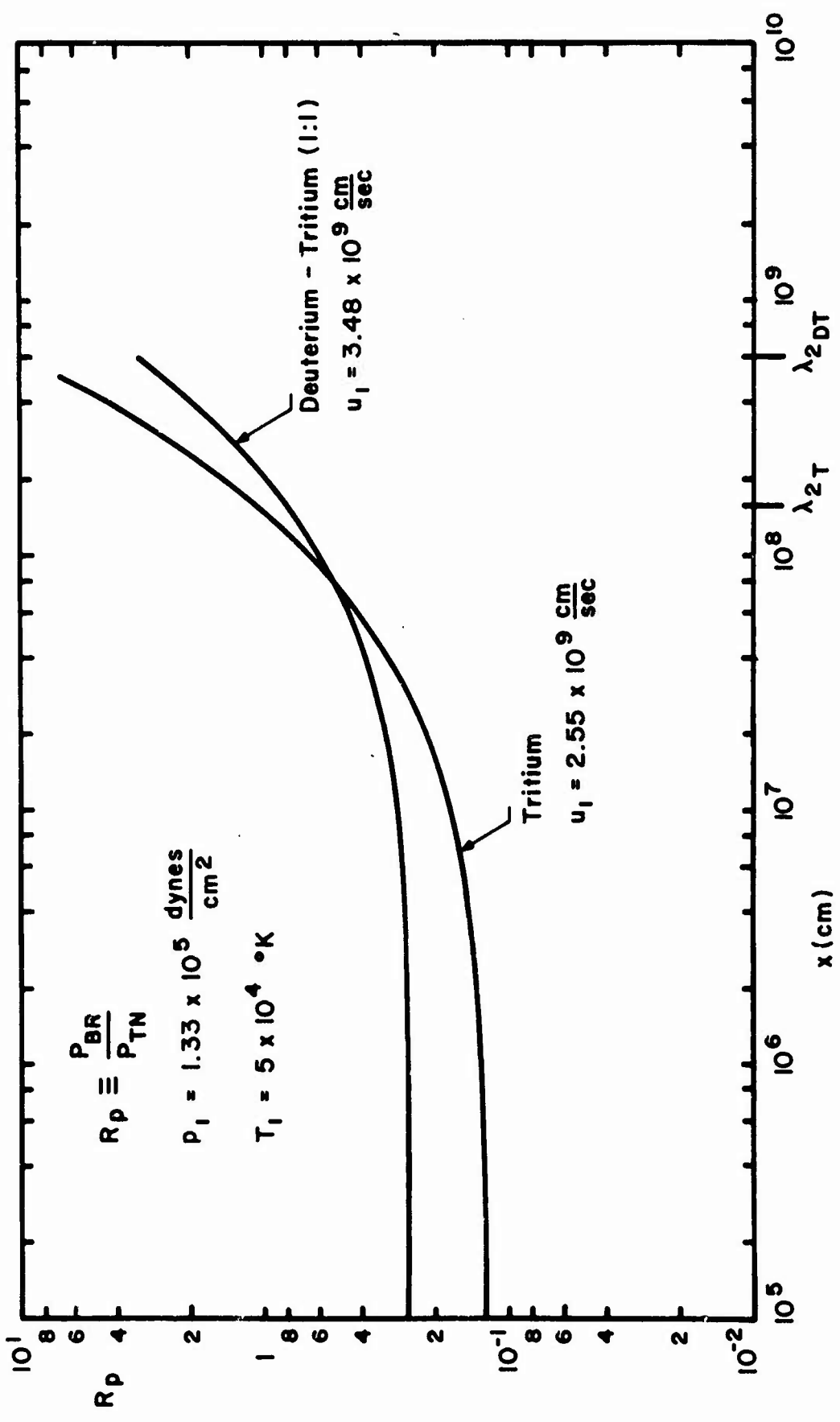


FIG. 29 RATIO OF RADIATIVE POWER LOSS TO THERMONUCLEAR POWER BEHIND GAS DYNAMIC SHOCK

maximum value of the reaction probability ($kT \approx 70$ kev).

Radiative effects become important as the shock speed is reduced to 1.10×10^8 cm/sec. The power ratio in the reaction zone is $\approx 8 \times 10^{-1}$. The larger power ratio occurs because the reaction probability decreases rapidly as kT falls from 40 kev to 4 kev. The power ratio decreases with distance behind the gas dynamic shock. Even though fuel is being replaced by inert reaction products which radiate but do not react, the reaction probability is rising very fast for the temperatures occurring in the reaction zone (3-4 kev) so that the reaction rate is increasing faster than the bremsstrahlung rate. The temperature profile does not look like the other profiles shown in figure 26 because radiative effects are significant. The temperature increases with distance behind the gas dynamic shock but does not reach a peak and then decrease because the condition for a temperature maximum, $R_p = 1$, is never satisfied.

One definition of the thickness of the reaction zone is the distance from the beginning of the reaction zone to the point where a fixed percentage of the gas has reacted. The reaction zone thicknesses for shocks travelling with the three different shock speeds given above have been computed

for four different percentages of reacted gas. The results are presented in Table 7.

α_m	u_1 ($\frac{\text{cm}}{\text{sec}}$)	Partial Thickness of Reaction Zone (cm)			
		0.01%	0.1%	1%	10%
0.001	1.10×10^8	8.5×10^4	7.9×10^5		
0.01	3.48×10^8	7.0×10^2	7.3×10^3	1.4×10^5	
0.1	1.10×10^9	2.7×10^3	2.7×10^4	2.9×10^5	7.9×10^6
1.0	3.48×10^9	2.8×10^4	2.8×10^5	2.8×10^6	3.3×10^7

TABLE 7. Thickness of Reaction Zone for a Given Degree of Reaction as a Function of Shock Speed

The thickness of the reaction zone depends on the temperatures and densities occurring in the reaction zone and the shock speed. $\langle \sigma v \rangle$ rises to a maximum value for $kT \approx 70$ kev and then falls off with increasing temperature. One would think that the reaction zone thickness would be minimized for shock speeds such that $T_2 = 70$ kev. However, the thickness depends on shock speed and the square of the density as well as on reaction probability. The thicknesses of the reaction zone (for small values of α) can be compared for two shocks travelling with different shock speeds in the

following way. It follows from the continuity equation that

$$\frac{\left(\frac{d\alpha}{dx}\right)_a}{\left(\frac{d\alpha}{dx}\right)_b} = \frac{A_b}{A_a} \frac{\langle\sigma v\rangle_a}{\langle\sigma v\rangle_b} \frac{\rho_a^2}{\rho_b^2}.$$

If $\Delta\alpha_a = \Delta\alpha_b$, then $\left(\frac{d\alpha}{dx}\right)_a / \left(\frac{d\alpha}{dx}\right)_b \approx \frac{\Delta x_b}{\Delta x_a}$. Since the initial density of the gas is the same for both cases, ρ_a^2 is $\approx \rho_b^2$. The ratio of the mass flow constant, $\frac{A_b}{A_a}$, is equal to $\left(\frac{T_2^b}{T_2^a}\right)^{\frac{1}{2}}$. Therefore,

$$\frac{\Delta x_b}{\Delta x_a} \approx \frac{\left(T_2^b\right)^{\frac{1}{2}} \langle\sigma v\rangle_a}{\left(T_2^a\right)^{\frac{1}{2}} \langle\sigma v\rangle_b}.$$

If T_2^b is $> T_2^a$, then

$$\frac{\Delta x_b}{\Delta x_a} \text{ is } < 1 \quad \text{if } \frac{\langle\sigma v\rangle_b}{\langle\sigma v\rangle_a} > \left(\frac{T_2^b}{T_2^a}\right)^{\frac{1}{2}}.$$

(For example, if $T_2^b = 70$ kev ($\langle\sigma v\rangle_b \approx 8.9 \times 10^{-16}$ cm³/sec) and $T_2^a = 29.3$ kev ($\langle\sigma v\rangle_a \approx 6.6 \times 10^{-16}$ cm³/sec), then

$\frac{\Delta x_b}{\Delta x_a} \approx 1.1$.) One can determine the shock speed

that gives the thinnest reaction zone from the graph of reaction probability vs. temperature for T-D reactions. The minimum thickness for a given degree of reaction occurs for $T_2 \approx 40$ kev which corresponds to a shock speed of 4.08×10^8 cm/sec.

The gas dynamic shock was assumed to be much thinner than the reaction zone for shocks travelling at the C-J speed. The validity of this assumption for shocks travelling with speeds below the C-J speed will now be examined. The thickness of the gas dynamic shock is assumed to be one collision mean free path evaluated at the end of the gas dynamic shock. It is found to be 168 m for shocks propagating at 3.48×10^8 cm/sec. (The collision mean free path varies roughly as the temperature squared.) Therefore, although it takes only 73 m for 0.1% of the gas to react for a shock speed of 3.48×10^8 cm/sec, 168 m or more are required for the gas temperature to build up to its final value behind the gas dynamic shock.

The behavior of the flow variables over a distance of 10 m behind the gas dynamic shock is relevant to shock tube experiments. The neutron flux as a function of space (or time, if viewed in the laboratory), is shown in Table 8 for shock speeds of 1.10×10^8 cm/sec and 3.48×10^8 cm/sec. The corresponding values of α are also noted. Much higher neutron fluxes are obtainable from deuterium-tritium mixtures than from hydrogen-tritium mixtures for shocks of the same speed.

For thermonuclear shocks to be obtainable in shock tubes, the thickness of the gas dynamic shock must be minimized.

However, the shock speed must be high enough so that reaction rates are appreciable. The gas dynamic shock is ≈ 1.68 m thick for a thermonuclear shock propagating at 1.10×10^8 cm/sec. Neutron fluxes of 10^{17} ($\text{cm}^{-2}\text{-sec}^{-1}$) are achieved in the reaction zone. About

u_1 ($10^8 \frac{\text{cm}}{\text{sec}}$)	α_m	ϕ ($\frac{1}{\text{cm}^2\text{-sec}}$)	x(m)	t(μsec)	α
1.10	0.001	1.24×10^{17}	2	1.82	2.34×10^{-7}
		2.48×10^{17}	4	3.64	4.68×10^{-7}
		3.72×10^{17}	6	5.46	7.02×10^{-7}
		4.96×10^{17}	8	7.28	9.35×10^{-7}
		6.20×10^{17}	10	9.10	1.17×10^{-6}
3.48	0.01	4.86×10^{19}	2	0.576	2.89×10^{-5}
		9.73×10^{19}	4	1.15	5.80×10^{-5}
		1.46×10^{20}	6	1.73	8.69×10^{-5}
		1.86×10^{20}	8	2.30	1.11×10^{-4}
		2.43×10^{20}	10	2.88	1.45×10^{-4}

TABLE 8. Neutron Flux Behind Gas Dynamic Shock in a Deuterium-Tritium Mixture as a Function of Shock Speed

0.0001% of the gas will have reacted 8 m behind the gas dynamic shock. The specific thermonuclear power is

$$\begin{aligned}
 P_{TN} &= n_{D_2} n_{T_2} \langle \sigma v \rangle_2 Q_R \\
 &\approx (2 \times 10^{16})^2 (1.66 \times 10^{-18}) (17.6 \times 1.602 \times 10^{-13}) \frac{\text{watts}}{\text{cm}^3} \\
 &\approx 2 \text{ kw/cm}^3.
 \end{aligned}$$

If the shock tube is 10 m long and has a radius of 10 cm, then the total power output is $\approx 5 \times 10^5$ kw. (Fission power reactors have power outputs of the same order of magnitude.)

A shock tube is a pulsed device so the power output is not continuous. A estimate can be made of the total energy released in reactions with each pulse. We assume that a given gas element will react from the time the shock wave initiates the reactions until the rarefaction wave following the shock wave quenches them. If the shock wave has travelled for a time, t , the distance between the shock front and the rarefaction wave (in the limit of very large initial Mach number) is (Gross²⁴)

$$l(t) = \frac{u_1}{4} t. \quad (5.15)$$

The energy released during the operation of the shock tube may be estimated by

$$\begin{aligned}
 E &= P_{TN} (\pi r^2) \int_0^{t_{op}} l(t) dt \\
 &= P_{TN} (\pi r^2) \frac{u_1}{4} \frac{t_{op}^2}{2}. \quad (5.16)
 \end{aligned}$$

The operating time, t_{op} , is equal to the length of the apparatus divided by the shock speed. If the shock speed is $\approx 10^8$ cm/sec, then the operating time for a 10 m long shock tube is ≈ 10 μ sec. Evaluating equation (5.16), (noting that $P_{TN} \approx 2\text{kw/cm}^3$ and $r=10$ cm), we see that the energy released is ≈ 750 joules. This particular figure is of course only a rough estimate. However, it indicates that an energy output of the order of hundreds of joules is feasible.

ACKNOWLEDGEMENTS

I would like to thank Professor Robert A. Gross for suggesting this problem and for his continued guidance and encouragement throughout the course of this dissertation.

I would like to express special appreciation to Professors Chia-Kun Chu and Paul Koch for helping to clarify many facets of the problem. I would also like to acknowledge the many useful discussions I have had with Stephen Call, Donald Chubb, Mrs. June Clearman, Jack Dorning, Professors Leon J. Lidofsky, Edward Melkonian and Alan Oppenheim, and Dr. Robert Taussig. Finally, I would like to thank Miss Patricia Hurd and Miss Elizabeth Rivera for the excellent job they have done on the typing of this manuscript.

My association with the plasma physics group has been a very rewarding experience. A large share of the credit must be given to Professor Gross who has helped to create an atmosphere in this laboratory which is unusually stimulating and cooperative.

This study was supported by the Air Force Office of Scientific Research under the grant AF 49 (638) - 1634

LIST OF SYMBOLS

A	mass flow constant
A	ion atomic weight
A'	constant in Gamov cross section
α	degree of fusion
α_m	maximum degree of fusion
B	momentum flow constant
B'	constant in Gamov cross section
C	energy flow constant
c	speed of light
D	function of radiative loss parameter
D'	constant that depends on A, B and C
δ	constant in shock structure differential equation
Δ	dimensionless radiative energy loss parameter
E_{cm}	energy in center of mass coordinates
E_L	energy in laboratory coordinates
e	internal energy
e	electron charge
ϵ	density ratio of protons to tritons
ϵ_R	constant that depends on ϵ
F	electron flow constant
G	proton flow constant
γ	ratio of specific heats

H	constant that depends on A, B and C
h	enthalpy
h	Planck's constant
j_ν	mass emission coefficient
k	Boltzmann constant
K_ν	mass absorption coefficient
κ	constant in shock structure differential equation
λ	de Broglie wavelength
λ_D	Debye shielding distance
λ_p^ν	photon absorption mean free path
λ_R	reaction mean free path
λ_2	reaction mean free path behind gas dynamic shock
m_α	alpha particle mass
m_D	deuteron mass
m_e	electron mass
m_N	neutron mass
m_H	proton mass
m_T	triton mass
m_T'	effective triton mass
n_α	alpha particle number density
n_D	deuteron number density
n_e	electron number density
n_N	neutron number density
n_H	proton number density

n_T	triton number density
ω	dimensionless speed
P_{BR}	power due to bremsstrahlung
P_{TN}	power due to thermonuclear reactions
P	pressure
Π	dimensionless pressure
ϕ	dimensionless density
Q	energy released in reactions per gram of initial gas mixture
Q_{eff}	effective energy released per gram of initial gas mixture
Q_R	energy released per reaction
q	radiative energy flux
q_{TN}	thermonuclear energy per unit mass
R	universal gas constant
R_p	ratio of bremsstrahlung power to thermonuclear power
ρ	density
σ	cross section
σ_{Gam}	Gamov cross section
σ_{Gov}	Govorov cross section
$\langle \tau v \rangle$	reaction probability
T	temperature
τ	dimensionless temperature
τ_c	self collision time

τ_{ce}	self collision time for electrons
τ_{c_N}	self collision time for neutrons
τ_{eq}	equilibration time
τ_R	reaction time
u	gas speed
u_1	shock speed (initial gas speed)
\bar{W}	mean molecular weight
w_i	production rate of ith specie
ξ	dimensionless spatial variable
Z	atomic number

REFERENCES

1. W. J. M. Rankine, Phil. Trans. Roy. Soc. London 160, 277 (1870).
2. H. Hugoniot, J. Ecole Polytech (Paris) 58, 1 (1889).
3. Lord Rayleigh, Proc. Roy. Soc. (London) A84, 267 (1910).
4. D. Gilbarg and D. Paolucci, J. Rat. Mech. Anal. 2, 617 (1953).
5. C. S. Wang Chang, App. Phys. Lab Report No. APL/JHO, CM503 (1948).
6. H. M. Mott-Smith, Phys. Rev. 82, 885 (1951).
7. K. Zoller, Zeitschrift fur Physik 8, 321 (1921-1922).
8. H. Grad, Comm. on Pure and App. Math. 5, 257 (1952).
9. M. Berthelot, Comptes Rendus, de l'Academie des Sciences, Paris, pp. 18-22.
10. D. L. Chapman, Phil. Mag., 47, 90 (1899).
11. E. Jouguet, J. Mathematique, 6th Series, 1, 367 (1905) and 2, 5 (1906).
12. J. von Neumann, OSRD Rep. 569 (1942).
13. W. Doring, Annalen der Physik, 43, 421 (1943).
14. Y. B. Zeldovich, JETP, 10, 542 (1940).
15. J. O. Hirshchfelder and C. F. Curtiss, J. Chem. Phys. 28, 1130 (1958).
16. E. L. Resler Jr. and B. Cary, The Threshold of Space, Pergamon Press, (1957).
17. H. Petschek and S. Byron, Ann. Phys. 1, 270 (1957).
18. V. A. Prokof'ev, Uch. Zap. Mos. Gos. Univ., Mech. 172, 79 (1952).

19. M. A. Heaslet and B. S. Baldwin Jr., *Phys. Fluids* 6, 781, 79 (1963).
20. R. E. Marshak, *Phys. Fluids* 1, 26 (1958).
21. S. C. Traugott, *Proceedings of the 1963 Heat Transfer and Fluid Mechanics*, edited by A. Roshko et al. (Stanford University Press, Stanford, California, 1963).
22. P. A. Koch, *Phys. Fluids* 8, 2140 (1965).
23. S. M. Scala and D. H. Sampson, Heat Transfer in Hypersonic Flow with Radiation and Chemical Reaction, edited by D. Olfe (Pergamon Press, New York 1963).
24. R. A. Gross, *Rev. Mod. Phys.*, 37, 724 (1965).
25. J. O. Hirschfelder, C. F. Curtiss and R. B. Bird, Molecular Theory of Gases and Liquids, (John Wiley and Sons, Inc., New York 1954).
26. T. von Karman, Aerothermochemistry (notes edited by G. Millan, Jan. 1958).
27. D. Brezing, Columbia U. Plasma Lab Rep't. 13 (September 1964).
28. S. Glasstone and R. H. Lovberg, Controlled Thermonuclear Fusion, (D. von Nostrand Company, Inc., Princeton, 1960).
29. R. T. Taussig, *Phys. Fluids*, 9, 421 (1966).
30. W. D. Hayes, Gasdynamic Discontinuities, (Princeton University Press, Princeton, 1960).
31. H. Taylor and A. V. Tobolsky, *Amer. Scientist* 46, 191 (1958).
32. L. Spitzer, Jr., Physics of Fully Ionized Gases (Interscience Publishers, New York, 1962).
33. D. J. Hughes and R. B. Schwartz ed, *Neutron Cross Sections*, BNL 325 (1959).
34. S. Glasstone, Principles of Nuclear Engineering (D. van Nostrand Company, Inc. Princeton, 1955).

35. R. K. Osborn, Fusion and Plasma Physics (lecture notes, University of Michigan Dep't. of Nuclear Engineering, June 1961).
36. R. D. Evans, The Atomic Nucleus (McGraw-Hill Book Company, Inc. New York, 1955).
37. Vincenti and C. Kruger, Introduction to Physical Gas Dynamics (John Wiley and Sons, Inc., New York, 1965).
38. R. Goulard, Fundamental Equations of Radiation Gas Dynamics (Purdue U. School of Aeronautical and Engineering Sciences, Lafayette, Indiana, 1962).
39. C. F. Wandel, T. Hesselberg Jensen and O. Kofoed-Hansen, Nuclear Instr., 4, 269 (1959).
40. I. Kaplan, Nuclear Physics (Addison Wesley, Reading, Massachusetts, 1955).
41. F. Ajzenberg-Selove and T. Lauritsen, Nuclear Phys., 11, 1 (1959).
42. N. Jarmie and J. D. Seagrave, Eds., USAEC Report LA-2014 (1957).
43. A. M. Govorov, Li Ka-yeng, G. M. Osetinskii, V. I. Salatskii, and J. V. Sizov, JETP, 15, 266 (1962).
44. W. B. Thompson, Proc. Phys. Soc. (London) B70, 1 (1957).

Unclassified

Security Classification

DOCUMENT CONTROL DATA - R&D		
<i>(Security classification of title, body of abstract and indexing annotation must be entered when the overall report is classified)</i>		
1. ORIGINATING ACTIVITY (Corporate author) Columbia University	2a. REPORT SECURITY CLASSIFICATION Unclassified	2b. GROUP
3. REPORT TITLE Thermonuclear Shock Wave Structure		
4. DESCRIPTIVE NOTES (Type of report and inclusive dates) Technical Report		
5. AUTHOR(S) (Last name, first name, initial) Fuller, Ann L.		
6. REPORT DATE July 1966	7a. TOTAL NO. OF PAGES	7b. NO. OF REFS
8a. CONTRACT OR GRANT NO. AF49(638)1634	9a. ORIGINATOR'S REPORT NUMBER(S) Plasma Laboratory Report No. 31	
b. PROJECT NO.	9b. OTHER REPORT NO(S) (Any other numbers that may be assigned this report)	
c.		
d.		
10. AVAILABILITY/LIMITATION NOTICES Qualified requestors may obtain copies of this report from DDC.		
11. SUPPLEMENTARY NOTES	12. SPONSORING MILITARY ACTIVITY Air Force Office of Scientific Research, Washington, D. C.	
13. ABSTRACT <input checked="" type="checkbox"/> The structure of a very strong shock wave propagating through a deuterium-tritium gas mixture and a pure tritium gas is studied. The temperature behind the shock wave is sufficiently high so that thermonuclear reaction probabilities are large. The wave structure is similar to that of detonations in chemically reacting gases. It is assumed that the characteristic times for collisions and reactions are such that the von Neumann-Zeldovich model of detonations is applicable; i.e., the shock can be treated as a viscous gas dynamic shock followed by a deflagration wave inside of which all the reactions occur. The physical and mathematical assumptions involved in the analysis of thermonuclear shock wave structure are examined. The reaction probabilities for deuterium and tritium fusion reactions are computed and the appropriate reaction kinetics equations are developed. The effect of energy losses due to bremsstrahlung on the wave structure is considered for a gas that is optically thin to radiation of all frequencies. The resulting set of structure equations are solved numerically for several physically interesting cases. The neutron flux and power output due to reactions is calculated for a shock propagating in a electromagnetically driven shock tube filled with a mixture of deuterium and tritium. A power of 1 kw/cm ² is predicted under specified operating conditions. CC		

DD FORM 1473
1 JAN 54

Unclassified

Security Classification

Unclassified
Security Classification

KEY WORDS	LINK A		LINK B		LINK C	
	ROLE	WT	ROLE	WT	ROLE	WT
Thermonuclear reactions						
Shock Wave						
Detonation						
Deuterium						
Tritium						

INSTRUCTIONS

ORIGINATING ACTIVITY: Enter the name and address of the contractor, subcontractor, grantee, Department of Defense activity or other organization (corporate author) issuing report.

REPORT SECURITY CLASSIFICATION: Enter the overall security classification of the report. Indicate whether "Restricted Data" is included. Marking is to be in accordance with appropriate security regulations.

GROUP: Automatic downgrading is specified in DoD Directive 5200.10 and Armed Forces Industrial Manual. Enter group number. Also, when applicable, show that optional markings have been used for Group 3 and Group 4 as authorized.

REPORT TITLE: Enter the complete report title in all capital letters. Titles in all cases should be unclassified. A meaningful title cannot be selected without classification, show title classification in all capitals in parentheses immediately following the title.

DESCRIPTIVE NOTES: If appropriate, enter the type of report, e.g., interim, progress, summary, annual, or final. Give the inclusive dates when a specific reporting period is covered.

AUTHOR(S): Enter the name(s) of author(s) as shown on the report. Enter last name, first name, middle initial. Military, show rank and branch of service. The name of principal author is an absolute minimum requirement.

REPORT DATE: Enter the date of the report as day, month, year, or month, year. If more than one date appears on the report, use date of publication.

TOTAL NUMBER OF PAGES: The total page count should follow normal pagination procedures, i.e., enter the number of pages containing information.

NUMBER OF REFERENCES: Enter the total number of references cited in the report.

CONTRACT OR GRANT NUMBER: If appropriate, enter applicable number of the contract or grant under which report was written.

PROJECT NUMBER: Enter the appropriate military department identification, such as project number, project number, system numbers, task number, etc.

ORIGINATOR'S REPORT NUMBER(S): Enter the official report number by which the document will be identified and controlled by the originating activity. This number must be unique to this report.

OTHER REPORT NUMBER(S): If the report has been signed any other report numbers (either by the originator or by the sponsor), also enter this number(s).

AVAILABILITY/LIMITATION NOTICES: Enter any limitations on further dissemination of the report, other than those

imposed by security classification, using standard statements such as:

- (1) "Qualified requesters may obtain copies of this report from DDC."
- (2) "Foreign announcement and dissemination of this report by DDC is not authorized."
- (3) "U. S. Government agencies may obtain copies of this report directly from DDC. Other qualified DDC users shall request through _____."
- (4) "U. S. military agencies may obtain copies of this report directly from DDC. Other qualified users shall request through _____."
- (5) "All distribution of this report is controlled. Qualified DDC users shall request through _____."

If the report has been furnished to the Office of Technical Services, Department of Commerce, for sale to the public, indicate this fact and enter the price, if known.

11. SUPPLEMENTARY NOTES: Use for additional explanatory notes.

12. SPONSORING MILITARY ACTIVITY: Enter the name of the departmental project office or laboratory sponsoring (paying for) the research and development. Include address.

13. ABSTRACT: Enter an abstract giving a brief and factual summary of the document indicative of the report, even though it may also appear elsewhere in the body of the technical report. If additional space is required, a continuation sheet shall be attached.

It is highly desirable that the abstract of classified reports be unclassified. Each paragraph of the abstract shall end with an indication of the military security classification of the information in the paragraph, represented as (TS), (S), (C), or (U).

There is no limitation on the length of the abstract. However, the suggested length is from 150 to 225 words.

14. KEY WORDS: Key words are technically meaningful terms or short phrases that characterize a report and may be used as index entries for cataloging the report. Key words must be selected so that no security classification is required. Identifiers, such as equipment model designation, trade name, military project code name, geographic location, may be used as key words but will be followed by an indication of technical content. The assignment of links, roles, and weights is optional.